

GRINDING AND ABRASIVE WEAR.

by

T.C. BATTERY B.Sc.

Thesis submitted under the requirements of the University of Leicester
for the Degree of Doctor of Philosophy.

May 1969.

UMI Number: U622268

All rights reserved

INFORMATION TO ALL USERS

The quality of this reproduction is dependent upon the quality of the copy submitted.

In the unlikely event that the author did not send a complete manuscript and there are missing pages, these will be noted. Also, if material had to be removed, a note will indicate the deletion.



UMI U622268

Published by ProQuest LLC 2015. Copyright in the Dissertation held by the Author.
Microform Edition © ProQuest LLC.

All rights reserved. This work is protected against
unauthorized copying under Title 17, United States Code.



ProQuest LLC
789 East Eisenhower Parkway
P.O. Box 1346
Ann Arbor, MI 48106-1346

X75301 2005

Thesis
362947
13.4.70



SUMMARY.

Abrasives are used in various forms to produce fine finishes on metal surfaces. Previously, grinding and abrasive processes have been studied in isolation; the present work however has shown that grinding can be usefully interpreted in abrasive wear terms.

Wear experiments using small grinding wheels on a pin and ring machine have been able to reproduce many of the effects observed not only in grinding but also in such specialised processes as super-finishing.

Abrasive wear theory has been re-examined, especially the parameters making up the K factor, and then applied to the grinding process. In order to test theoretical predictions a grinding dynamometer was constructed to measure forces in surface grinding.

Idealised indentors having simple geometrical shapes, similar to those assumed in abrasive wear theory, were tracked across smooth metal surfaces. Measurements of the scratches produced were then compared with theory.

Scratch tests on a range of heat-treated steels using both idealised indentors and abrasive grits showed that pile-up at the edge of scratches is a highly significant factor in determining wear rate in abrasion and cutting forces in grinding.

Finally a wide range of techniques for examining abrasives has been studied, the most notable of which involved the use of a scanning electron microscope.

Acknowledgements.

This work was carried out under the supervision of Dr. J.F. Archard whom I would like to thank for his helpful guidance and generous encouragement.

I am grateful to Mr. G. McTurk of the Department of Geology of the University of Leicester who carried out the scanning electron microscopy, made possible by the financial assistance given by A.A. Jones and Shipman Ltd., Leicester.

I am indebted to Mr. D.J. Whitehouse of Rank Taylor Hobson Ltd., Leicester for the use of a X 500 Talysurf attachment.

INDEX.

	page
Chapter 1. <u>INTRODUCTION.</u>	1
Chapter 2. <u>REVIEW OF SURFACE GRINDING AND ABRASIVE WEAR.</u>	
2.1 Introduction.	3
2.2 Surface grinding.	4
2.3 Abrasive wear.	17
2.4 Model experiments and scratch tests.	26
2.5 General conclusions.	37
Chapter 3. <u>ABRASIVE WEAR THEORY.</u>	
3.1 Introduction.	38
3.2 Predictions based on idealised indentors.	38
3.3 The application of abrasive wear theory to the grinding process.	46
3.4 Grinding force predictions.	53
3.5 Discussion and conclusions.	61
Chapter 4. <u>WEAR TESTS.</u>	
4.1 Introduction.	70
4.2 Apparatus.	70
4.3 Materials.	72
4.4 Preliminary experiments.	73
4.5 Wear rates.	77
Chapter 5. <u>GRINDING DYNAMOMETER AND ASSOCIATED TESTS.</u>	
5.1 Introduction.	85
5.2 Apparatus.	85
5.3 Materials.	87
5.4 Experimental procedure.	87
5.5 Results.	89

5.6 Discussion.	page 96
5.7 Conclusions.	97
Chapter 6. <u>SCRATCH TESTS WITH ROCKWELL AND VICKERS INDENTORS.</u>	
6.1 Introduction.	98
6.2 Apparatus and materials.	99
6.3 Experimental procedure.	100
6.4 Results of single scratches.	101
6.5 Microscopic observations of single scratches.	104
6.6 Repeated scratches.	106
6.7 Coefficients of friction.	107
6.8 Theoretical analysis of scratch geometry.	107
6.9 Discussion.	111
6.10 Conclusions.	114
Chapter 7. <u>EXPERIMENTS WITH ABRASIVES.</u>	
7.1 Introduction.	115
7.2 Apparatus.	115
7.3 Materials.	116
7.4 Preliminary scratch tests with single abrasive grits.	116
7.5 Effects of material hardness on the cutting process.	117
7.6 Scratch tests with grinding wheels.	119
7.7 Positive rake grits.	120
7.8 Scratch tests on ground surfaces.	121
7.9 Examination of abrasives.	122
7.10 Discussion.	126
7.11 Conclusions.	128
Chapter 8. <u>GENERAL CONCLUSIONS.</u>	129
<u>BIBLIOGRAPHY.</u>	136

1. Introduction.

Grinding wheels and abrasive papers although manufactured from similar materials exhibit certain structural differences. A grinding wheel is made up of abrasive particles held together by a bonding material, the proportion of which provides a method of controlling the hardness (grade) of the wheel. The wheel also contains voids; the amount of void (structure) can be regulated providing another method of adjusting performance.

Abrasive papers consist of abrasive particles glued onto a backing material. This type of construction limits the amount of abrasive which is available and is more susceptible to clogging than an abrasive wheel.

Despite differences in construction the ultimate performance of both a grinding wheel and abrasive paper depend on the abrasive grits from which they have been manufactured. These grits are randomly shaped and have been formed from the breakdown of larger pieces of abrasive. The surface of both wheels and papers are therefore made up of a large number of randomly orientated grits.

Grinding is a widely used commercial process and most of the work reported in the literature has been carried out under conditions similar to those encountered in practice. The bulk of results involved hard materials $\sim p_m = 800 \text{Kg/mm}^2$, coarse abrasives ~ 60 grit, high surface speeds $\sim 5,000$ ft/min. each portion of the grinding wheels surface being used repeatedly.

Abrasive wear studies, on the other hand, have been mainly concerned with elucidating the basic mechanism of the process. Most investigations have involved relatively soft materials, frequently pure metals, fine abrasives ~ 200 grit, slow speeds ~ 200 ft/min. and in many cases each portion of the abrasive paper was only used once.

The purpose of the present work was to study the broad pattern of behaviour of solid abrasives over a wide range of conditions and to see if a connection could be established between grinding and abrasive wear.

2. Review of Surface Grinding and Abrasive Wear

2.1 Introduction

Grinding is a specialised and expensive process which is used, for hardened steel components in particular, to obtain good surface finish and accurate control of dimensions. Many of the problems associated with grinding processes, such as high flash temperature, oxidation, the mechanism of chip formation and metallurgical changes are also important in abrasive wear.

The purpose of this review is to explore to what extent grinding and abrasive wear processes are related. Admittedly both processes use the same abrasive materials but the methods of constructing grinding wheels and abrasive papers differ considerably. Similarly the conditions under which each is subsequently used are not the same.

Theoretical treatments of both grinding and abrasion, discussed later, have considered them to be cutting rather than wearing processes. Cutting processes in this context are those processes where each contact between work and tool, be the tool a cutter or an abrasive grain, produces a chip. On the other hand a wear process involves contact between asperities but generally only a small proportion of these contacts produces a wear product.

Another significant difference between cutting and wear processes is the effect of lubricants. With cutting processes lubricants help to stabilise conditions and

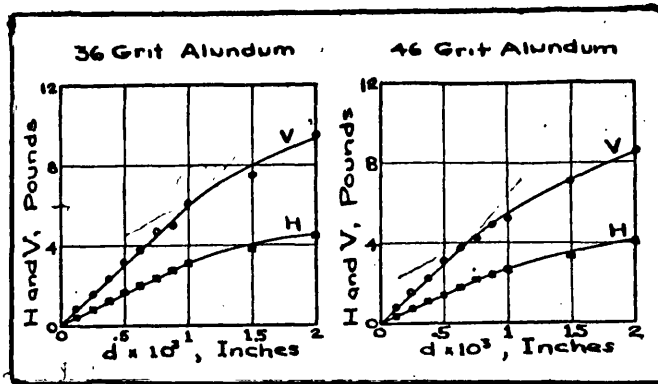


Fig 2.1 Variation of Grinding Forces With
Depth of Cut, d . (Marshall and Shaw 1952).

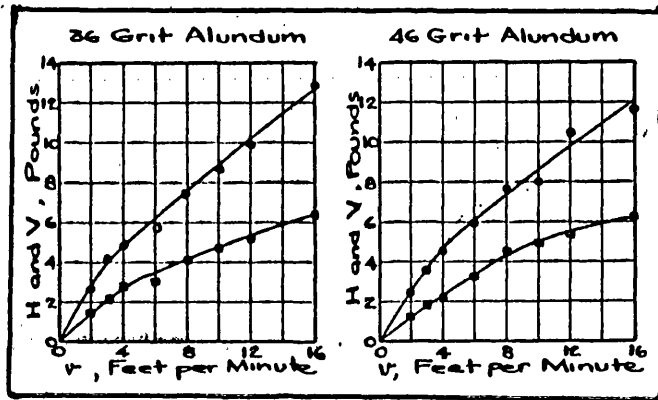


Fig 2.2 Variation of Grinding Forces With
Table Speed, v . (Marshall and Shaw 1952).

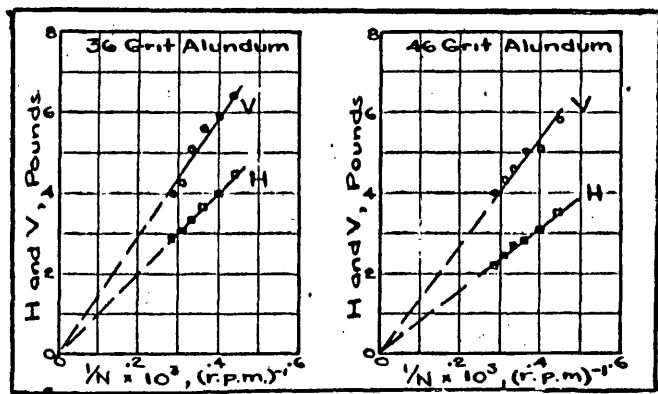


Fig 2.3 Variations of Grinding Forces With Inverse
Wheel Speed, N^{-1} . (Marshall and Shaw 1952).

4

improve the efficiency of the abrasive by preventing clogging. In a wear process, involving for example the rubbing together of two metal specimens, a suitable lubricant will drastically reduce the rate of wear.

2.2 Surface Grinding

2.2.1 Force Measurements

The first reported force measurements for surface grinding are due to Marshall and Shaw (1952). They designed a dynamometer which measured both tangential and normal forces and they took measurements over a considerable range of conditions. Their dynamometer could only be used at relatively slow work speeds; most of their results were obtained at table speeds of 4fpm, the maximum possible table speed being 16fpm, and their work was confined to dry grinding. These restrictions all served to increase the severity of the tests and make satisfactory operation more difficult. Despite these very obvious departures from normal grinding practice their results are of considerable interest. They showed that the vertical and horizontal grinding forces were proportional to the inverse of wheel speed and the width of workpiece fig(2.1); that the vertical and horizontal forces increase with table speed fig (2.2) and that vertical and horizontal forces are proportional to the depth of cut for depths below about 0.001 in. fig(2.3).

TABLE 2.1

Material	Al ₂ O ₃ 36	Al ₂ O ₃ 46	Al ₂ O ₃ 60	SiC 36
Mean grinding coefficient	0.57	0.52	0.52	0.47
Mean coefficient of friction	0.47	0.43	0.42	0.45

As a result of their experiments they postulated a 'grinding coefficient' which in formulation resembles the coefficient of friction, being defined as the ratio of the tangential to normal force. Indeed the value of the 'grinding coefficient' when the grinding wheel is cutting freely is only slightly greater than the coefficient of friction. Typical values are shown in Table 2.1.

The 'actual coefficient of friction' was measured by clamping the wheel and dragging it across the surface of the specimen; normal and tangential forces were recorded using the grinding dynamometer. It is questionable whether such conditions are any different from those which occur during grinding; scratch tests reported later have shown that in the situation already described the wheel will remove metal from the test piece. Since the conditions are now identical to those encountered in grinding, it is not surprising that similar values are observed for the 'grinding coefficient' and mean coefficient of friction. More significant than the actual value of the grinding coefficient is the very marked difference in its value and for that observed for other cutting processes such as turning where the ratio of:-

$$\frac{\text{tangential force}}{\text{normal force}} = 2 \quad (2.1)$$

The same ratio for grinding is about 0.5.

TABLE 2.2

<u>Process</u>	<u>Specific Energy</u>
Grinding	$10 - 25 \times 10^6 \text{ in}\cdot\text{lb}/\text{in}^3$
Single Point Cutting	$0.5 \times 10^6 \text{ in}\cdot\text{lb}/\text{in}^3$

Another major difference which they observed between grinding and other chip forming processes was the specific energy which in grinding is given by:-

$$u = \frac{\pi D N H}{12 v b d} \quad (2.2)$$

where u = energy expended per unit volume removed
(in lb/in³)

D = wheel diameter (in)

H = tangential force in (lb)

N = wheel speed (rpm)

v = table speed (ft/min)

b = specimen width (in)

d = wheel depth of cut (in)

The specific energy for grinding is very much greater than that for other chip forming processes; typical values are given in table 2.2.

Marshall and Shaw also observed that the grinding force components and the specific energy were independent of the hardness of the workpiece, a singularly unexpected result which any adequate theory must be able to explain.

This review of earlier work shows that both force coefficients and specific energies for grinding and single point cutting differ. The most obvious interpretation of these facts is to suggest that the basic mechanism of metal removal in the two processes differs. Backer et al (1952)

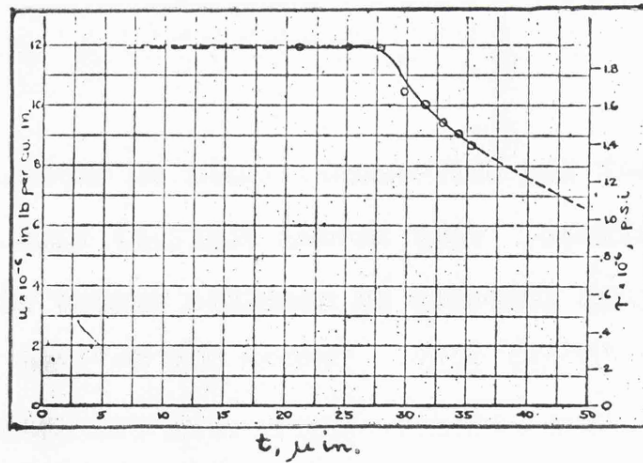


Fig 2.4 Specific Energy-Depth of Cut Curve for Grinding Tests. (Backer, Marshall and Shaw 1952).

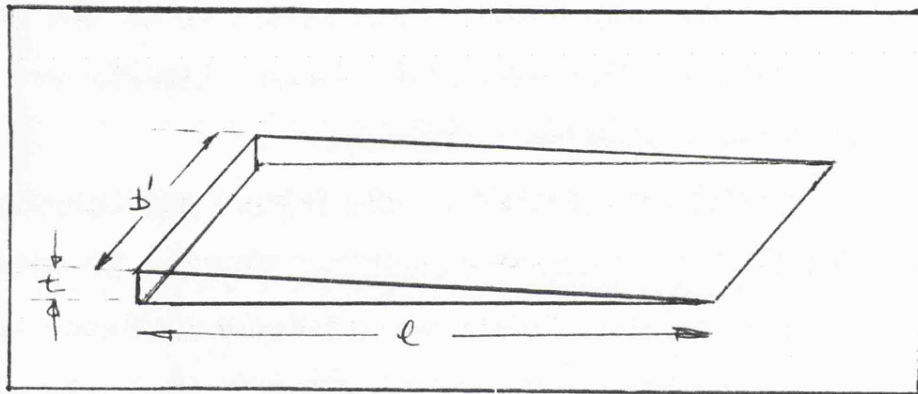


Fig 2.5 Chip Detail.

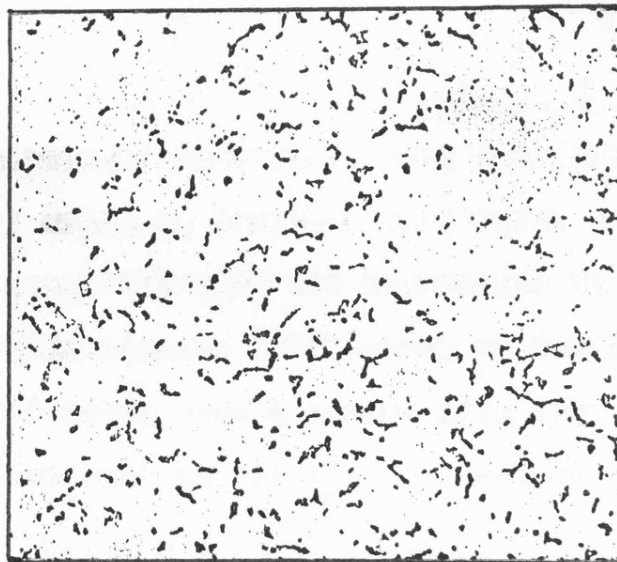


Fig 2.6 Carbon-Black Replica Showing Distribution of Grits in Surface of a Diamond-Dressed Grinding Wheel (32A46 - H8 - VBE) X5. (Backer et al 1952).

claim that the differences could be explained largely as a size effect. They showed fig(2,4) that there is a significant increase in specific energy with decrease in specimen (chip) size. Indeed the deduced shear strength involved when grinding under mild conditions roughly corresponds to the theoretical strength which is about 1.8×10^6 psi. for steel. They finally concluded that the smallness of chip size was apparently the most important distinguishing characteristic of the grinding operation, and the relatively large specific energy and shear stress important effects.

However, in grinding the forces are largely independent of workpiece hardness whereas in single point cutting the forces are strongly hardness dependent. Thus the balance of evidence suggests that grinding and single point cutting involve different methods of metal removal.

2.22 Chip Thickness

The earliest paper published concerning the size of grinding chips is attributed to Alden (1914). He developed an expression for chip thickness in cylindrical grinding based on geometrical relationships assuming that each grit will remove a chip whose dimensions are simple geometrical projections of the wheel and workpiece.

When expressed in surface grinding terms Alden's equation becomes:

$$x = \frac{2v}{Vn} \sqrt{\frac{d}{D}} \quad (2.3)$$

where n = the number of grits per unit length at the periphery cutting in the same groove
 v = work velocity (sfpm)
 V = wheel velocity (sfpm)
 d = wheel depth of cut (in)
 D = wheel diameter (in)

The quantity n is difficult to determine by direct measurement and consequently its value must be established from secondary variables.

More recently Backer, Shaw and Marshall (1952) developed the following expression for the grit depth of cut:

$$t = \left[\frac{48v}{\pi D N C r} \sqrt{\frac{d}{D}} \right]^{\frac{1}{2}} = \left[\frac{4v}{V C r} \sqrt{\frac{d}{D}} \right]^{\frac{1}{2}} \quad (2.4)$$

where t = grit depth of cut (in)
 v = work speed (sfpm)
 d = wheel depth of cut (in)
 D = wheel diameter (in)
 N = wheel speed (rpm)

- C = number of cutting points per square
inch of wheel surface
- r = ratio of width to depth of scratch
generated by a grit
- V = wheel velocity (sfpm)

It can be shown that equation 2.4 is simply a development of Alden's equation (2.3) for the grit depth of cut. Backer et al claim, as a result of microscopic examination of the grinding chips, that they are of constant width throughout their length and that as the conditions under which they are formed are similar to micro-milling, they will be wedge shape in character (fig 2.5).

The quantity n in Alden's equation (2.3) is then given by:

$$n = \frac{\pi D b' C}{\pi D} = b' C \quad (2.5)$$

but $b' = \frac{t r}{2}$ (2.6)

combining equations (2.5) and (2.6)

$$n = \frac{t r C}{2} \quad (2.7)$$

substituting for n in equation (2.3) gives

$$t = \frac{2 v}{V C r t/2} \sqrt{\frac{d}{D}} \quad (2.8)$$

which on rearranging is as before

$$t = \left[\frac{L v}{V C r} \sqrt{\frac{d}{D}} \right]^{\frac{1}{2}} \quad (2.4)$$

All the quantities in the Backer et al expression can be determined. The value of C is conveniently determined by making a wheel track on a glass plate covered with a uniform layer of carbon black about 0.0001 in. thick. The soot covered plate may be used as a photographic negative to make enlarged prints of the wheel track from which the value of C can be determined by counting the number of marks/in² fig (2.6). With a 46 grit wheel of structure 8, the number of contact points per square inch was found to be 1930, which gives a mean grit depth of cut of about 60μ in. for a wheel depth of cut of 0.001 in.

The width/depth ratio r may be determined from a taper section of a representative ground surface. The value of r was found to lie between 5 and 20, 15 being a good average for fine grinding.

Hahn (1955) has pointed out that in single-point theory the assumption is usually made that the tool forces arise from the chip bearing on the rake surface of the tool and that the clearance surface is free of rubbing forces. This assumption falls down however when very shallow cuts

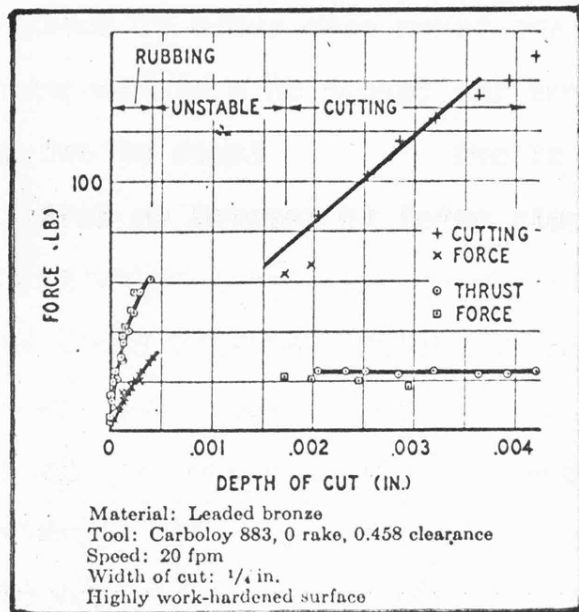


Fig 2.7 Force-Depth of Cut Relation for a Tool of Small Clearance Penetrating the Unstable "Transitional" Region. (Hahn 1956).

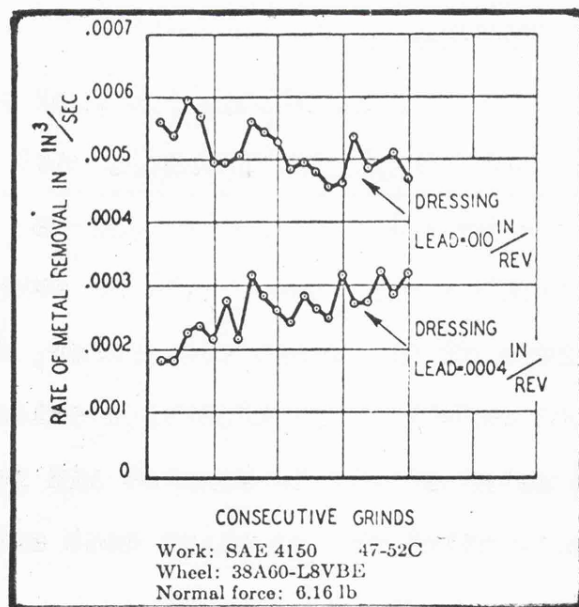


Fig 2.8 Progressive Changes in Cutting Ability of Grinding Wheel Surface. (Hahn 1956).

(0.0004 in.) are taken with tools of small clearance.

Fig (2.7) shows the forces on a single-point tool at very small depths of cut. Below a depth of cut of 0.0004 in. there is no chip, metal is removed as dust. All the forces on the tool act on the clearance surface. Furthermore, in this region the thrust (normal) force is about twice the (tangential) cutting force. Consequently, the assumption that the rubbing forces on the clearance surface in grinding are negligible appears to be very unrealistic and on the contrary, because of the relative magnitude of normal force to tangential force and the independence of work hardness, a more realistic assumption appears to be that the rubbing forces on the clearance surface of the grain are dominant and the rake surface of the grain are minor.

Moreover, it will be recognised that no formal clearance is provided on the grain so that interference must occur as a result of elastic effects.

A situation in which there are no cutting forces on the rake surface of the grain will occur, if one tries to grind tungsten carbide with aluminium-oxide wheels. In this case no metal at all is removed and yet there are normal and tangential forces which must originate entirely on the clearance surface.

2.23 The Rubbing-Grain Hypothesis

The observations quoted above lead Hahn (1956) to formulate his rubbing-grain hypothesis. Hitherto, most investigators have considered the grinding process to be essentially like a milling process, but on a microscopic scale. Generally, they have considered the forces, normal and tangential to the wheel surface, to arise from the chips acting against the rake surface of the grit and have neglected any frictional rubbing forces on the clearance surface of the grit.

Hahn suggests that there is considerable evidence which indicates that in the grinding process it may be more realistic to consider the frictional rubbing forces on the clearance surface and neglect the cutting forces on the rake surface.

In metal cutting with single-point tools where the chip forces predominate, the tangential force is generally about twice the normal force. If such tools were simply reduced to microscopic size and the forces for a number of them added together, there would be no reason for the ratio of the total force to be any different from that for any one tool. Consequently, if the rake surface forces are predominant one should find the ratio of tangential force (cutting) to normal force (thrust) to be the same as in single-point machining, namely, about two. In grinding the reverse is true; the

ratio is about $\frac{1}{2}$, and consequently, more nearly resembles the sliding-friction process where the ratio is about $\frac{1}{4}$.

Even with single point-cutting the ratio of cutting to normal force is about a $\frac{1}{2}$ not 2 when very shallow cuts are taken.

Further argument in support of the rubbing-grain hypothesis is obtained when abrasive wheels are dressed by a diamond. The diamond has been observed to actually cut through the grain. It is known that the lead of the diamond during dressing greatly influences the cutting action of a wheel. Clearly the dressing action is such as to provide zero clearance on the grain. The comparison between a slowly dressed and a rapidly dressed wheel is shown in fig (2.8). This data was derived from tests where the wheel was pressed against the workpiece with a prescribed force and the rate of stock removal measured. For the wheel dressed at 0.0004 in/rev diamond lead, the rate of stock removal for the freshly dressed wheel is 0.00018 cu in/sec corresponding to the first point on the lower curve. Subsequent grinding actually caused the wheel to sharpen as shown. The rate of stock removal for a freshly dressed wheel with diamond lead of 0.010 in/rev is 0.00056 cu in/sec, or three times that for the slowly dressed wheel. It is clear therefore that the clearance surfaces of the grits play an important role in the grinding process.

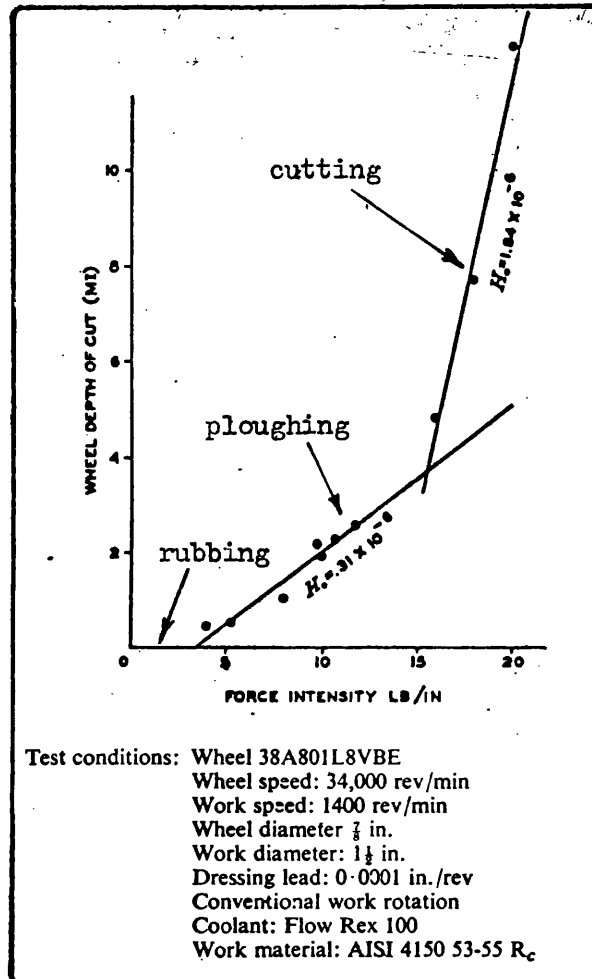


Fig 2.9 Wheel depth of cut versus force intensity.
 (Hahn 1962).

As a result of his controlled force grinding experiments Hahn (1962) suggested two methods of metal removal; namely a ploughing process where the abrasive grain plastically ploughs a groove and throws up alongside small particles of highly distorted metal, and secondly, a cutting process where a true chip is formed ahead of the grain. He also suggested that some grains may simply rub without removing any material whatsoever. The plough-cutting transition and the plough-rubbing transition are shown in fig (2.9).

Grisbrook (1960) observed that the force pattern on a grinding wheel changed progressively during a run and could be divided into four regions fig (2.10).

(i) An unstable region where the forces rise to peak and then fall to a steady value as the dulling effect, produced by wheel truing, wears off;

(ii) a region of stable grinding conditions where forces and speeds are constant and heat is in equilibrium;

(iii) in this region there is a progressive build-up of forces and power reflecting the reactions of the wheel to the particular combination of work speed, depth of cut and work material. Wheel grits become dull, overheating may develop and grinding becomes progressively less efficient;

(iv) the rate of increase of the forces becomes less; there is evidence of vibration and as this develops the magnitude of the forces commence to fall, as

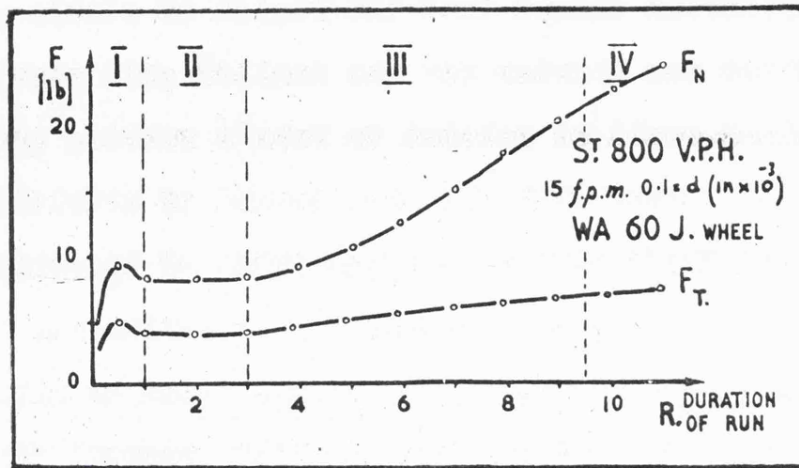


Fig 2.10 Pattern of forces in grinding. (Grisbrook 1960).

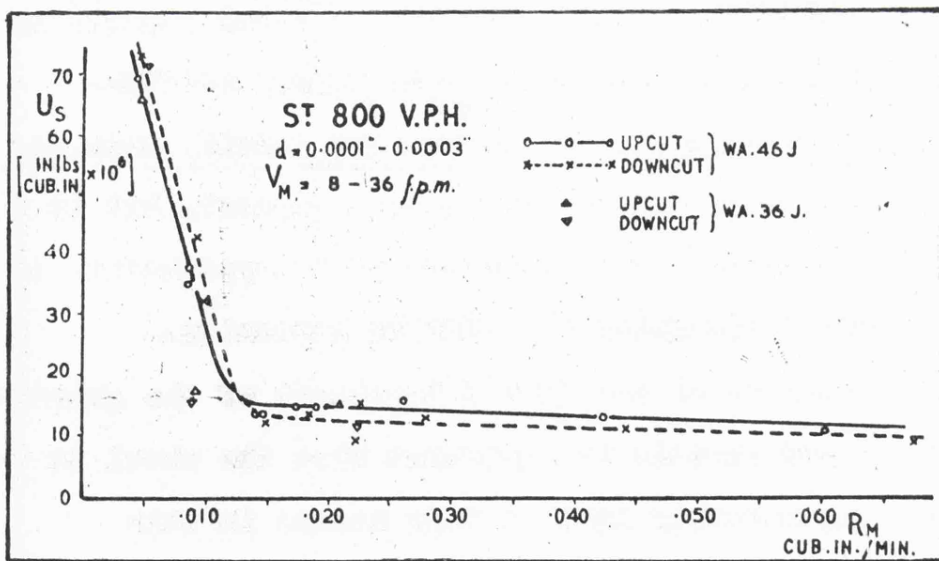


Fig 2.11 Specific energy - rate of metal removal upcut and downcut. (Grisbrook 1960).

observed by Landberg (1956).

Grisbrook showed that the region of stable grinding conditions was shorter for the smaller grit size, which he claimed could be related to Hahn's rubbing grain hypothesis since with the same amount of attrition on each grit there will be a higher rate of increase of area with the higher concentration of grits and therefore an increase in the rate of glazing. Also by plotting specific energy against rate of metal removal fig (2.11) further support for the rubbing grain hypothesis was obtained. As the rate of metal removal falls a critical condition (of critical chip thickness and degree of dullness of grit) will arise where the mechanism of grinding changes from one predominantly of cutting to one of abrasion. For conditions of metal removal above this critical value, there is an almost constant specific energy. Grisbrook did not clarify what was meant by the term abrasion in this context, but in view of his reference to the rubbing grain hypothesis, he envisaged a ploughing and rubbing mechanism.

Backer et al and Hahn's treatment of the grinding process are largely in agreement when the wheel is operating normally in that they assume in this situation metal is being removed as chips essentially by a cutting mechanism. It is only at very low rates of metal removal that their ideas diverge. The basic concept of grit depth of cut relies heavily on the

assumption that each 'active grit' removes a chip and that the chips formed have the precise geometry outlined earlier. Backer et al suggested that the high constant value of specific energy observed below a certain critical value of grit depth of cut was due to the material reaching its theoretical strength rather than a basic change in the mechanism of metal removal. Admittedly Hahn was studying a different type of grinding process, namely constant force grinding, but he attributed the changes of slope in the metal removal rate - normal force diagram to a change in the basic cutting mechanism (cutting-ploughing-rubbing).

It is concluded that the exact situation operating at the boundaries of the grinding process are in doubt but that when the process is operating satisfactorily metal is being removed by a cutting mechanism in the form of chips. In view of its critical importance in grinding theory it is rather surprising that little evidence is available in support of the assumption that each grit removes a chip; a notable exception is that due to Grisbrook (1962) discussed later.

2.3 ABRASIVE WEAR

2.31 Introduction

In abrasive processes it is assumed that the abrasive surface is harder than the material being abraded. The action of abrading a material produces grooves in its surface the contents of which ultimately become the wear product.

Quantitative expressions for abrasive wear have been developed by considering the abrasive particles to have simple geometrical shapes; the resulting expressions are of the general form

$V/L = KW/p_m$ where V is the volume loss, L the sliding distance, W the normal load and p_m the flow pressure of the material.

Although the exact value of the constant term K varies with particle geometry, abrasive wear theory predicts the wear volume to be inversely proportional to the hardness of the material being abraded and directly proportional to sliding distance and applied load.

2.32 Experimental observations of abrasive wear

Abrasive papers

The relationship between hardness and resistance to wear by abrasion when rubbed against emery paper has been studied for a wide range of metallic materials by Kruschov

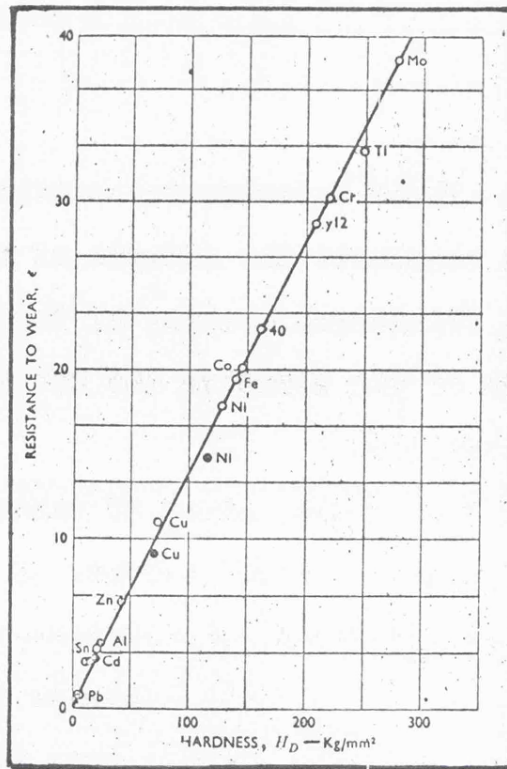
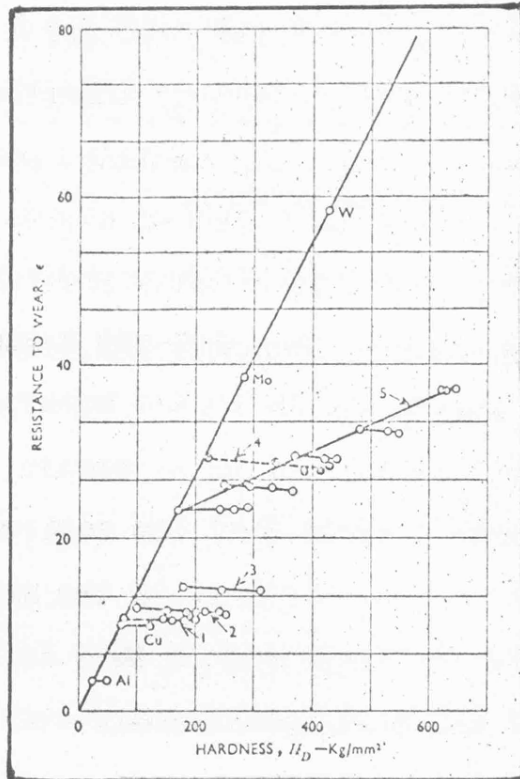


Fig 2.12 ϵ - H graph for Commercially Pure Metals.
(Kruschov and Babichev 1957).



- Materials. (1) Brass.
(2) Aluminium Bronze.
(3) Beryllium Bronze.
(4) Austenitic Stainless Steel.
(5) 0.4% Carbon Steel.

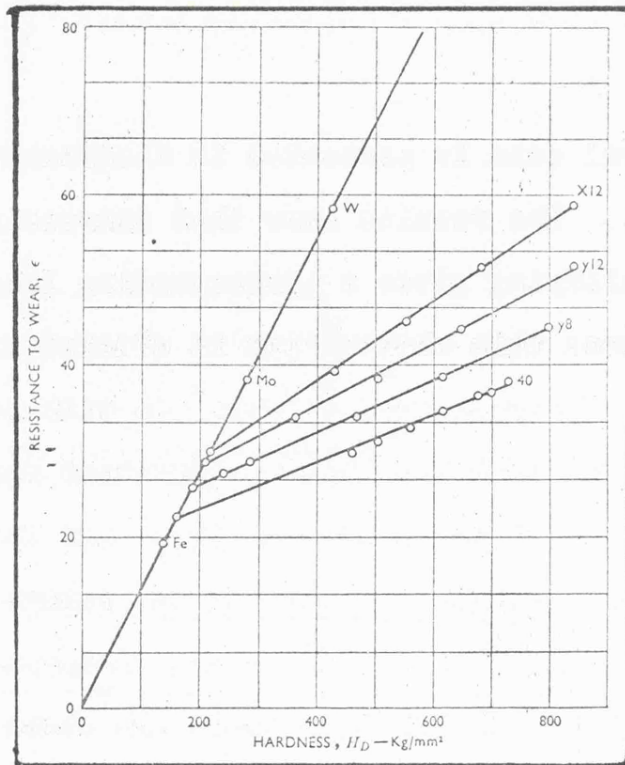
Fig 2.13 ϵ - H graph for Cold-worked Materials.
(Kruschov and Babichev 1957).

and Babichev (1957). Their experimental conditions were chosen so as to eliminate the effects of such factors as speed of sliding, frictional heating of the specimen, insufficient hardness of the abrasive and deterioration of the abrasive in service.

They found that for a large range of annealed pure metals the wear resistance ξ (the inverse of the abrasive wear rate) was directly proportional to hardness (fig 2.12), as would be predicted by abrasive wear theory. However, the situation was more complex when cold worked materials and heat-treated steels were tested.

The first unexpected result was that for a wide range of materials wear resistance is largely independent of the amount of cold working to which the material has been subjected (fig 2.13); since cold working increases hardness abrasive wear theory predicts a corresponding increase in wear resistance. Kruschov and Babichev suggested that this apparently anomalous behaviour was due to the intense work hardening which occurs during the abrasive process. They claimed that the resistance to abrasive wear depends on the hardness of the material in its maximum work hardened state and as this is attained during the course of the test, preliminary work hardening will have no effect.

The most interesting aspect of Kruschov and Babichev's work was that carried out on steels. A set of typical results for plain carbon steel are shown in fig.(2.14).



Materials:- 40 Carbon Steel 0.41%C.
 Y8 Carbon Steel 0.83%C.
 Y12 Carbon Steel 1.10%C.
 X12 Chromium Steel 2.35%C 11.9%Cr.

Fig 2.14 ϵ - H graph for Heat-treated Steels.
 (Kruschov and Babichev 1957).

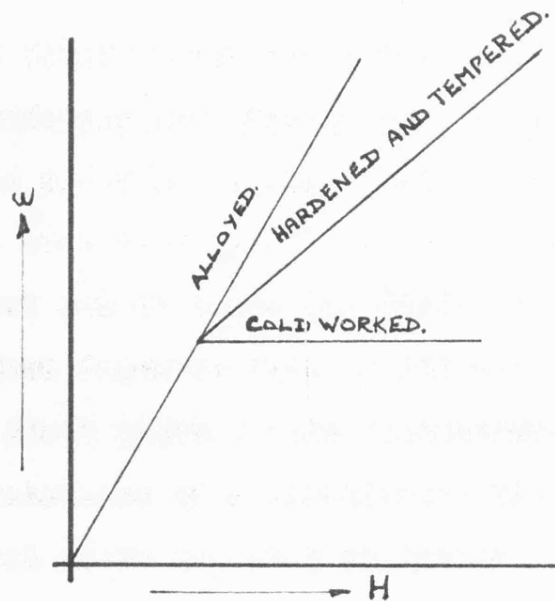


Fig 2.15 Sketch of ϵ - H graph showing the way
 in which plain carbon steels behave.
 (Kruschov and Babichev 1960).

and the general case is presented in diagrammatic form in (fig 2.15). The results show that increasing hardness by alloying gives a corresponding increase in wear resistance; this observation is consistent with abrasive wear theory. Cold working, as with pure metals, has no effect on wear resistance. Hardened and tempered steels exhibit anomalous behaviour; the wear rates for these materials falls off the linear relation between wear resistance and hardness. Compared with other materials, heat-treated steels are shown to wear more readily than would be expected from their hardness; this anomalous behaviour is perhaps related to the generally accepted fact that the forces produced when grinding hardened steels are substantially the same as those produced by soft steels.

More recently Nathan and Jones (1967) have reported on the influence of the hardness of the abrasive on the abrasive wear of a wide range of metallic materials of varying hardness. The abrasives used were carborundum, corundum, garnet, flint and glass in the form of abrasive belts and the experiments were arranged such that the specimen was continually encountering fresh abrasive. As a result of their experiments they concluded that each abrasive has an effective hardness which defines the maximum hardness of the material which it can abrade. When Nathan and Jones's results are replotted in the form of $\frac{1}{V}$ (wear resistance) against hardness (fig 2.16) instead

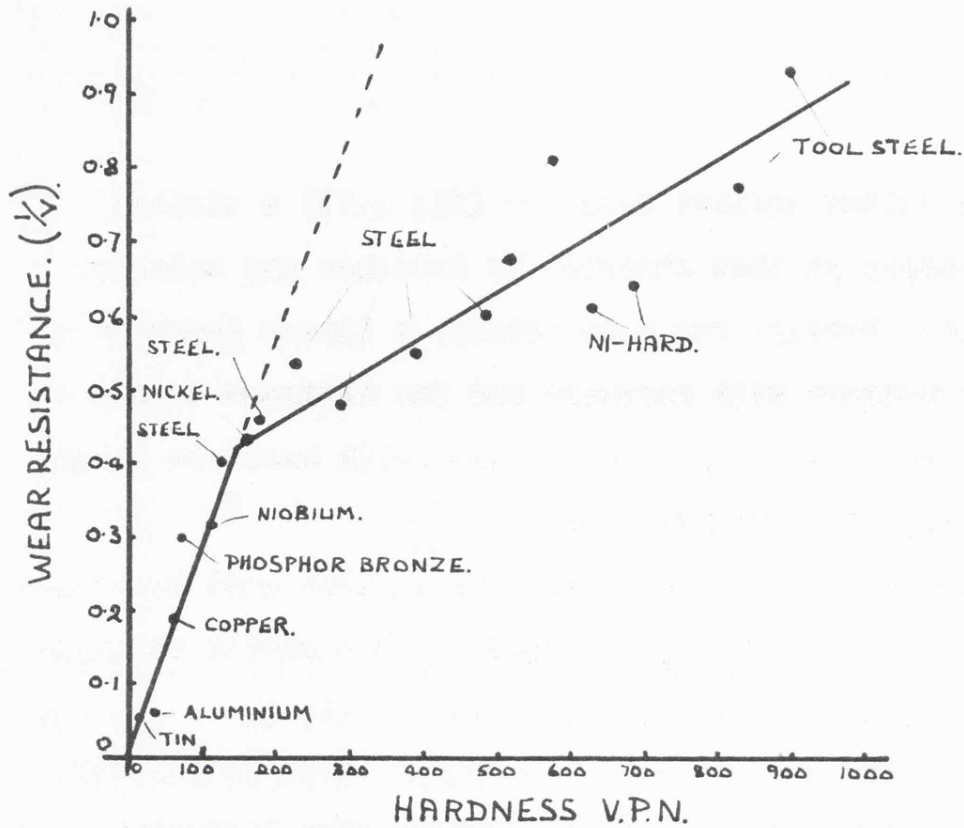


Fig 2.16 Relationship between wear resistance($1/V$) and hardness of metals for the abrasive carborundum.

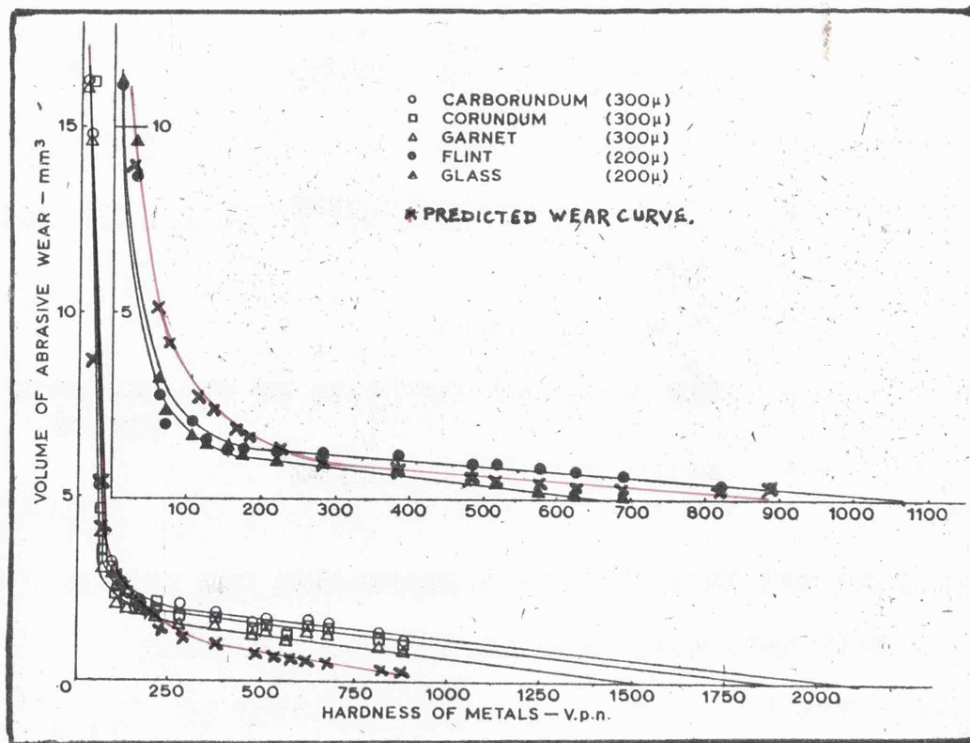


Fig 2.17 Relationship between the volume of abrasive wear and the hardness of metals for the abrasives carborundum, corundum, garnet, flint, and glass corresponding to 300-μ particle size at a load of 1 Kg, abrasive path 6 m, and velocity 0.5m/s. (Nathan and Jones 1967).

of wear volume against hardness (fig 2.17) a similar relationship to that observed by Kruschov and Babichev is obtained. Namely, for pure metals, a linear increase in wear resistance with hardness but for hardened steels a rate of increase in wear resistance with hardness which falls below the original line.

Unfortunately, the hardest pure metal used by Nathan and Jones was nickel p_m 157 Kg/mm². The harder materials were Ni-hard cast iron and hardened steel; the deviation of the later from the behaviour which would be expected from abrasive wear theory has already been discussed.

Nathan and Jones proposed an empirical relationship for the wear volume in abrasion in the following form:-

$$V = \frac{1}{2.5} W L \log_{10} \frac{H_a}{H_m} \text{ mm}^3/\text{Kg} \quad (2.9)$$

V = volume of abrasive wear

W = load in Kg

L = sliding distance

H_a = the effective hardness of the abrasive
Kg/mm²

H_m = material hardness Kg/mm²

They pointed out that the above expression was unreliable for very soft materials such as tin and aluminium (hardness less than 50Kg/mm²). The validity of the formula therefore relies heavily on the results for hardened and tempered steels whose behaviour is known to

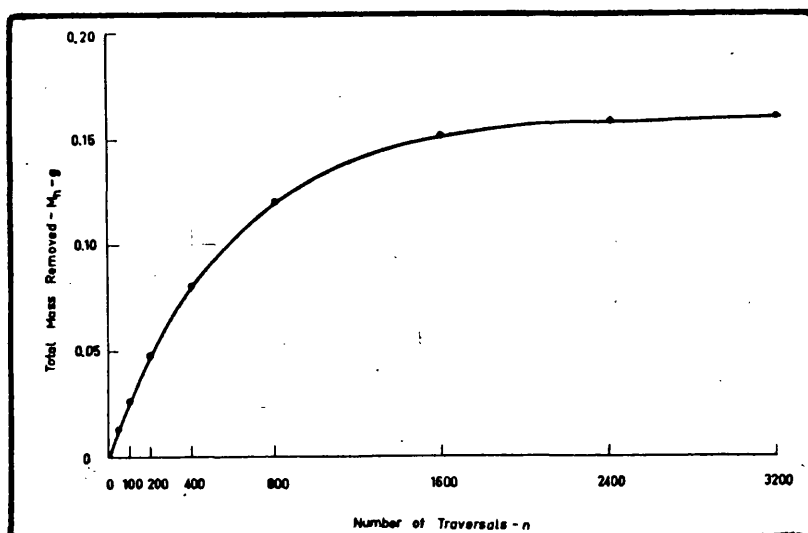


Fig 2.18 Variation in total mass removed from the specimen with number of specimen traverses on the same track. Steel abraded on 220-grade silicon carbide abrasive paper. (Mulhearn and Samuels 1962).

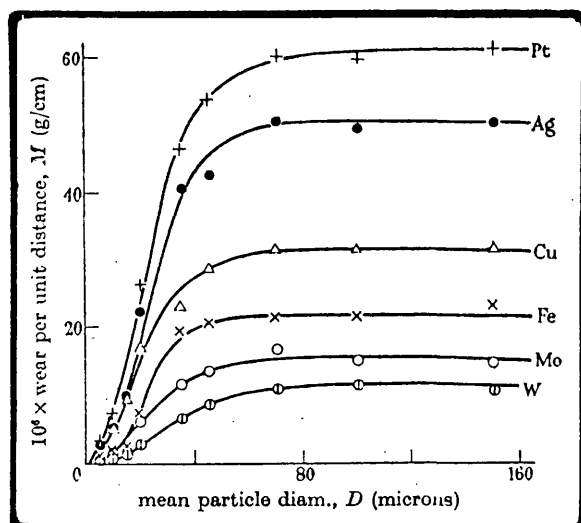


Fig 2.19 Variation of M with D for various metals at the equilibrium stage of pick-up of abrasive, on dry emery papers at 1 Kg load. (Goddard and Wilman 1962).

be unusual. The fact that the results for the harder materials fit may therefore be purely fortuitous. The function $\log_{10} \frac{H_a}{H_m}$ varies with the hardness of the work material but it may well be that the mechanism of metal removal may vary in a similar manner with the hardness of the workpiece, particularly in view of the fact that most of the harder materials were the same, namely steels.

In the work just described the effects of clogging and blunting of the abrasive were largely eliminated as the metal specimens were constantly encountering fresh abrasive. The results are not therefore directly applicable to the more practical situation where the work is traversed repeatedly over the surface of the abrasive.

Mulhearn and Samuels (1962) carried out abrasive wear tests where the surface of the abrasive was used repeatedly; they used silicon carbide papers, the work material being fully cold worked mild steel. Their results showed that the rate of abrasion gradually fell with increase in sliding distance (fig 2.18), a finding which is not altogether unexpected as one would anticipate that the abrasive would be gradually used up during the course of a test. The efficiency of the paper will also be reduced as a result of clogging by wear debris. Mulhearn and Samuels found that the abrasive action stopped earlier with fine than with course papers which supports the suggestion of a clogging mechanism. It must also be

remembered that the quantity of abrasive material on the surface of the paper will be less with finer grades.

As a result of their experimental work Mulhearn and Samuels developed an expression for the mass loss M_n of the form

$$M_n = M(1 - e^{-\beta n}) \quad (2.10)$$

where n = number of revolutions (sliding distance)
 M_n = mass loss after n revolutions
 M = mass loss after an infinite number of revolutions
 β = a constant

They showed that this expression was in good agreement with their practical observations. It is of interest to note that with abrasive papers there is a definite limit to the quantity of material which can be removed as the abrasive eventually is completely used up. With the grinding process, on the other hand, there should be no change in the rate of metal removal provided the wheel is self sharpening. The experimental results obtained under these conditions will be the same as those produced in wear tests when the specimen is continually encountering fresh abrasive paper. If conditions are such that the wheel glazes however the abrasive grits will become blunted and the rate of metal removal will

fall progressively, a condition similar to that observed by Mulhearn and Samuels.

2.33 Particle Size

Although abrasive wear theory takes account of and is sensitive to the geometry of the abrasive grits, their actual size is not considered. It would be expected therefore that the wear rate should be largely insensitive to changes in particle size.

Many investigators have found that when the material-abrasive combination is fixed and only the particle size of the abrasive varied there is a certain critical particle size which determines the exact nature of the wear process. Above the critical value the wear rate is independent of particle size but below the critical value the wear rate is very dependent on particle size. A typical set of results due to Goddard and Wilman (1962) are shown in (fig 2.19).

The experimental observations can be explained in two ways; either the value of θ in the wear equation 3.30 depends critically on particle size for fine abrasives but for coarse particles is independent of particle size or the finer grades of abrasive may be more readily clogged by wear debris. A refinement of the second mechanism has been postulated by Rabinowicz (1965) who suggests that it is not so much the clogging of the abrasive which occurs, but the formation of large particles

which prevent the abrasive contacting the work surface.

Grinding forces have been shown to be unaffected by variations in grit size; it should be remembered however that grinding usually involves the use of fairly coarse abrasives well above the critical particle size reported for abrasive papers.

2.34 Groove Volume

It is generally accepted that the abrasive particles produce grooves in the surface being abraded, the volume of these grooves becoming the wear product. When wear predictions and experimental results were compared it soon became apparent that there were considerable discrepancies; several investigators (Stroud and Wilman (1962), Mulhearn and Samuels (1962), Goddard et al (1959)) have shown that the observed wear rate was well below that predicted often as much as by an order of magnitude. Obviously only a proportion of the groove volume displaced by the abrasive was appearing as a wear product. Mulhearn and Samuels (1962) suggested that only a proportion of the grits cut the material, the remainder merely plough a groove displacing but not removing material; thus if only 10% of the grits are cutting the wear rate observed will be one tenth of that predicted. An alternative explanation due to several workers (Stroud and Wilman (1962) and Goddard et al (1959)) is that only a proportion of the groove volume displaced by each grit

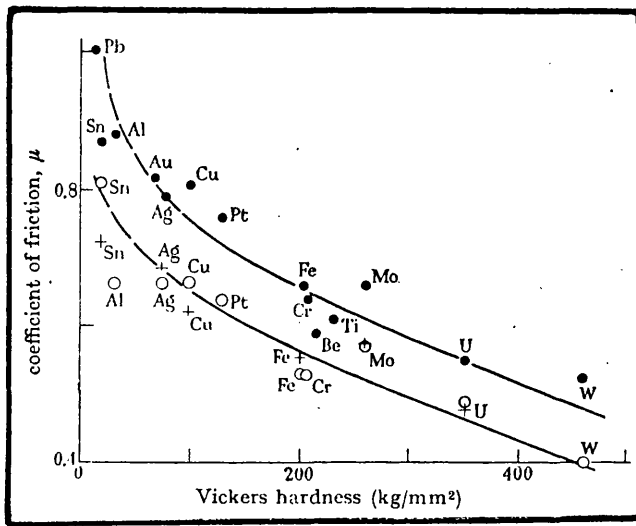


Fig 2.20 Variation of coefficient of friction with hardness for various metals.
(Goddard and Wilman 1962).

is removed, again if it is assumed that only 10% of the volume of each groove is removed the wear rate obtained experimentally will be one tenth of that predicted theoretically. In view of the importance of these concepts in abrasive wear theory they will be discussed in greater detail at a later stage.

2.35 Coefficient of Friction

Many investigations of abrasive wear have also included the measurement of the coefficient of friction. The main conclusions from such experiments with emery paper is that above a critical particle size the coefficient of friction is independent of particle size but below the critical particle size the coefficient of friction is related to particle dimensions. The coefficient of friction is also a function of the work material; in general the harder the work material the lower the coefficient of friction. A typical set of results due to Goddard and Wilman (1962) are shown in (fig 2.20).

2.4 Model Experiments and Scratch Tests

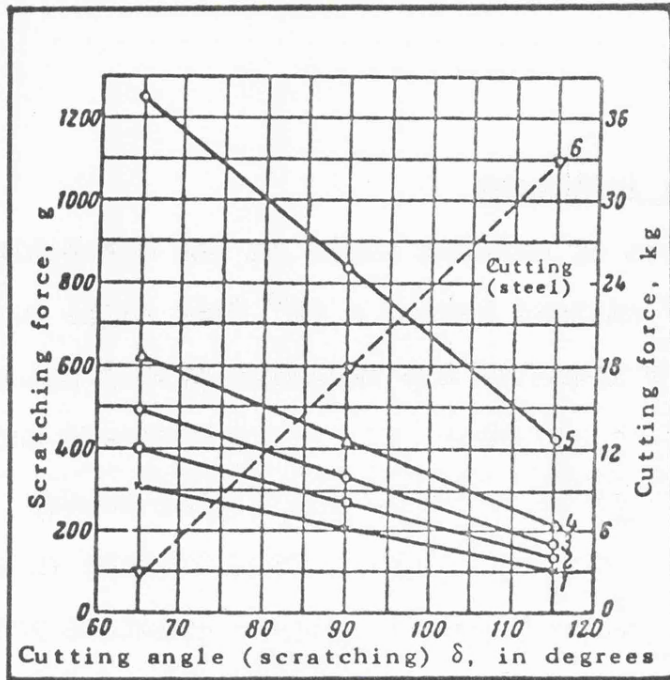
2.41 Introduction

Practical observations of the wear debris produced by a number of abrasive processes, covering a wide range of conditions, show the wear product to be chip-like in form, similar to that produced by single point cutting.

Theoretical treatments of abrasive wear have therefore assumed that material is removed essentially by a cutting mechanism involving a large number of randomly orientated tools of indeterminate geometry.

One of the most significant differences between cutting using abrasives and single point cutting is the rake angle of the cutting tool, thought to be negative for most abrasive grits and generally positive in single point cutting.

A number of workers have reported on scratch tests involving both idealised tools and single abrasive grits. The main object of such experiments has been to provide more information concerning the basic mechanism by which material is removed during abrasion. It should be emphasised however that the application of the findings of scratch tests involving idealised indentors, soft materials and slow speeds to a process such as grinding, where the cutting tool is an abrasive grit, the work material a hardened steel and the cutting speed $\sim 5000'$ /min, can only be made with extreme caution.



Scratching force: 1 - solder, $P = 0.1$ Kg.
 2 - lead, $P = 0.1$ Kg.
 3 - brass, $P = 0.1$ Kg.
 4 - stearin, $P = 0.1$ Kg.
 5 - brass, $P = 0.5$ Kg.

Cutting force: 6 - Steel 5, $t = 2$ mm, $s = 0.28$ mm/rev
 (data from Wul'f et al 1948).

Fig 2.21 Scratching and cutting forces against cutting angle for a series of metals.
 (Kruschov and Babichev 1960).

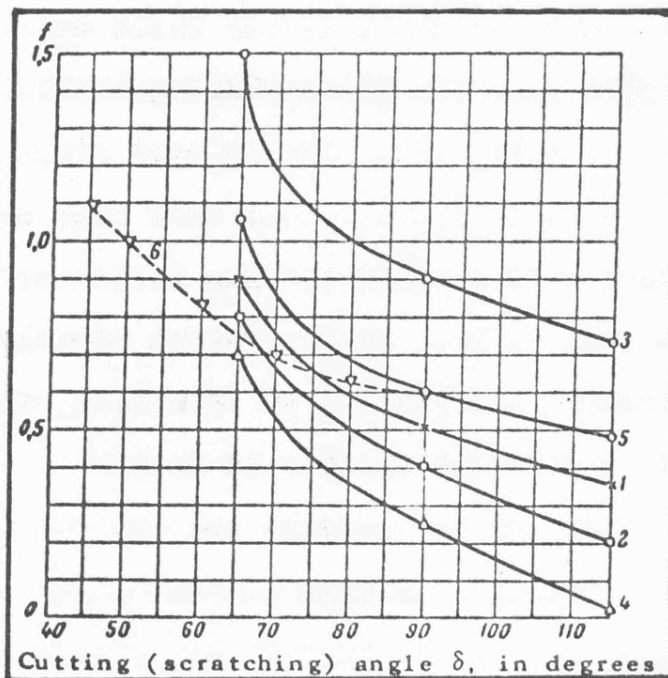


Fig 2.22 Coefficient of friction of facet during scratching and cutting against cutting angle δ (same conditions as fig 2.21).
 (Kruschov and Babichev 1960).

2.42 Idealised Indentors

The effects of cutting angle on the scratching performance of cutters having a 90° face angle has been studied by Kruschov and Babichev (1960) using tools of rake angle $+25$ zero and -25 . They measured scratch force for a number of metals ranging from solder $p_m 4.2\text{Kg/mm}^2$ to brass $p_m 102\text{Kg/mm}^2$ when cutters were tracked across their surfaces under a constant load. They reported that cutters with rake angles of $+25^\circ$ and zero produced a chip when scratched over a metal surface but the cutter with a negative rake angle caused the metal to separate in the form of soft crushed turnings. With solder the negative lead angle cutter ploughed a groove in the surface without producing a turning.

Force measurements (fig 2.21) showed that the tangential force depends on the material being scratched and it decreases with increase in scratching angle. Kruschov and Babichev also quote, on the same graph, results due to Wul'f et al (1948) which show that the cutting force during single point cutting increases with an increase in cutting angle. This apparent anomaly is due to the experimental conditions; in scratching the normal force is kept constant whereas in machining processes the depth of cut is constant and consequently the forces will vary. Obviously in both processes the cutting mechanism will be the same; for example the coefficient of friction of the facet during scratching and cutting against

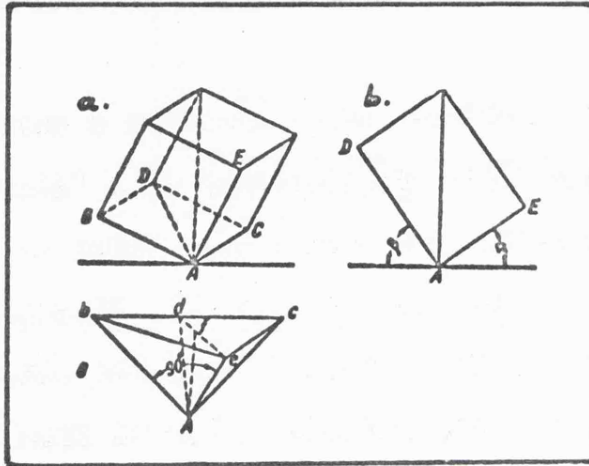


Fig 2.23 Basic geometry of scratching point
in Bierbaum's equipment
(Kruschov and Babichev 1960).

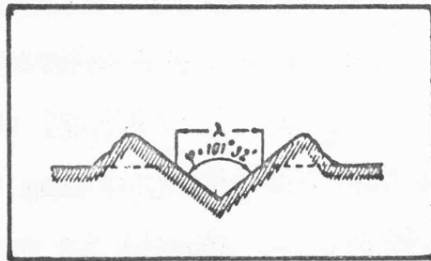


Fig 2.24 Cross-section of scratch produced by
Bierbaum's equipment.
(Kruschov and Babichev 1960).

cutting angle follows the same trend as shown in (fig 2.22), namely negative rake angles give a low coefficient of friction positive rake angles a high coefficient of friction.

Kruschov and Babichev also describe a series of scratch tests made with the indenter of a 'Bierbaum micro-characteriser'. The scratching point in the Bierbaum test is a cube set so that its diagonal is perpendicular to the test surface with the cube edge AE forward (fig 2.23). The material removed from the scratch forms ridges on its sides (fig 2.24). Tests on a series of annealed and cold worked materials showed that the Bierbaum hardness was sensitive to cold working in exactly the same way as hardness by impression. However if the Bierbaum test was modified so that scratching is by cube facet instead of in the normal test cube edge, a different type of scratch is produced with the separation of a chip. Under these conditions the scratch hardness was shown to be insensitive to cold work (work hardening) which indicates that the material had reached its limiting work hardened condition during the test. It should be pointed out that the material used for these tests was nickel which, of course, is well known for the rapidity with which it work hardens.

As a result of their experiments Kruschov and Babichev concluded that two types of scratch were possible one involves the formation of a groove by a ploughing action

material being displaced but not removed, the other a cutting mechanism the groove volume being removed as a turning. Their results also suggest that the transition from cutting to ploughing depends on the material being scratched, the cutting angle of the indenter and its orientation relative to the surface being scratched (facet cuts, edge ploughs). Confirmatory evidence for this later observation has been provided by a number of workers (Tabor (1954) NEL (1962)), who have reported that when scratching with the facet of an indenter a chip is removed but when scratching by edge plastically impressed grooves are produced without removing material.

The existence of cutting and non-cutting grits on abrasive papers has been explained by Mulhearn and Samuels (1962) in terms of critical 'attack angle'; the attack angle being the angle between the cutting facet of indenter and the work material (in cutting tool nomenclature $90^\circ +$ the rake angle). They concluded as a result of experiments with idealised cutting tools that the critical 'attack angle' for fully work hardened mild steel was 90° . Applying the results obtained with idealised indentors to abrasive grits they suggested that the grits with attack angles less than the critical value plough a groove without removing material, grits with greater attack angles remove a chip. Using elegant metallographic techniques they found that only 10% of the grits on their abrasive papers had attack angles exceeding the critical value. They

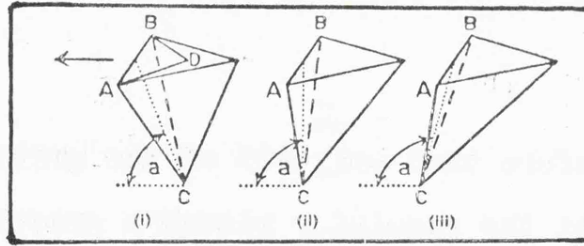


Fig 2.25 Pyramidal tools used to simulate abrasive particles. Face ABC is in contact with the material. Angle $ACB = 90^\circ$ in all cases. Angle "a" is referred to as the "attack angle". The arrow indicates the direction of sliding. (Mulhearn and Samuels 1962).

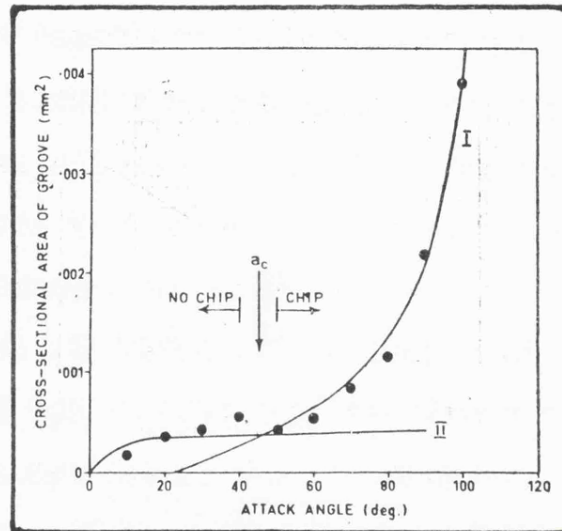


Fig 2.26 Curves I and II represent the variation of the cross-sectional area of the groove with attack angle as calculated from eqns.(1) and (2) respectively. The experimentally measured values are shown by black circles. (Copper workpiece). (Sedriks and Mulhearn 1964).

Equation 1.

$$A = \frac{W(1 + \mu \tan b)}{c p (\mu - \tan b)}$$

Equation 2.

$$A = \frac{\mu' W}{c \sec \alpha + c p}$$

where;

- A = cross-sectional area of groove.
- p = yield pressure of workpiece material.
- b = rake angle = $\alpha - 90^\circ$ (α = attack angle).
- c = constant
- μ = coefficient of friction between the contacting surfaces.
- μ' = coefficient of friction between the tool face and the material.
- s = shear strength of the workpiece material.
- W = applied load.

concluded therefore that only 10% of the grits were cutting and that the remainder plough a groove without removing material.

More recently Sedriks and Mulhearn (1963 & 1964) have used pyramidal tools of known geometry and orientation to simulate scratching by abrasive particles. Previous treatments of abrasive wear have considered the load to be carried by one or more of the inclined faces which stay in contact with the work (fig 2.25). Sedriks and Mulhearn point out that for particles with 'attack angles' greater than 90° there is no frontal facet to support the load and the tool would dig into the work material; obviously in this situation conventional abrasive wear theory is inapplicable. They therefore discussed the two mechanisms of material displacement namely scratching by ploughing and scratching by cutting in terms which are valid for all values of 'attack angle'. The ploughing mechanism was analysed in terms of the shearing and ploughing term as used by Bowden and Tabor (1950) to predict frictional force. The cutting mechanism was analysed in terms of the orthogonal cutting tool theory developed by Merchant (1945). Sedriks and Mulhearn (1963 & 1964) suggested, as a result of plotting their scratch width predictions and experimental results on the same graph (fig 2.26), that the critical 'attack' angle occurs at the point where the two curves intersect. The graph also shows very good agreement between the

predicted and experimental figures. They concluded that the change from ploughing to cutting depends on the coefficient of friction between the tool face and the material and the critical 'attack' angle. It is of interest to note that abrasive wear theory would predict a graph of a similar shape to that shown in (fig 2.26) but seizure would occur at an 'attack' angle of 90° . The fact that seizure does not occur could be explained by assuming that the tool is not absolutely sharp and a sufficient area is provided to support the normal load in the form radiused cutting edge, wear land or built up edge. In orthogonal cutting the tool is assumed to be supported by friction; when tools having a positive rake are used the coefficient of friction up the tool face has to have unusually high values if the frictional force is to be great enough to balance the normal force.

Abrasive wear theory is very sensitive to the width/depth ratio of the scratches produced on the abraded surface, in other words the shape of the grit. The use by both Sedriks and Mulhearn (1963 & 1964) as well as Kruschov and Babichev (1960) of indentors having a width/depth ratio of 1:1 does not therefore seem entirely justified in view of the fact that most investigators have reported ratios of between 5:1 and 10:1 when scratching with actual abrasives. Mulhearn and Samuels (1962) found that single-point cutting tools which had an apex

angle of about 90° produced grooves with an apex angle of 160° . They did not further explore this highly significant observation but it could be advanced as a reason for using tools with a width/depth ratio of 1:1. Moreover in their theory Mulhearn and Samuels (1962) followed other workers in assuming that the groove form was identical with that on the indenter. This large difference between tool apex angle and groove angle has not been noted in other experiments including those of the present author which are reported later.

When a sphere or cylinder is tracked across a surface deformation can occur elastically or plastically. Plastic deformation in this situation involves the formation of a groove either by displacement (material being ploughed but not removed) or by a cutting action (material piles up in front of the indenter and under favourable conditions is removed). Kragelskii (1965) has analysed the ploughing-cutting transition for both a sphere and a cylinder and his findings show that the significant factors are μ the true molecular coefficient of friction between the work material and the indenter and the ratio h/R (h being the depth of the groove and R the radius of the sphere or cylinder). The analysis shows that the greater the value of μ the smaller the value of the ratio h/R for cutting to occur. In the case of a sphere cutting begins at a value of $h/R = 0$ if $\mu = 1$ and for a cylinder cutting begins at $h/R = 0$ if $\mu = 0.39$ showing that material is more readily

removed by a cylinder than a sphere.

Sedriks and Mulhearn's analysis of cutting with a pyramidal indenter and Kragelskii's analysis for a sphere and for a cylinder all involve the molecular coefficient of friction between the indenter and the work material; the other significant factors being for pyramidal indentors critical 'attack' angle and for spheres and cylinders the ratio h/R . However, in the context of the present work, the most significant aspect of Kragelskii's findings is that they cast some doubt on the concept of a critical 'attack' angle as they show that material can be removed under favourable conditions by tools which are very blunt and have effectively very small 'attack' angles.

2.43 Experiments involving files and abrasive surfaces

Spurr and Newcomb (1957) have studied the wear behaviour of a number of materials when rubbed against files under loads of 10-70Kg. Their tests were unusual in that the direction of sliding was opposite to that used in the normal filing process and the file teeth therefore had 'attack' angles of between 11° and 19° . The results produced showed that the wear rate was directly proportional to the product of the load and $\tan \theta$ (θ being the angle of inclination of the file teeth. Having developed an expression for the rate of metal removal based on the assumption that the frontal

TABLE 2.3

Material	p_m Kg/mm ²	$K_1 \times 10^{-1}$
Indium	1	0.30
Lead	6	1.20
Tin	10	0.80
Zinc	40	1.04
Antimony	106	3.82
Platinum	115	2.30
Copper	133	2.42
Brass	170	5.44
Silver Steel	330	4.20

facets of the file teeth support the normal load Spurr and Newcomb pointed out that the actual quantity of material removed was less than that predicted. Table 2.3 shows the coefficients of wear K_1 for a range of materials calculated from experimental results and the expression:-

$$W = \frac{K_1 L}{p \tan \theta} \quad (2.11)$$

where

- W = volume loss per unit sliding distance
- L = normal load
- p = the flow pressure of the material
- θ = the angle of inclination of the file teeth

Since the values of the coefficients of wear K_1 are all less than unity, the process is obviously less than 100% efficient; indeed under the most favourable conditions only 50% of the predicted wear volume is actually removed. A notable feature of the values of K_1 is that they tend to increase for the work materials of greater hardness showing that proportionally higher wear rates can be achieved with harder metals.

Spurr and Newcomb's findings are of particular interest when compared with the critical 'attack' angle concept suggested by Mulhearn and Samuels (1962) and further developed by Sedriks and Mulhearn (1963 & 1964). Mulhearn et al. interpreted the critical 'attack'

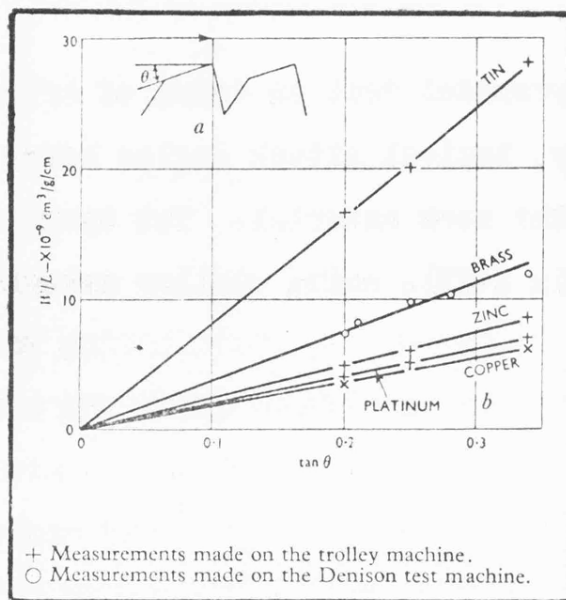


Fig 2.27 Wear of Metals Sliding Over Files Plotted Against Tangent of the Angle of Inclination θ of the File Teeth. (Spurr and Newcomb 1957).

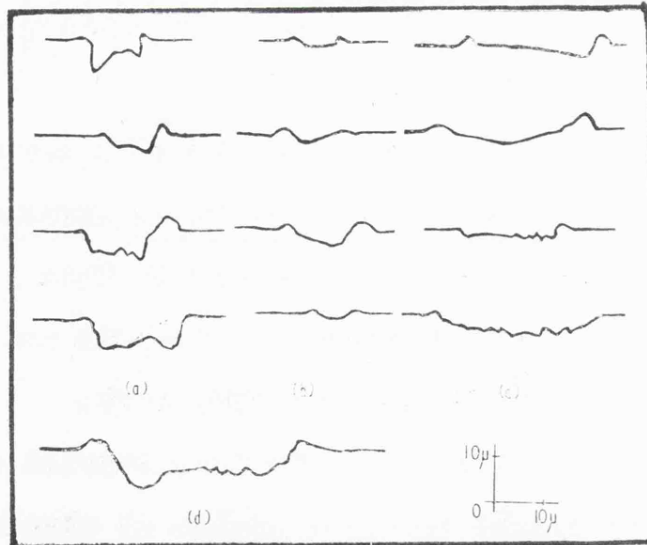


Fig 2.28 Traces of hair shadows (at X260) across some typical grooves on a specimen of silver. Note that there is usually higher pile-up at the deeper side of the grooves. (Stroud and Wilman 1962).

angle for a pyramidal tool in terms of orthogonal cutting theory, typical attack angles being about 50° - 90° depending on the work material. Yet Spurr and Newcomb have shown (fig 2.27), using similar materials, that material can be removed by tools having very small attack angles under conditions which are a better approximation to orthogonal cutting. Indeed, they suggest that tools with even shallower angles than those which they used (11° - 19°) might remove material. These marked variations in findings may be partially explained by geometrical differences between the cutters and differences in the experimental conditions (the pyramidal tool was tracked across the surface once whereas the specimen encounters a succession of cutting edges when rubbed against a file).

The most widely quoted aspect of Spurr and Newcomb's work is their correlation of rates of abrasion with the elastic modulus of the material, rather than its hardness; this result is very difficult to explain and remains unsupported by any other published work.

A number of investigators have carried out experiments using either single abrasive grains or abrasive surfaces; typical of this work is that due to Stroud and Wilman (1962). They showed by traversing a block of silver a short distance ~ 1 mm over emery paper that only a proportion of the groove volume was removed, $\sim 10\%$ the

remainder of the material being displaced by a ploughing mechanism. Using a light profile technique they observed a ploughed up ridge at the edge of the grooves (fig 2.28). Pile up at the edge of surface scratches has been observed by other workers both with idealised indentors and abrasives.

One of the most striking omissions in the literature is the lack of experimental data on the scratching of hard materials such as hardened steel. Admittedly idealised indentors are difficult to manufacture and could easily be chipped when used on hard materials; this argument does not apply however to abrasives. The fact that more investigators have not studied hard materials is all the more surprising since such materials are frequently machined by abrasive processes.

2.5 General Conclusions

A study of the literature has shown that despite the marked similarity of grinding and abrasive wear processes they have been studied very largely in isolation. There seems to be little justification for this state of affairs particularly because theoretical treatments of both processes have regarded them as cutting on a micro scale.

Another noticeable feature common to both grinding and abrasive wear is the anomalous behaviour of heat-treated steels; grinding forces have been found to be largely independent of the hardness of the workpiece and abrasive wear tests reveal that hardened steels have less resistance to wear than would be anticipated.

In both types of process the precise mechanism by which material is removed is still in doubt. In abrasive processes it has been suggested that often only a proportion of the grits are cutting whereas in grinding it is generally assumed that all the grits are cutting.

SQUARE BASED PYRAMID.

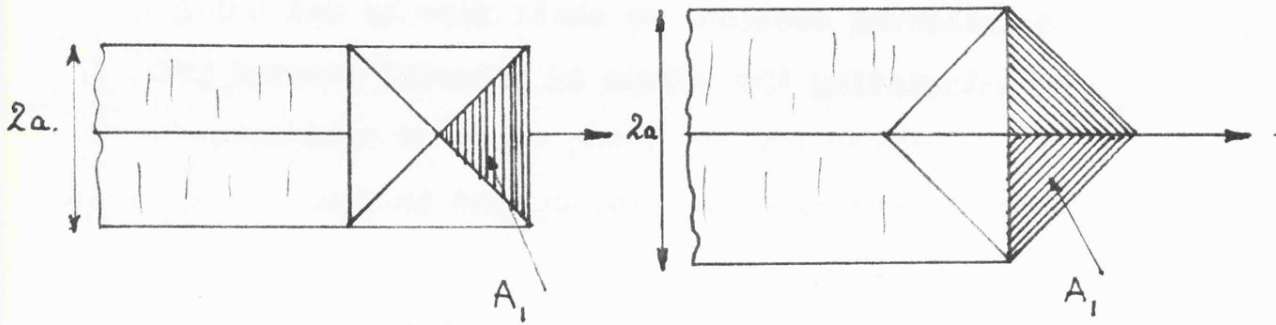


FIG 3.1. FACET FACE ORIENTATION.

FIG 3.2. FACET EDGE ORIENTATION.

TRIANGULAR BASED PYRAMID.

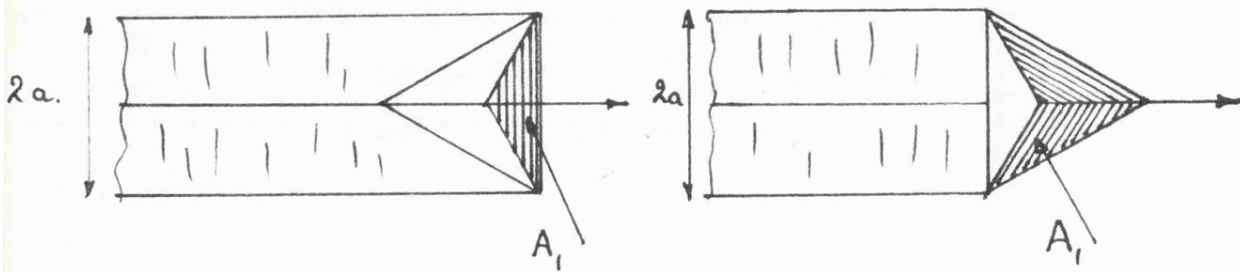


FIG 3.3. FACET FACE ORIENTATION.

FIG 3.4. FACET EDGE ORIENTATION.

CONE

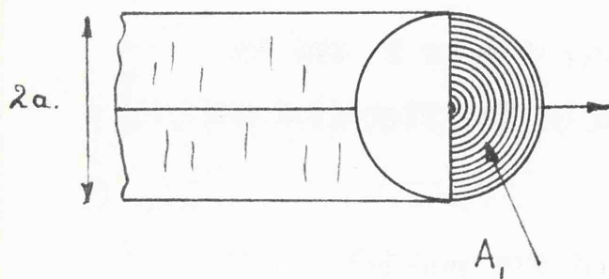


FIG 3.5. CONE.

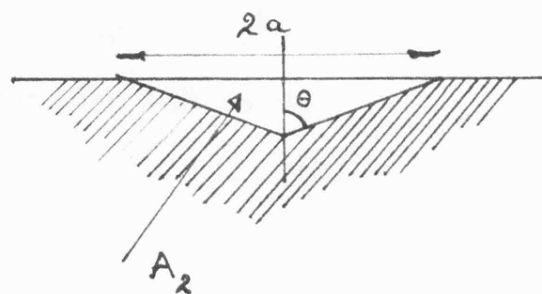


FIG 3.6. CROSS-SECTION OF A SCRATCH.

3 Abrasive Wear Theory

3.1 Introduction

In the following sections we shall firstly set out the methods of calculating the volume of material removed per unit sliding distance for differing types of indentors. Secondly this theory will then be applied to the conditions of grinding.

For the purpose of calculation it will be assumed that the abrasive grits are pyramidal or conical in shape. It is also assumed that the abrasive has very sharp cutting edges and when tracked across a surface under load will cut a groove, the dimensions of the groove being determined by the geometry of the particle, the hardness of the material being abraded and the applied normal force.

3.2 Predictions based on Idealised Indentors

3.2.1 Square Based Pyramid

(1) Cutting by facet

Let the base angle of the scratch be 2θ and the width of the scratch formed be $2a$. figs (3.1 and 3.6)

The area of cross-section of the scratch is given by

$$A_2 = a^2 \cot\theta \quad (3.1)$$

For a typical particle the area supporting a load ∂W is A_1

$$A_1 = a^2 = \frac{\partial W}{P_m}$$

therefore

$$a^2 = \frac{\partial W}{P_m} \quad (3.2)$$

In a sliding distance ∂L the volume of metal removed ∂V is

$$\partial V = \partial L a^2 \cot \Theta$$

$$\frac{\partial V}{\partial L} = a^2 \cot \Theta \quad (3.3)$$

Combining (3.2) and (3.3):

$$\frac{\partial V}{\partial L} = \frac{\partial W \cot \Theta}{P_m} \quad (3.4)$$

For a total load W and assuming all the grits have the same geometry,

Volume loss per unit sliding distance

$$= \frac{W \cot \Theta}{P_m} \quad (3.5)$$

(11) Cutting by edge

For a scratch base angle 2θ and width $2a$

figs (3.2 and 3.6)

The area of the scratch is given by

$$A_2 = a^2 \cot\theta \quad (3.6)$$

In a sliding distance ∂L the volume removed ∂V is

$$\partial V = a^2 \cot\theta \partial L \quad (3.7)$$

The normal load is supported by the area A_1

but

$$A_1 = a^2 = \frac{\partial W}{P_m} \quad (3.8)$$

Combining (3.7) and (3.8):

$$\frac{\partial V}{\partial L} = \frac{\partial W \cot\theta}{P_m} \quad (3.9)$$

For a total load W assuming all particles to be of a similar shape:

$$\text{Volume loss per unit sliding distance} = \frac{W \cot\theta}{P_m} \quad (3.10)$$

3.2.2 Triangular based pyramid**(1) Cutting by facet**

With a scratch of width $2a$ and base angle 2θ
 figs (3.3 and 3.6) the area supporting the normal
 load is given by

$$A_1 = \frac{a^2 \sqrt{3}}{3} = \frac{\partial W}{p_m} \quad (3.11)$$

Therefore $a^2 = \frac{3 \partial W}{\sqrt{3} p_m} \quad (3.12)$

The area of the scratch is

$$A_2 = a^2 \cot \theta \quad (3.13)$$

Combining equations (3.12) and (3.13)

$$A_2 = \frac{\sqrt{3} \partial W \cot \theta}{p_m} \quad (3.14)$$

If the total load is carried by a number of
 particles of the same shape

Volume loss per unit sliding distance

$$= \frac{\sqrt{3} W \cot \theta}{p_m} \quad (3.15)$$

(ii) Cutting by edge

With a scratch of width $2a$ and base angle 2θ
 figs (3.4 and 3.6) the area supporting the normal
 load is given by

$$A_1 = \frac{2 a^2 \sqrt{3}}{3} = \frac{\partial W}{p_m} \quad (3.16)$$

$$\text{Therefore } a^2 = \frac{3 \partial W}{2\sqrt{3} p_m} \quad (3.17)$$

The area of the scratch is

$$A_2 = a^2 \cot \theta \quad (3.18)$$

Combining equations (3.17) and (3.18)

$$A_2 = \frac{\sqrt{3} \partial W \cot \theta}{2 p_m} \quad (3.19)$$

If the total load is carried by a number of grits of the same shape

Volume loss per unit sliding distance

$$= \frac{\sqrt{3} W \cot \theta}{2 p_m} \quad (3.20)$$

3.2.3 Conical indenter

Let the base angle of the indenter be 2θ and the width of the scratch $2a$. figs (3.5 and 3.6)

The area of cross-section of the scratch

$$A_2 = a^2 \cot \theta \quad (3.21)$$

Area supporting the load ∂W is A_1 where

$$A_1 = \frac{\pi a^2}{2} = \frac{\partial W}{p_m} \quad (3.22)$$

$$\text{therefore } a^2 = \frac{2 \partial W}{\pi p_m} \quad (3.23)$$

Let there be N particles when the total load

$$W = N \partial W \text{ or } \partial W = \frac{W}{N} \quad (3.24)$$

From (3.23) and (3.24)

$$a^2 = \frac{2 W}{N \pi p_m} \quad (3.25)$$

For a sliding distance L the worn volume V is

$$\text{given by } V = N A_2 L \quad (3.26)$$

Combining (3.21), (3.25) and (3.26)

$$\frac{V}{L} = \frac{W \cot \Theta}{\frac{\pi}{2} p_m} \quad (3.27)$$

3.2.4 Discussion

The general form of the equation for the volume loss per unit sliding distance is

$$\frac{V}{L} = \frac{C W \cot \Theta}{p_m} \quad (3.28)$$

where the constant C is some function of the geometry of the abrasive particle.

In the initial calculations no allowance was made for the build up at the front of the indentors or ploughing

TABLE 3.1

Indenter	Presentation	Value of C	
		Calculated	Modified
Square pyramid	edge	1.0	0.5
Square pyramid	facet	1.0	0.5
Triangular pyramid	edge	1.73	0.87
Triangular pyramid	facet	0.87	0.87
Cone	-	0.64	0.5*

* experimental value by author

at the edge of the scratches.

Sedricks and Mulhearn (1963) have shown that when an idealised tool is tracked across a flat surface facet first, the chip formed runs up the tool face to about the same extent as the scratch depth, thus increasing the load bearing area by a factor of two. This effect halves the value of C in the case of facet first scratches in equation 3.28.

Similar tests carried out by Kruschov and Babichev (1960) using a diamond cube indenter showed, when scratching annealed electro-deposited nickel, that scratching by facet produced a chip but scratching with the cube edge ploughs a groove. Experiments reported later in this thesis confirm the importance of ploughing when scratching by edge but have shown that material can be removed by this mechanism. The ploughing mechanism will be assumed to reduce the efficiency of edge scratching by a factor of two thus halving the calculated value of C.

The calculated and modified values of C are shown in table (3.1).

In further calculations a representative value of $C = 0.5$ will be used giving a wear equation

$$V = \frac{0.5 W \cot \theta L}{P_m} \quad (3.29)$$

where

W = load in Kg

Θ = half angle of a typical scratch

L = sliding distance in cms

p_m = flow pressure or hardness in Kg/cm²

The mean value of Θ is obtained experimentally. Values of Θ observed in fine grinding and abrasive wear give width/depth ratios of between 50 and 5 to 1, an average value being about 20:1.

Even when the width/depth ratio is taken into account abrasive wear theory has been found to be in error when applied to actual wear situations, the predicted figures being greater than the observed. Two possible explanations for this discrepancy are (i) only a proportion of the grits are cutting at any one time or alternatively (ii) only a proportion of the scratch volume is actually removed. To allow for both possibilities equation (3.29) requires modification, two new parameters being incorporated; α proportion of grits actually cutting and β proportion of groove volume removed. The equation now becomes:

$$\frac{V}{L} = \frac{0.5\alpha\beta W \cot \Theta}{p_m} \quad (3.30)$$

Experimental evidence supporting the concept that only a proportion of the grits are cutting is provided by Mulhearn and Samuels (1962); who have shown that for

any material there is a critical attack angle and grits with an attack angle less than the critical value do not remove a chip. The second mechanism has been observed by Stroud and Wilman (1962) when rubbing silver over an abrasive surface; they concluded that only a proportion of the scratch volume is removed, the remainder being displaced to the edge of the groove. The present work also provides further experimental support for this latter mechanism.

In wear studies the discrepancies between the theoretical and practical wear rates are accounted for by the so called K factor. In abrasive wear theory the K factor has effectively been subdivided into three distinct parts.

$$K = \alpha \cdot \beta \cdot \cot \theta \quad (3.31)$$

Not only does each individual parameter have a definite physical significance but they can all be measured for any particular process.

3.3 The Application of Abrasive Wear Theory to the Grinding Process

3.3.1 Introduction

Any attempt to reconcile grinding and abrasive wear theory must rely heavily on the basic premise, fundamental to both processes, that when the abrasive is performing

satisfactorily metallic particles are being removed essentially by a cutting action.

The very marked similarities between the results reported for both processes are all the more remarkable in view of the very different conditions under which experiments have been carried out.

Grinding is a widely used commercial process and most of the work reported in the literature has been carried out under conditions similar to those encountered in normal practice. The bulk of results involved hard materials $\sim p_m = 800 \text{ Kg/mm}^2$, coarse abrasives ~ 60 grit, high surface speeds $\sim 5,000 \text{ ft/min}$ each portion of the grinding wheels surface being used repeatedly. Abrasive wear studies, on the other hand, have been directed in the main to elucidating the basic mechanism of the process. In most studies relatively soft materials have been used, frequently pure metals, fine abrasives ~ 200 grit, slow speeds $\sim 200 \text{ ft/min}$ and in many investigations each portion of the abrasive paper was only used once.

Theoretical treatments of grinding have regarded the process essentially as one of cutting using very small single-point tools. Each grit is assumed to remove a chip. Experimental observations have shown that the ratio of normal to tangential force is 0.5 in grinding and 2 for single point cutting. Abrasion, on the other hand, has been regarded as a scratching process. Each particle cuts a groove in the work surface whose contents is

removed as a wear product, probably some form of chip. The abrasive particles are assumed to have a negative rake and allowance can be made for ploughing and rubbing grits. The coefficient of friction is about 0.5 similar to that observed with grinding.

Despite the very obvious differences in experimental conditions and theoretical treatment the marked similarities of practical results are considered to justify an attempt to interpret the grinding process in abrasive wear terms. Indeed it will be suggested later that some of the anomalies of the present theories of grinding can be explained by adopting an abrasive wear approach.

When applying the expressions developed from abrasive wear theory to grinding it is assumed that the same conditions are applicable. That is to say, the geometry of the groove cut is determined by the shape of the abrasive grits, the hardness of the material being ground and the applied normal force.

In order to apply abrasive theory to grinding the rate of metal removal per unit sliding distance must be expressed in terms of the parameters of the type of grinding being studied, i.e. surface, cylindrical or internal. The resulting expression is then substituted in the wear equation (3.30) to obtain the normal grinding force.

3.3.2 Surface grinding

An expression for the normal force in surface grinding for example is derived as follows:

Let:

- D = wheel diameter in inches
- r = wheel speed in revs per minute
- T = table speed in feet per minute
- d = wheel depth of cut in inches
- p_m = hardness of material being ground in Kg/mm^2
- w = work width in inches (plunge grinding)
or cross feed in inches per
traverse

Then

$$\text{Wheel surface speed} = 2.54 D r \pi \text{ cm/min} \quad (3.32)$$

$$\text{Work speed} = 2.54 12 T \text{ cm/min} \quad (3.33)$$

Combining (3.32) and (3.33)

$$\text{Sliding speed (up cut)} = 2.54 (D r \pi + 12T) \text{ cm/min} \quad (3.34)$$

and

$$\text{Sliding speed (down cut)} = 2.54 (D r \pi - 12T) \text{ cm/min} \quad (3.35)$$

The rate of metal removal is

$$V = 12 2.54^3 T d w \text{ cm}^3/\text{min} \quad (3.36)$$

Combining (3.32) with (3.34) and (3.33) with (3.34), the

rate of metal removal per unit sliding distance is given by the expressions:-

$$\text{Up cut } \frac{V}{L} = \frac{12.2.54^3 T d w \text{ cm}^3/\text{cm}}{2.54(D r \pi + 12T)} \quad (3.37)$$

$$\text{Down cut } \frac{V}{L} = \frac{12.2.54^3 T d w \text{ cm}^3/\text{cm}}{2.54(D r \pi - 12T)} \quad (3.38)$$

Since the table speed in surface grinding is only 1/100 of the wheel speed an average value for the rate of metal removal will be assumed.

$$\frac{V}{L} (\text{average}) = \frac{12.2.54^3 T d w \text{ cm}^3/\text{cm}}{2.54(D r \pi)} \quad (3.39)$$

substituting the above expression in the wear equation (3.30) and rearranging in terms of W

$$W = \frac{12.2.54^3 T d w p_m 10^2 \text{ Kg}}{2.54(D r \pi) \alpha \beta 0.5 \cot \theta} \quad (3.40)$$

The normal force in pounds $N = 2.27$; thus evaluating the constant terms

$$N = \frac{10,830 T d w p_m \text{ lbs}}{D r \alpha \beta \cot \theta} \quad (3.41)$$

3.3.3 Cylindrical Grinding

Let:

- D = wheel diameter in inches
- D_w = work diameter in inches
- d = wheel depth of cut in inches
- r_1 = wheel speed in rpm
- r_2 = work speed in rpm
- w = work width plunge grinding or
cross feed/rev conventional
grinding

then

$$\text{Wheel surface speed} = D r_1 \pi 2.54 \text{ cm/min} \quad (3.42)$$

$$\text{Work speed} = D_w r_2 \pi 2.54 \text{ cm/min} \quad (3.43)$$

Therefore combining (3.42) and (3.43)

$$\begin{aligned} \text{Sliding speed (conventional)} \\ = 2.54\pi(D r_1 + D_w r_2) \text{ cm/min} \end{aligned} \quad (3.44)$$

$$\begin{aligned} \text{Sliding speed (climb)} \\ = 2.54\pi(D r_1 - D_w r_2) \text{ cm/min} \end{aligned} \quad (3.45)$$

$$\begin{aligned} \text{The rate of metal removal} = d\pi D_w r_2 w 2.54^3 \text{ cm}^3/\text{min} \\ (3.46) \end{aligned}$$

Combining (3.44) with (3.46) and (3.45) with (3.46) the rate of metal removal per unit sliding distance is:

$$\text{conventional } \frac{V}{L} = \frac{d \pi D_w r_2 w 2.54^3}{2.54 \pi (D r_1 + D_w r_2)} \quad \text{cm}^3/\text{cm} \quad (3.47)$$

$$\text{climb } \frac{V}{L} = \frac{d \pi D_w r_2 w 2.54^3}{2.54 \pi (D r_1 - D_w r_2)} \quad \text{cm}^3/\text{cm} \quad (3.48)$$

Putting the above expressions in the wear equation (3.30) and rearranging in terms of W

$$\text{conventional } W = \frac{d p_m \pi D_w r_2 w 2.54^3 10^2}{2.54 \pi (D r_1 + D_w r_2) 0.5} \quad \text{cot } \Theta \quad \text{Kg} \quad (3.49)$$

$$\text{climb } W = \frac{d p_m \pi D_w r_2 w 2.54^3 10^2}{2.54 \pi (D r_1 - D_w r_2) 0.5 \alpha \beta \cot \Theta} \quad \text{Kg} \quad (3.50)$$

Evaluating the constant terms and converting to pounds the normal grinding force is:

$$\text{conventional } N = \frac{2,840 p_m D_w r_2 w d}{(D r_1 + D_w r_2) \alpha \beta \cot \Theta} \quad \text{lb} \quad (3.51)$$

$$\text{climb } N = \frac{2,840 p_m D_w r_2 w d}{(D r_1 - D_w r_2) \alpha \beta \cot \Theta} \quad \text{lb} \quad (3.52)$$

Abrasive wear theory can be applied to other grinding processes by substituting the rate of metal removal per unit sliding distance in the wear equation. Thus the parameters required to interpret grinding in abrasive wear terms are:

- (i) the rate of metal removal per unit sliding distance.
- (ii) the width/depth ratio of the scratches formed on the surface.
- (iii) α the proportion of the grits cutting.
- (iv) β the proportion of the groove volume removed.
- (v) the hardness of the material being ground.

3.4 Grinding Force Predictions

3.4.1 Introduction

Many studies of the grinding process involving dynamometer force measurements have been reported and in the first instance we will use this earlier published work to test the theoretical predictions of the normal grinding force obtained using abrasive wear theory. Unfortunately some of the parameters required for calculation were not measured or even considered by other workers and it has therefore been necessary in most cases to assume representative values. The parameters in question were those which make up the K

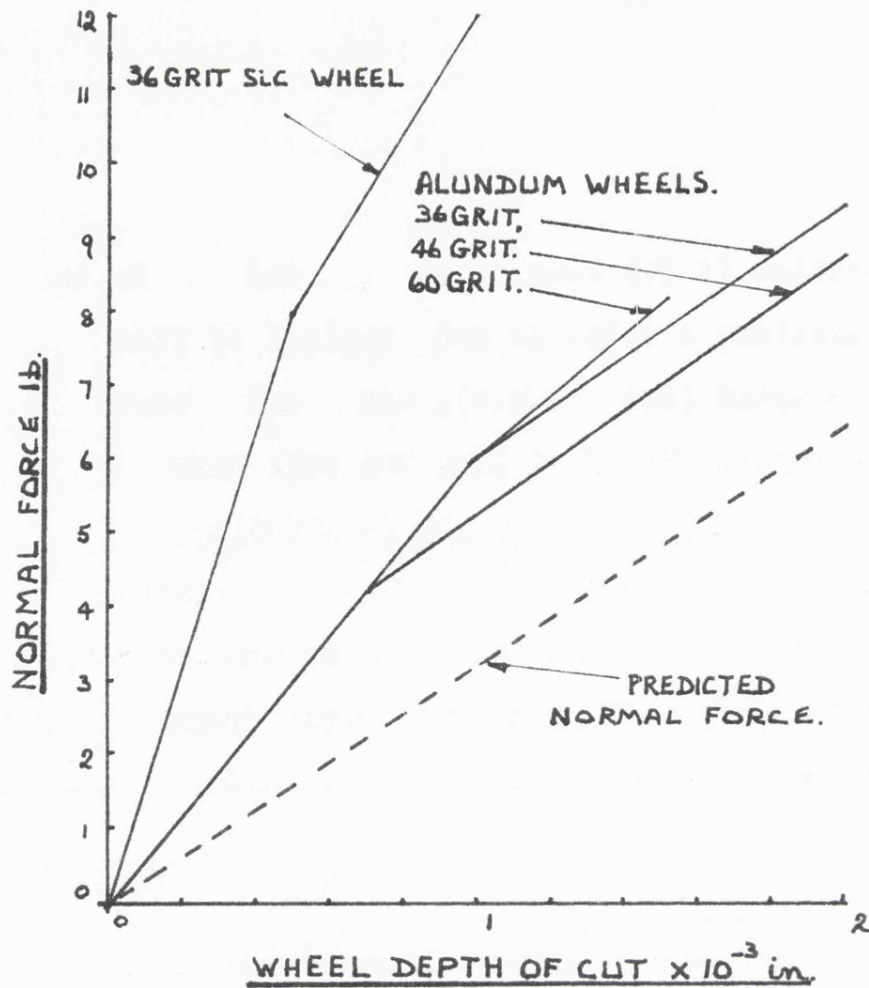


Fig 3.7 Wear theory predictions compared with Marshall and Shaw's (1952) experimental results.

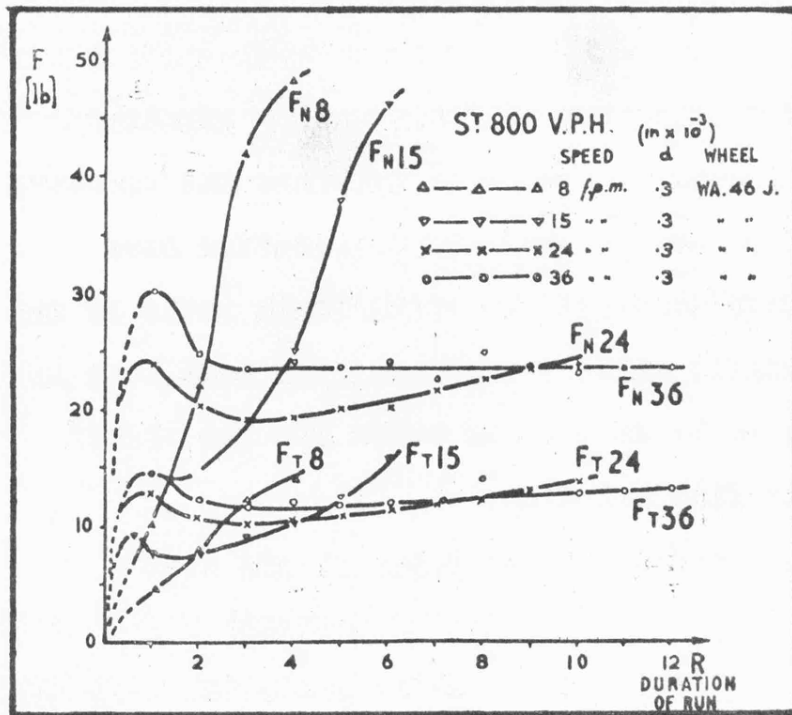


Fig 3.8 Grinding forces for various table speeds. (Grisbrook 1962).

factor in equation (3.31) namely $\cot\Theta$, α and β . In the initial calculations a value of $\cot\Theta$ typical of fine grinding was adopted ($\cot\Theta = 0.1$), and α and β were assumed to be unity. The fact that the well known expression for the grit depth of cut in grinding (equation 2.4) assumes that all the grits are cutting and that the whole of the groove volume is removed would seem to justify a value of unity for α and β when applied to the grinding process.

3.4.2 Surface Grinding

The first reported force measurements for surface grinding are due to Marshall and Shaw (1952). Their dynamometer could only be used at relatively slow table speeds; most of their results were obtained at table speeds of 4fpm; the maximum possible table speed being 16fpm, and their work was confined to dry grinding. These restrictions all served to increase the severity of the tests and make satisfactory operation more difficult. They measured the width/depth ratio of the grinding scratches using a taper section technique and they found 15 to be an average value for the width/depth ratio in fine grinding.

Force predictions using Marshall and Shaw's results for a steel of hardness 43 Rockwell C (420 DPN) are shown in fig (3.7). The forces predicted were below

TABLE 3.2

Grinding Force Components for Specimens of Different Hardness

Hardness of specimen Kg/mm ²	Calculated force lb.	Observed force lb.
830	4.76	5.1
545	3.12	5.1
230	1.32	5.1

those observed in all cases and for the silicon carbide wheel were considerably in error.

One of the most significant and surprising of the findings of Marshall and Shaw was that the grinding forces were independent of the work piece hardness. The results of abrasive wear calculations based on this work are given in table 3.2.

For hardened steel the force predictions are within 10% of the observed value. For the same material in the annealed condition the calculated values are only 25% of the experimental value. It would appear therefore that hardened steel is a unique case; the force calculations suggest that both the whole of the scratch volume is removed and every grit is cutting. Re-examining the earlier calculations for the steel having a hardness of Rockwell C43 (420 VPN) showed that the forces observed with the alumina wheel were consistent with those predicted for a steel having a hardness of Rockwell C65 (830 VPN).

Grisbrook (1962) extended the work of Marshall and Shaw, using a similar type of dynamometer, to more practical conditions; namely higher table speeds and wet grinding. He observed that the force pattern on a grinding wheel changed progressively during a run and could be divided into four regions fig (2.10). Force predictions were made, using abrasive wear theory, for the steady state regions of the force pattern curves fig (3.8).

TABLE 3.3

Table speed fpm	Calculated normal force	Observed force
15	10.2 lb	14 lb
24	16.4	19
36	24.5	24

The tests carried out at the higher table speeds gave longer periods of grinding stability, and the best agreement between the theoretical predictions and experimental force measurements.

Observed and predicted forces for several table speeds are shown in table 3.3

3.4.3 Cylindrical Grinding

Landberg (1956) has reported on the cylindrical grinding of steel. Using measuring centres tangential and normal forces are measured. A particularly interesting feature of Landberg's work was the selection of grinding conditions which gave an exceptionally long period of grinding stability (~ 120 mins of continuous grinding). Applying abrasive wear theory the forces predicted were considerably less than those observed; in fact they were only 25% of the observed force.

Table 3.4.

In view of the extended period of grinding stability, it would appear that this discrepancy must be accounted for by some difference in grinding mechanism possibly the width/depth ratio or more likely the proportion of groove volume removed or grits cutting (assumed to be unity in all the initial calculations).

TABLE 3.4

Wheel	Predicted force Kg	Observed force Kg
46R	4.95	21
46L	4.95	18.5
46I	4.95	16.1

The experiments carried out by Marshall and Shaw and by Grisbrook were mainly concerned with hardened steels, although they did observe the independence of the grinding forces from the workpiece hardness. Force predictions for hard steels were in good agreement with the practically observed values. Landberg's work however was performed entirely with mild steel and force predictions were well below the practical values. Calculations based on Marshall and Shaw's results for soft materials were also in error by a similar amount. It is suggested that some differences in wear mechanism operate between the grinding of hardened steel and softer materials.

Landberg also observed that a hard wheel gave the highest forces, a soft wheel the lowest. The hard wheel is more likely to glaze, the soft wheel to self sharpen. It is to be expected therefore that the soft wheel will have sharper grits and these will give grinding scratches with a smaller width/depth ratio and consequently lower cutting forces.

3.4.4 Constant Force Grinding

Constant force grinding is a recent innovation and the set-up shows considerable similarity to the pin and ring machine reported later. Usually small diameter wheels are employed and these are loaded against the

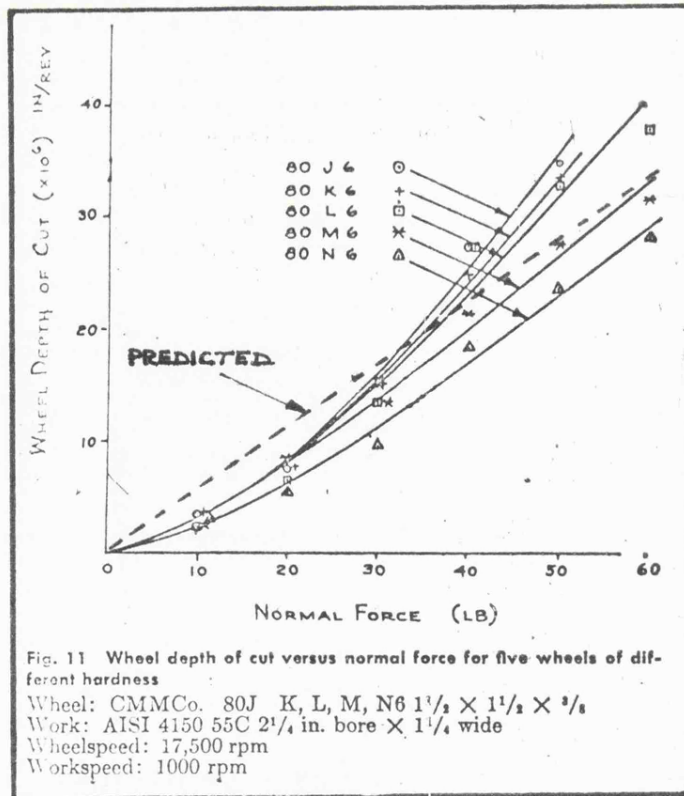
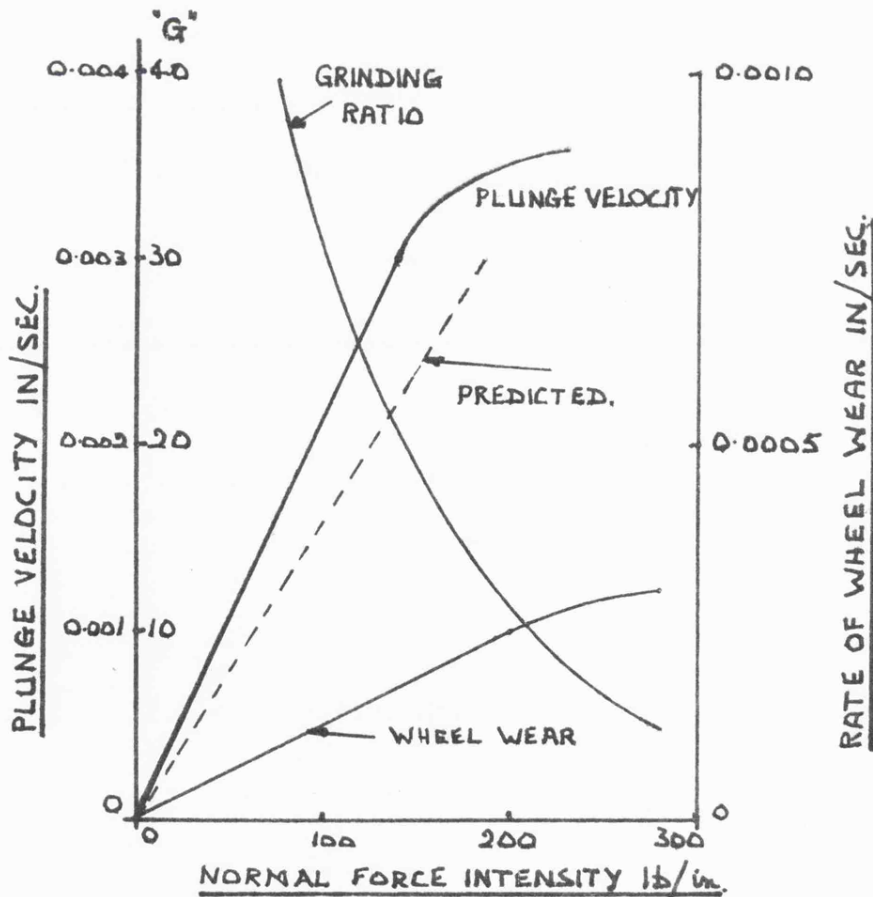
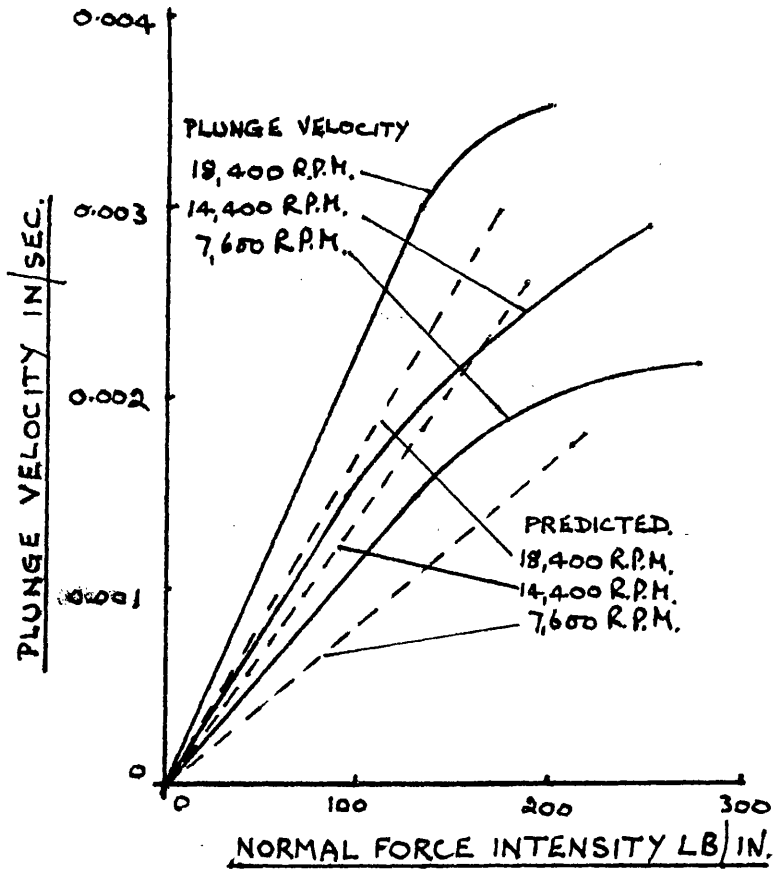


Fig 3.9 Theoretical predictions compared with Hahn's (1964) experimental results.



Conditions: Wheel speed 18,400 rev/min, Wheel diameter 1.750 in.
 Work speed 1950 rev/min, Work diameter 2.315 in.
 Work material AISI 4150 $R_c = 53 - 55$.

Fig 3.10 Theoretical predictions compared with Hahn's (1965) results.



Conditions: Wheel speed 18,400 rev/min, Wheel diameter 1.40 in.
 Work speed 1,950 rev/min, Work diameter 1.75 in.
 Work material AISI 4150, $R_c = 53-55$.

Fig 3.11 Wear theory predictions compared with Hahn's (1965) experimental results.

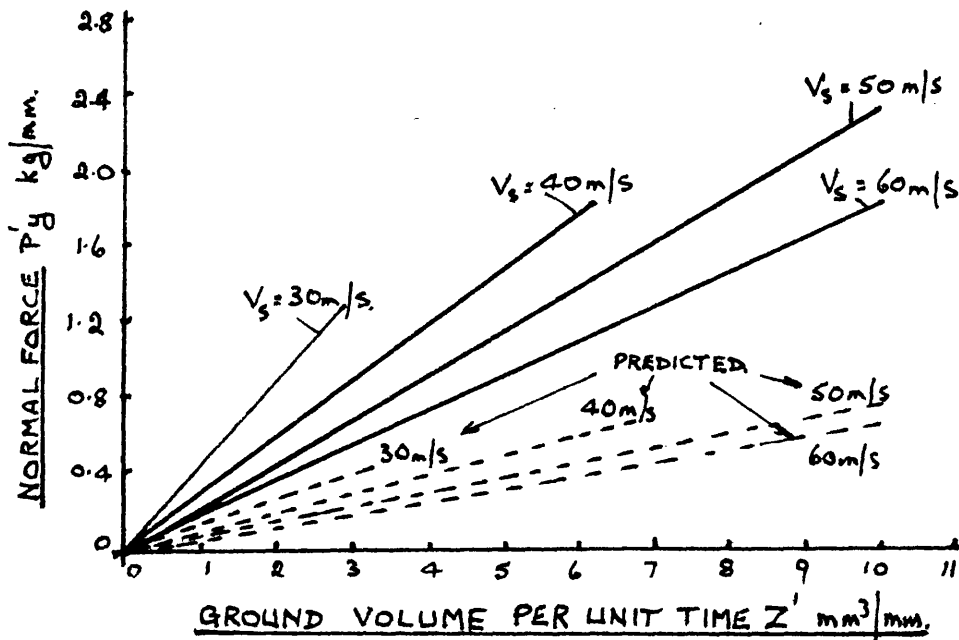


Fig 3.12 Comparison of Optiz et al's (1965) experimental results with wear theory predictions.

work under the action of a constant force. Hahn (1955, 1956, 1962, 1964, 1965) has reported extensively on this type of grinding. When the process is operating satisfactorily the rate of metal removal versus time shows a linear relationship; similarly the rate of metal removal versus normal force is linear fig (3.9).

The relationship between observed and predicted normal forces in the case of Hahn's results for controlled force grinding are shown in figs (3.10 and 3.11). In all cases the predicted forces are greater than those observed, the error being an over estimate of about 25%. This may well be accounted for by the value of the width/depth ratio assumed namely 20:1.

Opitz et al (1965) have also studied controlled force grinding and their results show a linear relationship between normal force and ground volume per unit time. The steel being ground was of relatively low hardness $\sim 200 \text{ Kg/mm}^2$ compared with $\sim 600 \text{ Kg/mm}^2$ in Hahn's experiments. Force predictions based on Opitz et al's work, shown in fig (3.12) are in error by a factor of four; the predicted figures being only 25% of the observed.

3.4.5 Abrasive Wear

Abrasive wear theory can equally well be applied to the rubbing of materials against abrasive papers such

as emery. Unless the specimen is constantly presented with fresh abrasive paper the wear rate gradually falls as the abrasive is used up.

Mulhearn and Samuels (1962) performed experiments in which the abrasive surface was used repeatedly. They showed that metal was removed in the form of chips and that the wear rate fell progressively as the surface of the paper gradually lost its abrasive properties. Their theoretical predictions were in error by a factor of ten; this was due they postulated to the fact that only 10% of the grits were cutting; the remainder merely plough the surface as they do not have suitable 'attack angle'. A typical wear curve is shown in fig (2.18).

Abrasive wear calculations were carried out for the linear portion of the test at the beginning of the run; these gave a wear rate three times that of the experimental figure. It should be pointed out that the metal being abraded was mild steel p_m 255Kg/mm² so the discrepancy is similar to that observed when grinding soft materials.

Kruschov and Babichev's (1957) experiments using abrasive papers differed from those already mentioned in that the specimen was continuously encountering 50% fresh emery paper; changes in the properties of the wearing surfaces in some cases due to clogging and in others due to blunting of the abrasive will largely be eliminated. Their results were expressed in terms of wear resistance and they showed that with pure metals this

Table 3.5.

Experimental wear results for a range of materials run against carborundum for a distance of 6 m. under a load of 1 Kg at a velocity of 0.5 m/s (due to Nathan and Jones 1967) compared with theoretical wear rates.

Material	V.P.N.	Carborundum	Theory *
		Vol. removed mm ³ .	Vol. removed mm ³ .
Tin.	10.8	16.15	27.9
Aluminium.	33.9	14.78	8.85
Copper.	61.9	5.27	5.15
Phosphor Bronze.	70.5	3.28	4.26
Niobium.	109.3	3.19	2.74
Steel.	123	2.48	2.44
Nickel.	157	2.30	1.91
Steel.	177.5	2.13	1.69
Steel.	222	1.85	1.35
Steel.	286.5	2.06	1.05
Steel.	384	1.80	0.78
Steel.	484	1.65	0.62
Steel.	516	1.46	0.58
Steel.	576	1.23	0.52
Ni-hard type 4.	628	1.63	0.48
Ni-hard type 1.	689	1.55	0.44
Tool steel.	824	1.29	0.36
Tool steel.	891	1.07	0.34

* Theory using equation 3.30 assuming $\alpha = 1$, $\beta = 1$ and $\cot\theta = 0.1$

varied in a linear manner with hardness. Steels on the other hand behaved differently; with a hardness variation of 4:1 (200 Kg/mm² soft to 850 Kg/mm² hard) the wear rate only changed by a factor of two. This observation adds further support to the idea that the efficiency of the abrasion process is greater for hard than soft materials; this applies even when the abrasive is performing satisfactorily, ignoring the effects of clogging fig (2.12 and 2.14).

In a study of the influence of the hardness of abrasives on the abrasive wear of metals Nathan and Jones (1967) used abrasive belts and a very large range of metals of widely differing hardnesses. The tests were arranged so that the specimen was constantly being presented to fresh abrasive. Their results showed the relationship between wear volume and metal hardness for a number of different abrasives fig (2.17). Thus with carborundum changing the hardness of the steel being abraded from p_m123 to p_m891 Kg/mm² a factor of about 8:1 only produces a change in wear rate of 2.4:1. As in previous work already discussed it appears that hardened steel is more readily abraded than would be expected relative to a soft steel. The results of applying abrasive wear theory are shown in table 3.5 and fig (2.17). With carborundum corundum and flint the theoretical and practical curves meet at a hardness value of about 150 Kg/mm², the predicted wear rates for

hardened steel being well below those observed practically. This apparent departure from the previous pattern of results, namely good agreement between observed and predicted forces with hardened steels poor with soft steels, is probably due to the value of the width/depth ratio assumed which was 20:1. This figure although typical of fine grinding is probably inaccurate for abrasive belts and if adjusted to give the correct wear rate for hardened steel, that for steel with a hardness of 123 Kg/mm^2 will be about three times the practically observed value.

3.5 Discussion and Conclusions

Undoubtedly the most significant fact which emerges from a study of experimental results reported in the literature is the very marked difference in the wear behaviour of hard and soft steel. Force predictions were in good agreement with the practically observed values with hardened steels assuming the parameters α and β were unity. Similar calculations for soft materials were in error; observed forces being greater than predicted by as much as 4:1. Several explanations are possible; the width/depth ratio assumed could be in error for example; this would imply that the scratches formed on a hardened steel are sharper than those produced

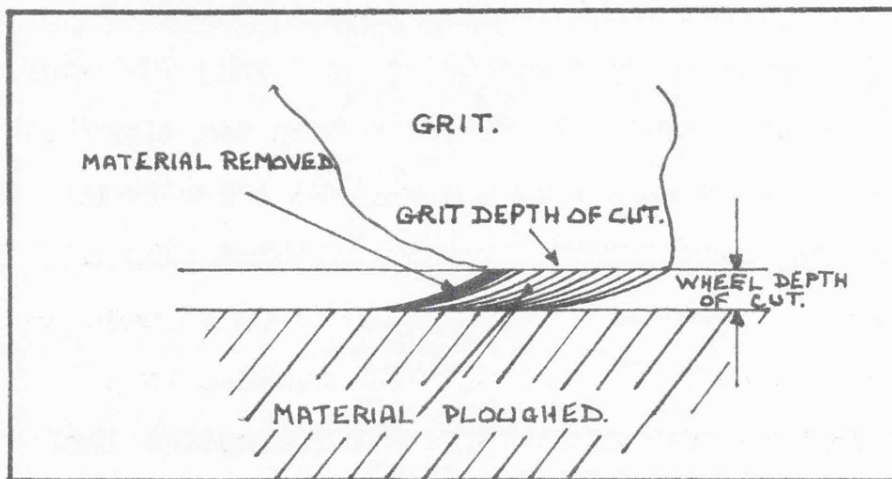


Fig 3.13 Showing a possible effect of ploughing on the cutting mechanism of a single grit.

on a soft steel under similar conditions. There is no practical evidence to support suggestion. Alternatively only a proportion of the scratch volume may be removed or only a proportion of the grits may be cutting. Obviously adjusting either or both α and β to values of less than unity would reconcile the practical results with the theoretical predictions. Altering either parameter will considerably influence the basic cutting mechanism. If it is assumed that only a proportion of the abrasive grits are cutting, the others merely ploughing a groove, it would imply when only 10% were active that each grit will remove a chip ten times as large as it would have done had all the grits been cutting. The alternative explanation, that only a proportion of the groove volume is removed, appears to give a more acceptable result. For example, in a process such as surface grinding the assumption that only 10% of the groove is removed leads to the rather surprising conclusion that each grit will still remove a chip of the same size but this will, of course be a proportion of a much larger groove fig (3.13). The mechanism by which a proportion of a groove can be removed must be fairly complex and probably very different from that of single point cutting; the breakaway of the built up edge of the groove may well be a significant factor. Experimental support for the second

suggestion is provided by Stroud and Wilman (1962), who, as a result of tests with abrasive papers concluded that only a proportion of the groove volume was actually removed; a value of $\sim 20\%$ was quoted as a result of their work. Additional evidence is provided by Grisbrook (1962), who carefully determined the number of 'active' grits in the surface of a grinding wheel and then counted the number of chips produced when grinding with the same wheel. He deduced that the number of active grits was substantially the same as the number of chips formed so that each grit could be said to have removed a chip. These observations fully support the suggestion that in certain circumstances only a proportion of the groove volume is removed; if it is assumed that only a proportion of the grits are cutting there should be a corresponding reduction in the number of chips produced. Consequently one would have expected a significant difference between the number of chips and the number of grits.

Backer, Marshall and Shaw (1952) claimed that the grinding process should be interpreted in terms of grit depth of cut and specific energy; these parameters do not form a part of an abrasive wear treatment of grinding. The grit depth of cut is difficult to determine; its value depends critically on the width/depth ratio of the scratches on the ground surface and the number of cutting points per square inch of wheel surface. It is the latter

factor which is the most difficult to obtain and for which the widest variations have been observed. For example, in the case of a 36 grit wheel values of C ranging from 900 to 15,000 have been reported. Obviously this casts considerable doubt on the final grit depth of cut figures which have been derived. Despite the difficulty of obtaining a precise value for the grit depth of cut it provides a useful parameter in terms of which the grinding process can be discussed. It enables one to predict the possible effects of alterations in the grinding conditions (wheel speed, wheel depth of cut, cross-feed and grit size) on the behaviour of the wheel and the quality of the surface produced. The equivalent factor in abrasive wear theory is the rate of metal removal per unit sliding distance.

The second parameter, specific energy, is a measure of the work done to remove a specific volume of work material and is calculated using the tangential force developed in the grinding process. Abrasive wear theory as such makes no direct prediction of the tangential force but practical values when grinding steel have been of the order of 0.4 to 0.6 of the normal force. Provided alteration of the grinding conditions has no effect on Θ , α and β there would be no corresponding change in specific energy. Any drastic change in Θ , α , and β would produce a corresponding change in the tangential

force and therefore in the specific energy. If the process becomes less efficient Θ very large and α and β considerably below unity the specific energy will increase, but at no time would a condition be predicted at which a constant value would be obtained as suggested by Backer et al. The more recent work of both Hahn (1962) and Grisbrook (1960), although supporting a rubbing cutting transition does not further the concept of a critical limiting value for the specific energy.

Surface finish is an important feature of the grinding process and in many applications accounts for its use in preference to other machining methods. Abrasive wear theory makes no direct predictions concerning surface finish; however one could surmise that the lower the rate of metal removal per unit sliding distance the better will be the resulting surface finish. As grit size does not feature in the theory presumably surface finish will be substantially independent of this factor; Grisbrook's (1960) results support this statement although the range of grit sizes used was relatively small. More recently an experimental study by Farmer, Brecker and Shaw (1968) has shown that the most important variable to produce a good surface finish in surface grinding was a low table speed. The variables listed below being only a half to a third as important and should be adjusted in the direction indicated for a good finish.

<u>VARIABLE</u>	<u>FOR GOOD FINISH</u>
Wheel dressing	Fine
Wheel grade	High
Grain size	Fine
Type of grind	Up
Wheel speed	High
Wheel depth of cut	Low
Work hardness	Hard

It is highly significant that those variables which give a good surface finish are also moved in the same direction to reduce the rate of metal removal per unit sliding distance, namely table speed, wheel speed, wheel depth of cut and work hardness.

The rapid removal of metal is therefore incompatible with a good surface finish; and the variable which is most significant in controlling metal removal rate, namely table speed, has the greatest effect on surface finish.

In most precision grinding processes the wheel is dressed using a diamond; a number of studies involving various techniques have been reported. It is necessary to develop a standard technique if subsequent grinding experiments are to give consistent results. Although there is no general agreement as regards the method to be adopted (type of diamond, cross feed per rev, wet

or dry) most workers have shown that marked variations occur in grinding forces, for example when different dressing procedures are used. No very precise reasons have been advanced for these force variations, except for the suggestion that in general terms they are a function of grit sharpness. An abrasive wear treatment shows that the rate of metal removal depends critically on the width/depth ratio of the scratches formed by the individual grits. If the method of dressing produces grits with a small included angle, the grinding forces will be low; grits with a very large included angle on the other hand would give high cutting forces. The variables α and β are largely a function of the material being ground and the effect of the grinding conditions on the abrasives performance; glazing or loading will reduce the abrasive's effectiveness.

Grisbrook (1960) has shown that the grinding forces can gradually change during a test; in the latter stages forces increase. Such changes are compatible with an abrasive wear treatment if it is assumed that Θ gradually changes as grinding proceeds; it would be necessary to use a larger value of Θ which implies that the grits are getting blunter. In a process such as super-finishing the value of Θ probably approaches 90° .

In wear studies the discrepancies between the theoretical and practical wear rates are accounted for by

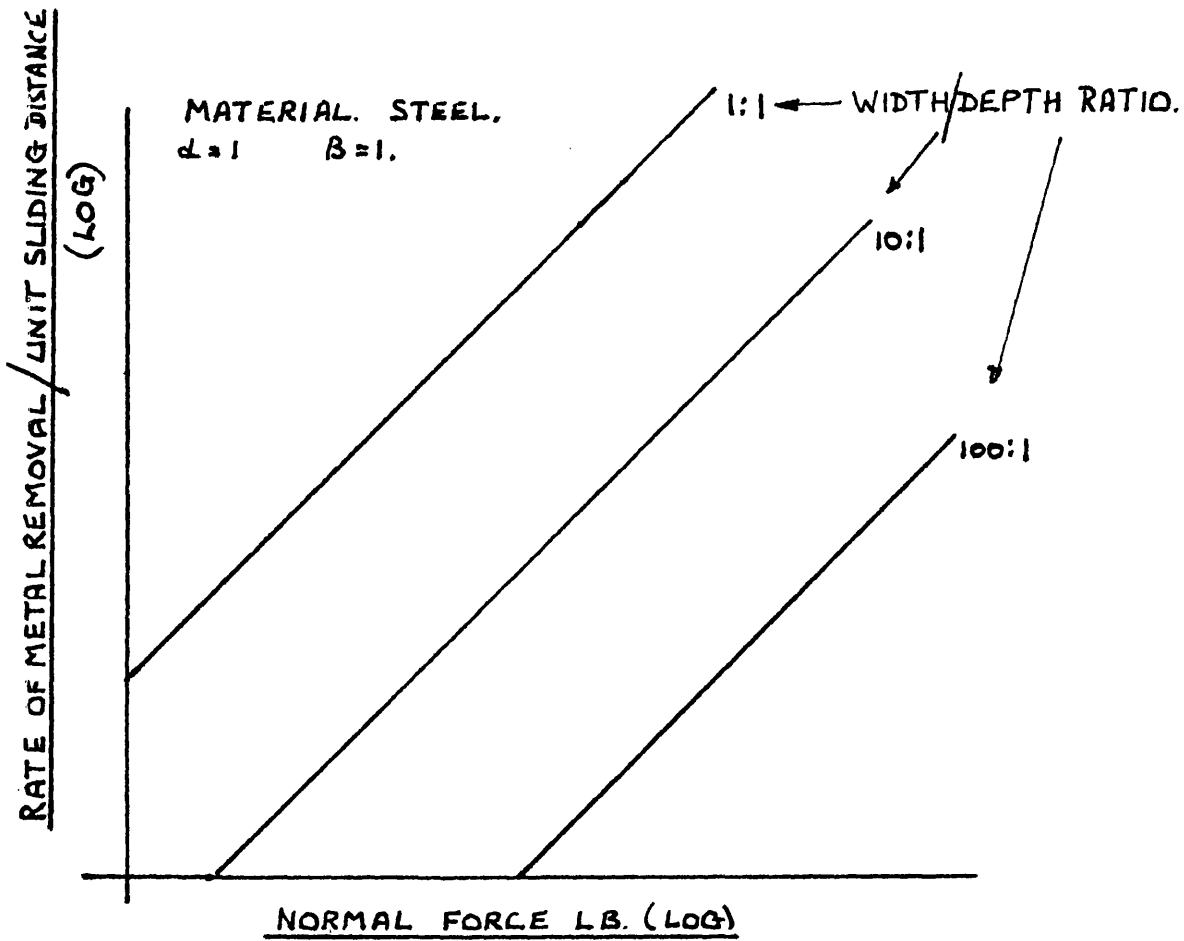


Fig 3.14 Showing the effect of width/depth ratio on normal force for a given steel (α and β constant).

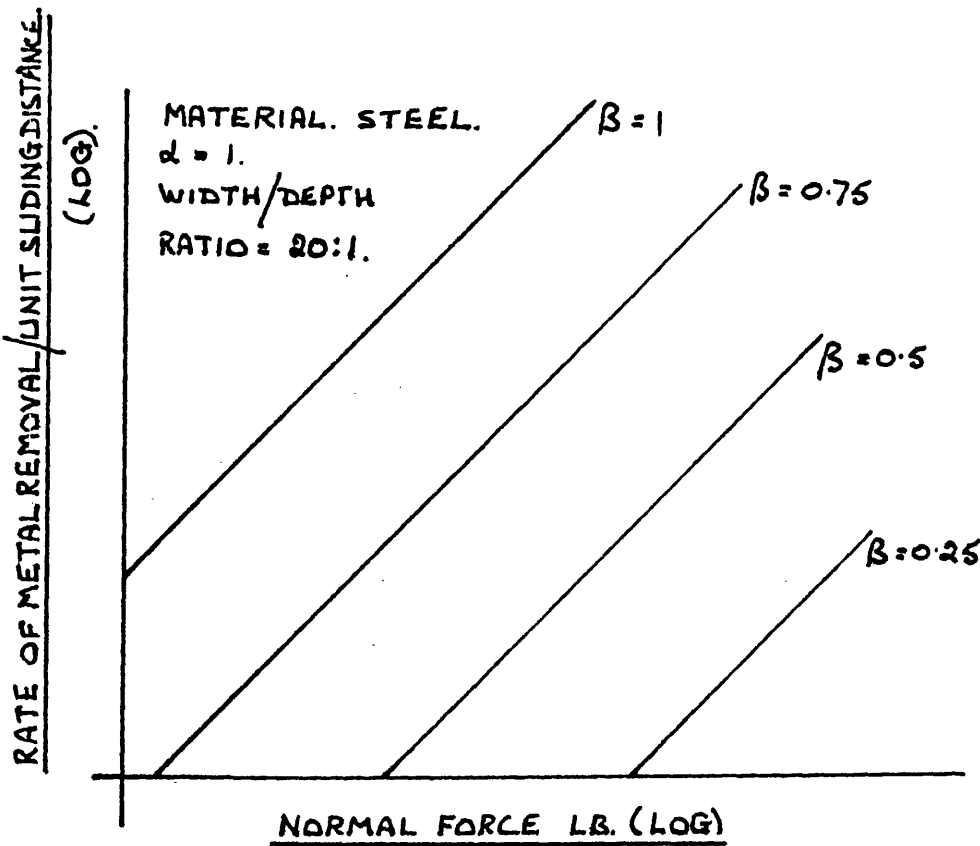


Fig 3.15 Showing the effect of variations in the value of β on normal force for a given steel (α and width/depth ratio constant).

the so-called K factor. In abrasive wear theory the K factor has effectively been subdivided into three distinct parts, all of which can be measured for any particular process.

$$K = \cot\theta \cdot d \cdot \beta$$

Knowing the hardness of the work material, the rate of metal removal per unit sliding distance, the width/ratio of the scratches on the ground surface and the proportion of the groove volume removed, it is now possible to predict grinding forces. It is suggested that curves similar to those shown in figs (3.14 and 3.15) could be used for estimating forces provided the process is operating satisfactorily.

CONCLUSIONS

- (i) Grinding can be regarded as an abrasive wear process; the most important parameter being the rate of metal removal per unit sliding distance.
- (ii) The grinding wheel must be cutting 'freely' if force predictions are to be made. If metallic particles are not being removed abrasive wear theory will give a qualitative assessment of the process, e.g. super finishing.
- (iii) In order to make accurate force predictions the width/ratio of the scratches made on the ground surface must be known.

- (iv) The high forces observed when grinding soft materials can be accounted for if it is assumed that only a proportion of the groove volume is removed, or only a proportion of the grits are cutting. These factors must be taken into account when making force calculations.
- (v) To predict grinding forces the hardness of the work material must be known.

4. Wear Tests.

4.1. Introduction.

Probably the most obvious and significant difference between grinding and abrasive wear is the rubbing speed used in each of the processes. Typical surface speeds in grinding are $\sim 5,000$ ft/min, those for abrasive wear ~ 200 ft/min. Indeed a number of studies of the basic mechanism of abrasive wear have been carried out at extremely low sliding speeds ~ 1 ft/min.

The main purpose of the present work with solid abrasives (grinding wheels and abrasive sticks) has been to explore the types of wear behaviour which occur over a wide range of speed and loads. It was hoped to obtain some indication of whether a similar mechanism applies throughout the range and ascertain whether the results could be usefully compared with those reported elsewhere in the literature for adhesive wear, in particular the mild-severe wear transition reported for steels (Welsh 1965).

Experiments with solid abrasives also provide an opportunity of assessing to what extent the removal of material by a grinding wheel can be regarded as an abrasive wear mechanism, especially when the results are compared with those predicted by wear theory.

4.2 Apparatus.

Two pin and ring machines were used. One was capable of covering a wide range of speeds and loads (1-30,000 rpm. and 40g-10Kg), the other a low speed machine (1rpm) could also accommodate loads of 40g to 10Kg. The essential

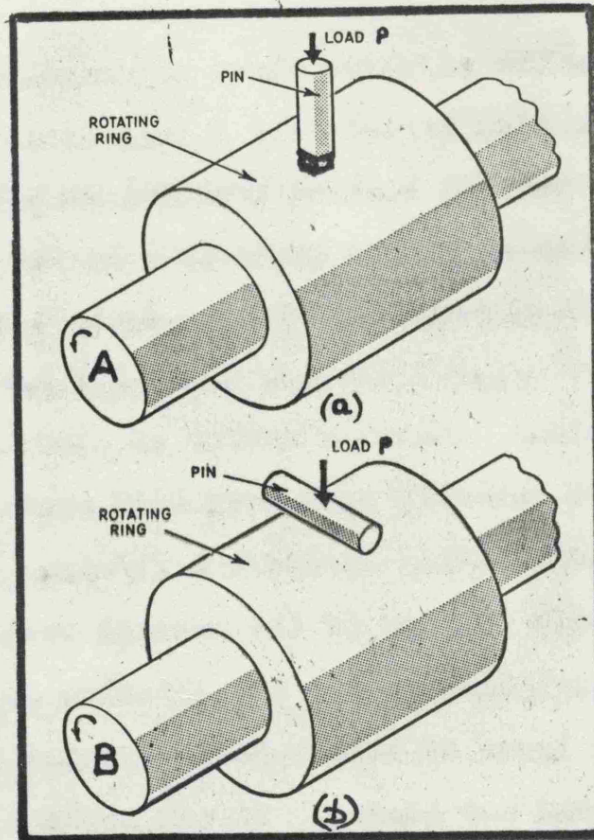


Fig. 4.1 Two arrangements of the pin and ring wear machine.

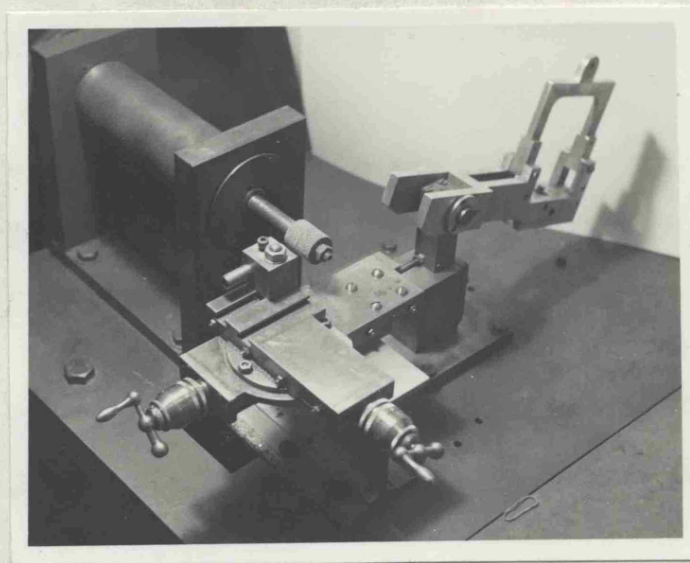


Fig. 4.2 Diamond dressing attachment fitted to the pin and ring wear machine.

details for the abrasive wheel experiments are shown in fig.4.1a; a ring B nominally 1 inch diameter mounted on a shaft A is rotated against a preformed pin C under a load P. The ends of the $\frac{1}{4}$ " diameter steel pins were machined to 0.175" square and then preformed by grinding to a $\frac{1}{2}$ " radius. A square preformed pin was used to ensure that a constant nominal area of contact was maintained since changes in mechanism may be sensitive to pressure. In order to avoid excessive vibration, particularly at high speeds, it was found necessary to dress the abrasive wheels when they were in position on the machine. To this end a small cross slide was fitted (fig. 4.2) the wheels being diamond dressed; a standard procedure was adopted and subsequent wear tests with steel gave reproducible results. The wear of the pin was measured by weighing using a chemical balance; that of the wheel was generally too small to be measured reliably except when using very high loads ~ 10 Kg. High loads produced excessive wear of the abrasive probably due to bond post rupture and crushing of the grits.

For tests with abrasive pins a cross-cylinders configuration was used, fig.4.1b; the wear of the abrasive pin was measured by observing the wear scar on the pin and that of the steel ring by weighing.

Both the pins and rings made from steel had a ground finish and were degreased immediately prior to use.

The tests were carried out, unlubricated.

Table 4.1.

Analyses of the steels used.

B.I.S.R.A. Code.	%C	%Ni	%Cr	%Si	%Mn	%S	%P	V.P.N.
AO	0.025	0.01	0.01	0.001	0.006	0.011	0.002	210
CN	0.63	0.13	0.05	0.24	0.87	0.048	0.04	263
DAK	0.985	0.12	0.07	0.23	0.64	0.05	0.032	350
28%Cr	Ferritic stainless steel					28%Cr		198

4.3 Materials.

A range of both steels and abrasives were tested. Most of the materials listed were used for wear, grinding and scratch tests.

Steels.

The steels were provided by the British Iron and Steel Research Association and their analyses are shown in Table 4.1.

Abrasives.

The abrasive materials, which were supplied by the Carborundum Company Ltd., were in the form of sticks and grinding wheels. Complete details of the materials used are given below.

Abrasive sticks.

$\frac{1}{4}$ " diameter Medium Grade Silicon Carbide (equivalent to C 180 - Q5 - VG).

Grinding wheels.

Aluminium oxide vitrified bonded wheels were used in three grit sizes, hardness and structure being kept constant.

1" diameter wheels for the pin and ring machine

BA36 - L5 - VFBLU.

BA60 - L5 - VFBLU.

BA120 - L5 - VFBLU.

7" diameter wheels for Jones and Shipman 540 surface grinder.

BA36 - L5 - VFBLU.

BA60 - L5 - VFBLU.

AA100 - L5 - VF8.

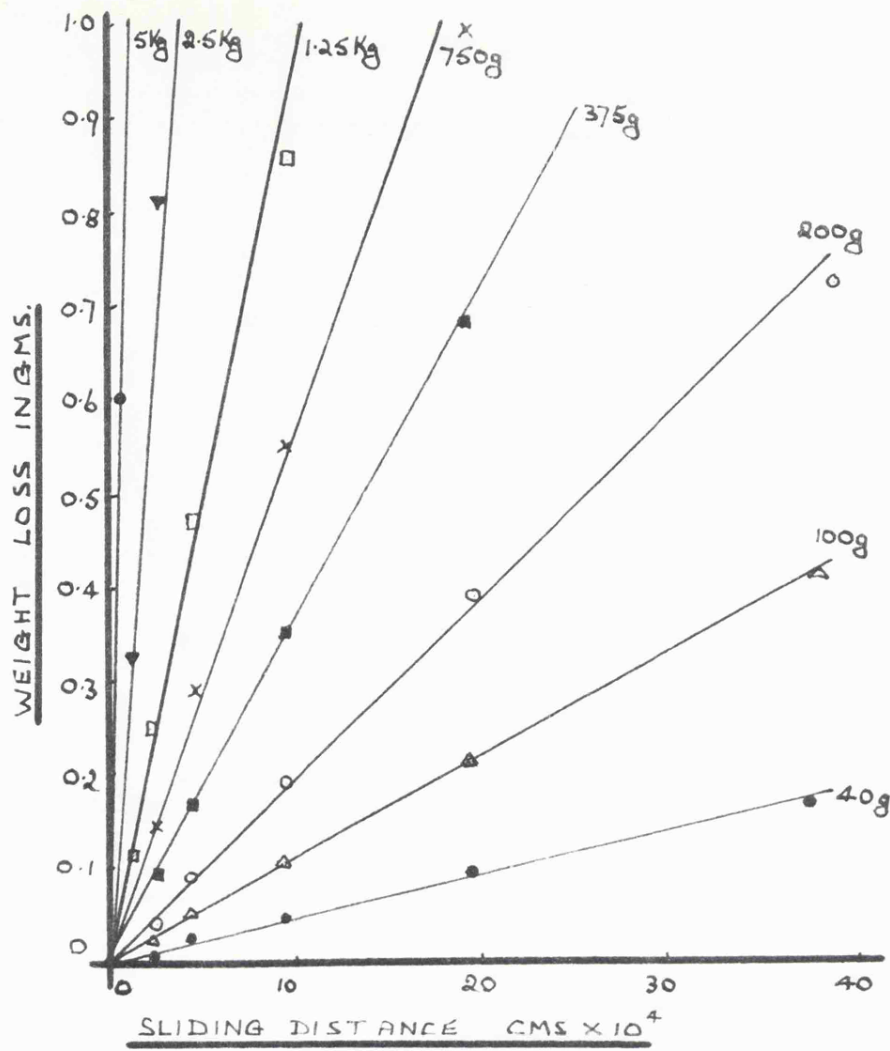


Fig. 4.3 Graphs of wear against sliding distance for 28%Cr Steel pins on 1" diameter 60 grit wheels at various loads, speed 750r.m.

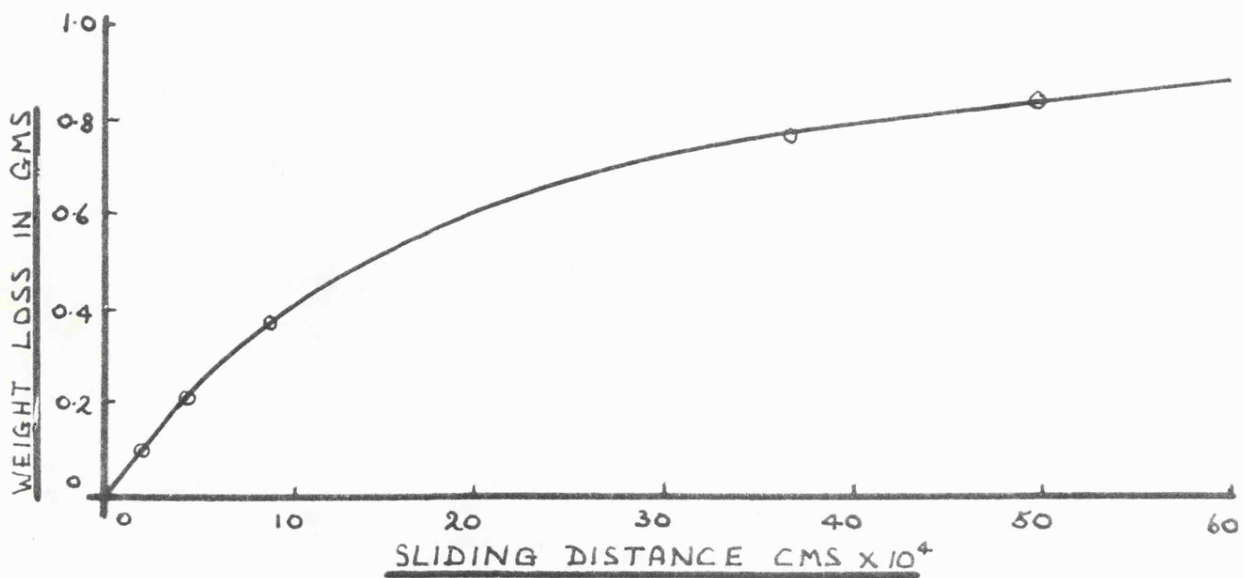


Fig 4.4 Graph of wear against sliding distance for a L.C steel (D.K.K 5) pin on a 1" diameter 60 grit wheel, load 750g, speed 5000r.m.

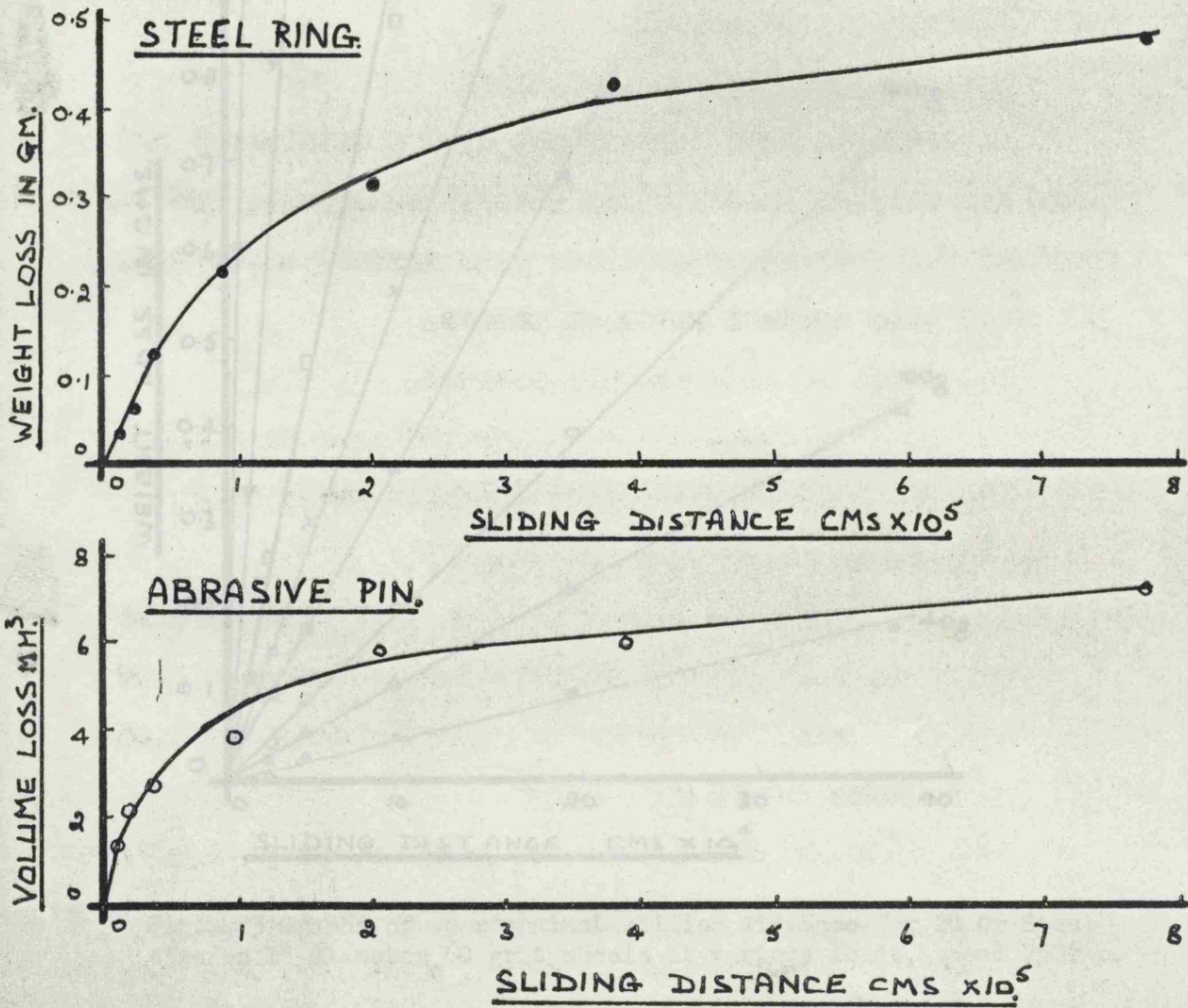


Fig. 4.6 Wear curves of $\frac{1}{4}$ " diameter silicon carbide pin and 1" diameter 0.6% C steel ring rubbing together under a load of 375g and at a speed of 750 rpm.

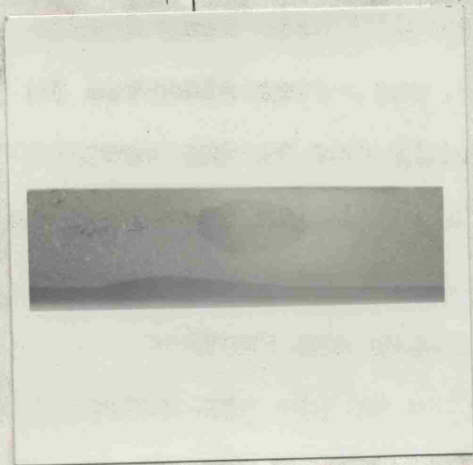


Fig. 4.5 Glazed abrasive pin.

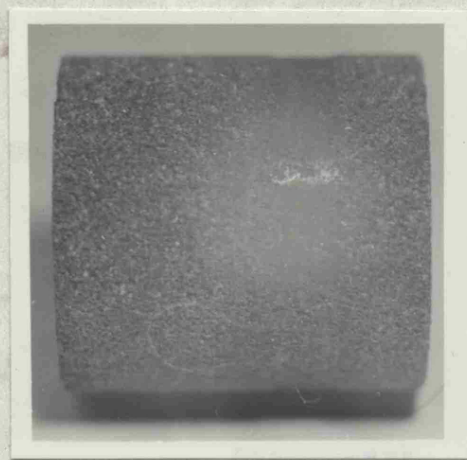


Fig. 4.7 Glazed abrasive wheel.

4.4 Preliminary Experiments.

Wear/Sliding distance behaviour.

Experiments were carried out over a wide range of loads and sliding speeds using several materials; the tests involved the rubbing of abrasive pins against steel rings and steel pins against abrasive wheels.

Two types of wear pattern emerged.

(1) Wear was directly proportional to sliding distance, the wear product being metallic chips (c.f. severe wear).

(2) The wear rate gradually fell with sliding distance. The wear product changed during the test from finely divided metallic debris to finely divided oxidised metallic material (c.f. mild wear).

Generally the abrasive wheel experiments gave linear rates of wear (fig 4.3) but if conditions were particularly unfavourable a progressively changing wear rate was observed (fig 4.4). This decline in wear rate was usually associated with glazing (fig 4.5). Experiments with abrasive pins always showed a reduction in wear rate with sliding distance (fig 4.6); the fall in wear rate was again associated with glazing and clogging of the abrasive with wear debris (fig 4.7). A linear wear rate was never observed in the abrasive pin experiments, probably due to the severity of the conditions. The same area of the pin is always in contact with the steel ring thus clogging and glazing are more likely to occur, effects which are further aggravated by the relatively fine grain size of the pin material (180 grit).

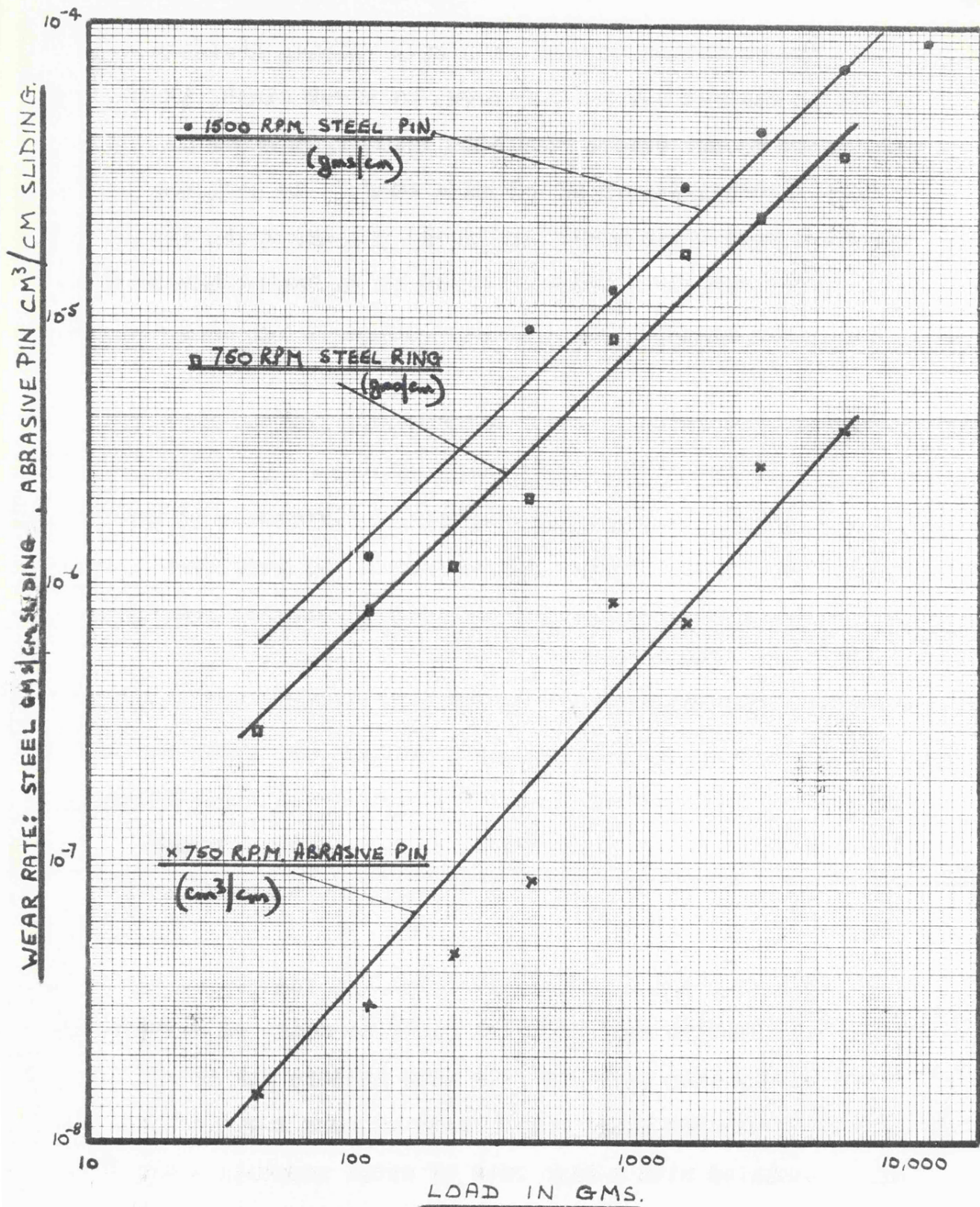


Fig 4.8 Wear rates of 180 grit abrasive pins and 0.6% C steel rings rubbing together under various loads at a speed of 750 rpm; and wear rate of 0.6% C steel pins on 60 grit wheels at 1,500 rpm.

The variation in wear rate with sliding distance shown in Figures 4.4 and 4.6 seem, at first sight, to be analagous to the severe wear/mild transition noted in earlier investigations of adhesive wear. In both the adhesive wear experiments and in the present tests the transition clearly represents a change in the mechanism of wear. For example, when using an abrasive pin (Fig 4.6) the tests started with the abrasive removing metallic particles and the wear rate gradually diminished until, in the final stages, the debris consisted entirely of finely divided oxide. However the important difference is that under abrasive conditions the transition is much more gradual. These more gradual changes in rates of removal, which occur with abrasives, indicate a progressively changing wear situation. At the outset sharp grits cause removal of metallic fragments; at the end the grits are blunt and highly polished and this glazing is accompanied by clogging with oxide debris. The role of different factors in the glazing of abrasive wheels requires further investigation.

In the abrasive pin experiments the wear rates of both the abrasive and the steel could be measured accurately. These showed (fig 4.8) that the wear pattern for both materials was the same; a high rate of wear for the abrasive was associated with a high rate of metal removal; a low rate of wear in the abrasive resulted in a correspondingly low rate of metal removal.

A qualitative assessment of the surfaces produced in the abrasive pin experiments showed that a glazed abrasive

pin was associated with a highly polished steel surface and a free cutting abrasive with a ground finish on the steel surface.

The effects just described in the wear cycle for abrasive pins are very similar to those of the superfinishing process. This process is claimed to "remove the roughness of the ground surface, produce any reasonably selected smoothness, and then automatically cease removing metal". The superfinishing process is normally applied to ground surfaces the object being to improve surface finish. The process is carried out at relatively slow speeds 50 to 60 feet per minute and the same area of the abrasive is continuously in contact with the work under a pressure of about 10 to 40 lbs. per square inch and a low viscosity lubricant is applied. A fine abrasive of about 600 grit is normally used.

The superfinishing cycle has been described as follows (Gisholt Machine Company 1947) :-

When the stone is first applied to the rough surface, it only contacts the ridges. If the correct bond hardness of stone is used it will break down to some extent, thus exposing new and sharp grits which will remove the peaks rapidly in the form of comparatively large chips. As the peaks are reduced the surface becomes smoother and more grits make contact reducing the pressure on the individual grits. Instead of the blunt grits being torn out they now remain in place becoming gradually duller. Metal is now removed in progressively smaller particles; these oxidise

immediately and are deposited in the pores of the abrasive. These deposits aid in the building up of a glazed abrasive surface which will produce a highly polished surface of greatly improved geometry. Finally the abrasive and metal surface effectively "run in", the lubricant forms a fluid film and the removal of metal ceases.

The wear cycles for the two processes just described are virtually identical; the only departure is the terminal stage (no metal removal) which is not shown in the abrasive pin experiments. This may well be due to the conditions used and the fact that finer abrasives are used in superfinishing. Another important difference is the use of a lubricant in the superfinishing process. Initially a lubricant would assist the abrasive process by removing wear debris; however, once two smooth surfaces have formed the lubricant can prevent contact and therefore wear.

The preliminary experiments show that many of the effects observed in the grinding process can be reproduced, using suitable abrasives, on a pin and ring machine. This applies not only to normal grinding processes but also to such specialised processes as superfinishing.

A basic difference between grinding processes and pin and ring experiments is stability. In surface grinding for example, if a grit becomes dull the forces on it increase and it will either be torn out exposing fresh grits or fracture producing new abrasive surfaces. The process is therefore self sustaining; effects such as glazing will only occur when conditions are particularly unfavourable.

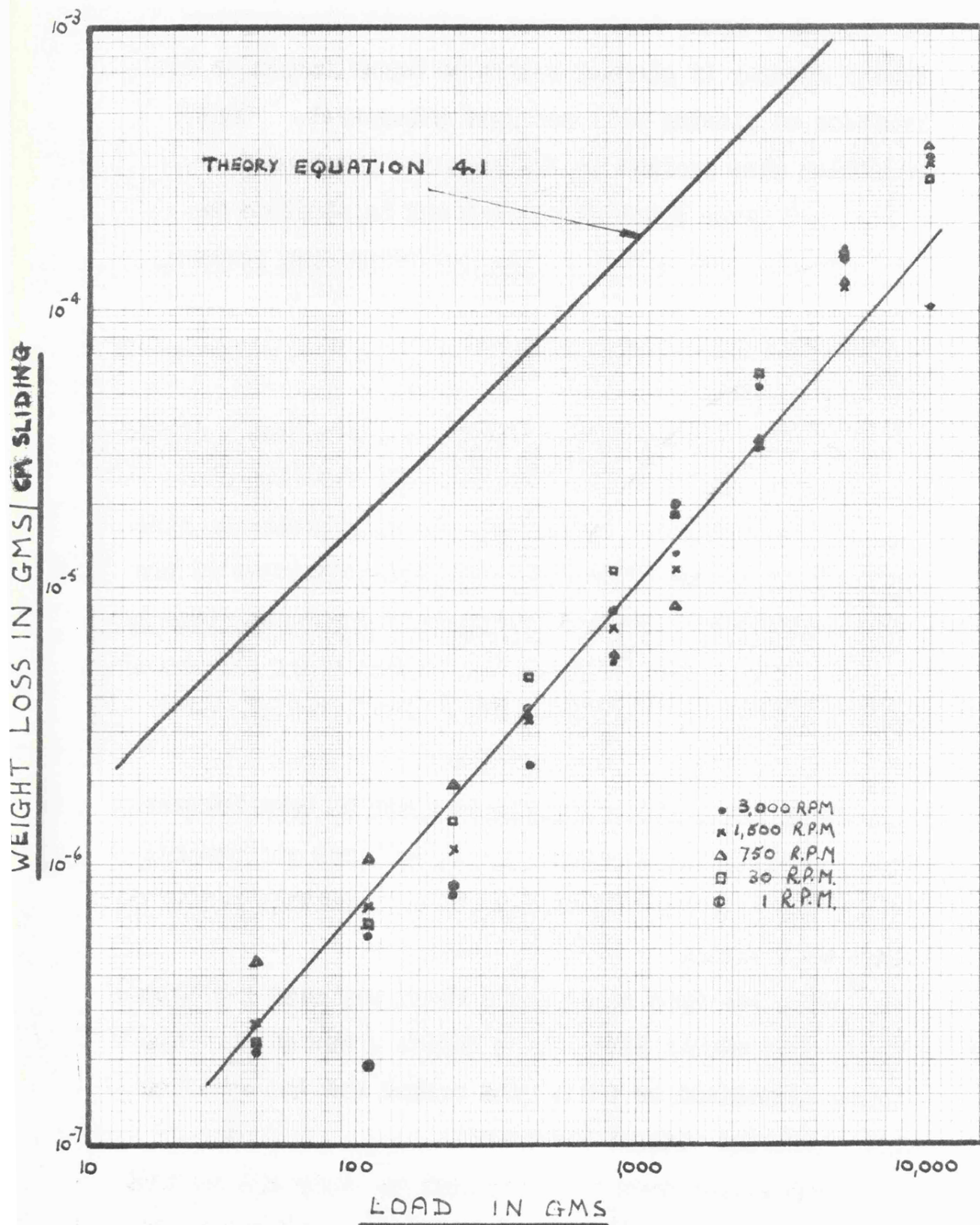


Fig 4.9 Wear rate against load for 28Cr steel rubbing against 60grit wheels at various speeds.

On the other hand, tests using a pin and ring machine favour change; if glazing starts to occur forces do not increase so glazing will continue unhampered. This situation also applies in the recently introduced controlled force grinding process and is utilised to particularly good effect in the superfinishing process.

4.5 Wear rates.

4.5.1 Introduction.

The preliminary experiments had shown that a linear rate of wear could not be obtained with abrasive pins. It was therefore decided to concentrate on experiments with abrasive wheels as these were more representative of the grinding process. Ferritic stainless steel was found to give the most consistent results, so the broad pattern of behaviour will be discussed mainly with reference to this material for which most results were obtained.

Some interesting similarities can be seen between abrasive wheel and abrasive pin experiments particularly when these are compared on the basis of initial rather than final wear rates.

Only one type of abrasive wheel was used for these experiments namely BA60 - L5 - VFBLU. The steels were either normalised or fully cold worked and the experiments were performed without lubricant.

The experiments were designed to study the effects of sliding speed, load, sliding distance, materials and configuration on wear rate. The effects of grit size and heat-treatment on wear rates will be discussed later.

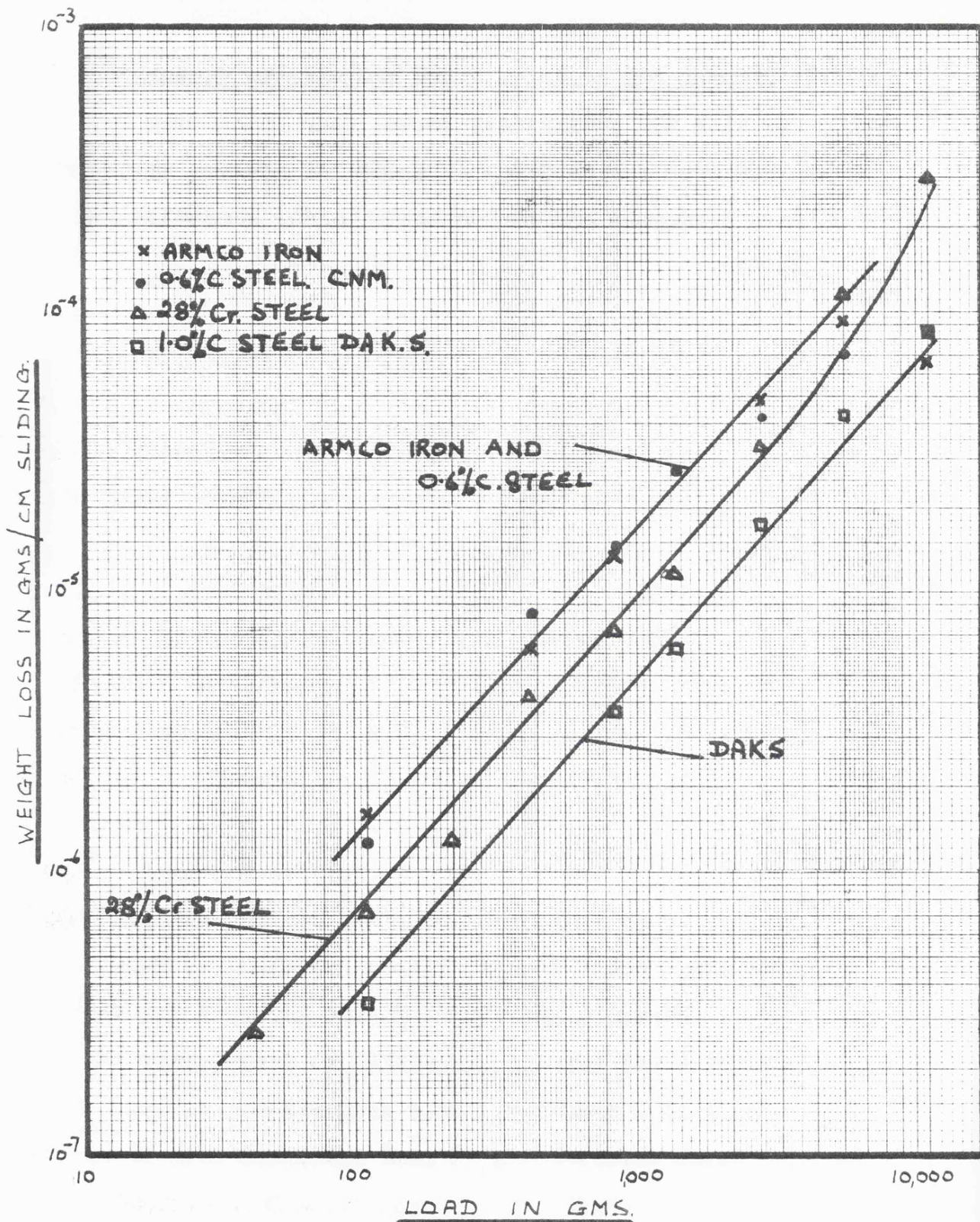


Fig 4.10 Graphs of wear rate against load for a range of steels rubbing against 60grit wheels (1" diameter) at a speed of 1500rpm.

4.5.2 Changes due to load, speed and sliding distance.

As with the preliminary tests, wear rates were determined over a wide range of loads and speeds; the steel pins were preformed and the abrasive wheels nominally one inch diameter.

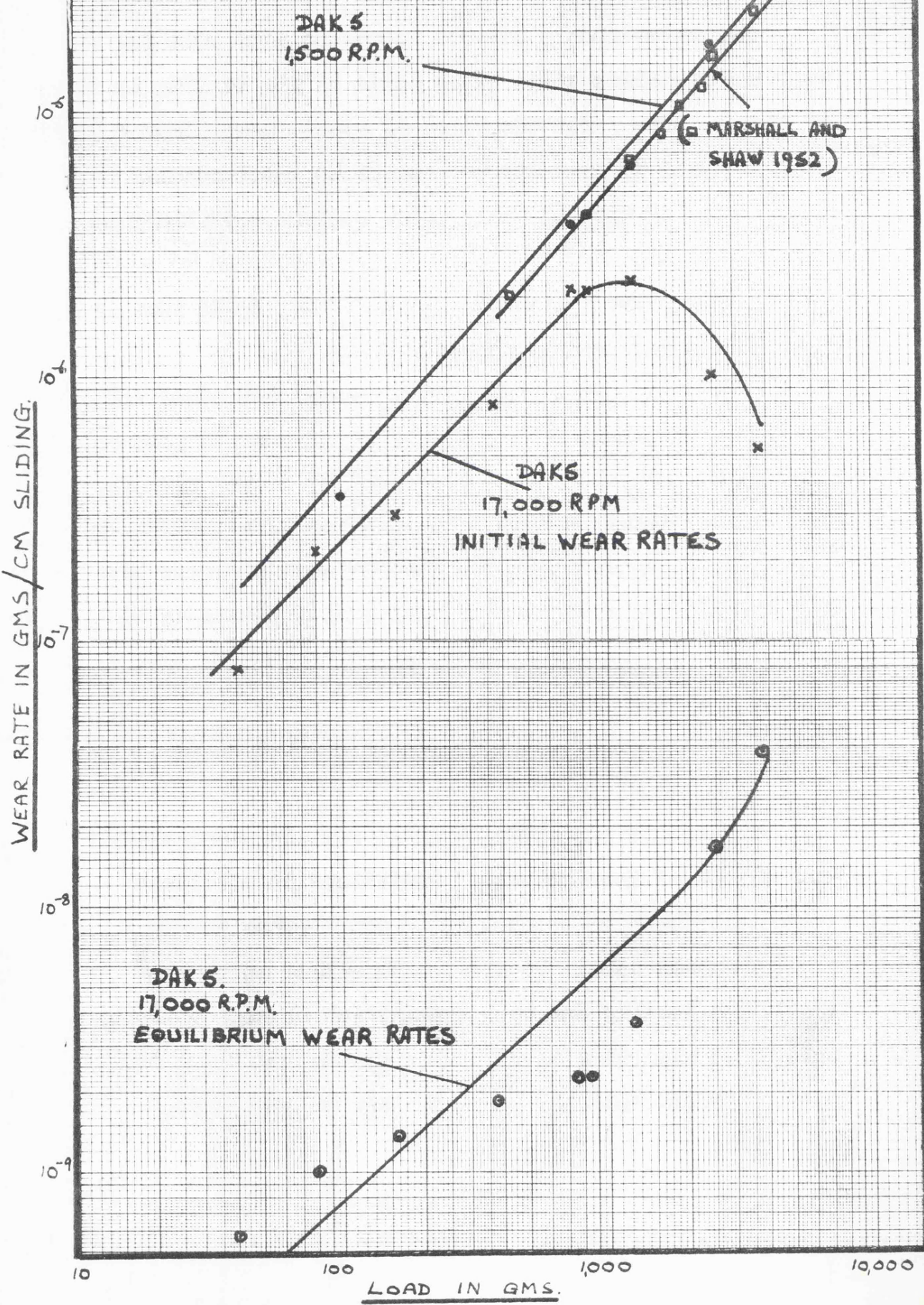
Load.

The effects of load on the wear rate of ferritic stainless steel are shown in figure 4.9; wear rate is almost directly proportional to load. The slight deviation at the heavier loads is probably due to thermal effects, breakdown of the abrasive and vibration.

A comparative set of results for Armco iron, 1% C steel DAK5 and a 0.6% C steel CNM are shown in figure 4.10. These results confirm that over the range of conditions studied, wear rate is directly proportional to load. Moreover even when a transition in the mechanism of wear occurred during the experiment it was found that both the initial and final equilibrium wear rates were proportional to the load. For example, in figure 4.11, this is shown for experiments with the 1.0% C steel DAK 5 running against an abrasive wheel at 17000 rpm. Figure 4.11 also shows the Marshall and Shaw (1952) results for grinding expressed in wear terms; not only is wear rate almost directly proportional to load but the wear rates observed are in good agreement with those for the DAK5 steel at 1,500 rpm. Both these observations provide further support to the idea that grinding is an abrasive wear process.

10⁻⁴

Fig. 4.11 Wear rates of 1% C steel pins rubbing against 60grit wheels under various loads at speeds of 1,500 and 17,000rpm. Marshall and Shaw's (1952) surface grinding results are shown on the same graph for comparison.



Speed.

The relationship between speed and wear rate for the ferritic stainless steel using loads of 40g to 10Kg is shown in figure 4.12. For the range of speeds used (1rpm - 3,000 rpm) the rate of wear can be seen to be substantially independent of speed. Only under extreme conditions is there a tendency for wear rate to be influenced by speed. For example heavy loads/high speeds (10Kg. 3,000 rpm) or at light loads/slow speeds (40g. 1rpm.).

The series of experiments using the 1% C steel DAK5 is of particular interest as these were extended to particularly high speeds (17,000rpm.). They show that even when the speed is increased by more than an order of magnitude from 1,500 rpm. to 17,000 rpm. the initial abrasive wear rate per unit sliding distance falls by only a factor of two. This is demonstrated in figure 4.11 for loads of less than 1 Kg. At 17,000rpm. and loads greater than 1Kg the pin became visibly hot and the wear rate started to fall with further increases in load.

It is concluded that the wear rate is substantially independent of speed provided conditions do not favour a change in mechanism. Changes in wear mechanism are obviously more likely to occur with either extensive frictional heating due to a combination of high speed/heavy load or at the other extreme slow speeds and light loads when a clogging/glazing mechanism may be initiated.

WEAR RATE. (LOSS IN GMS / CM SLIDING)

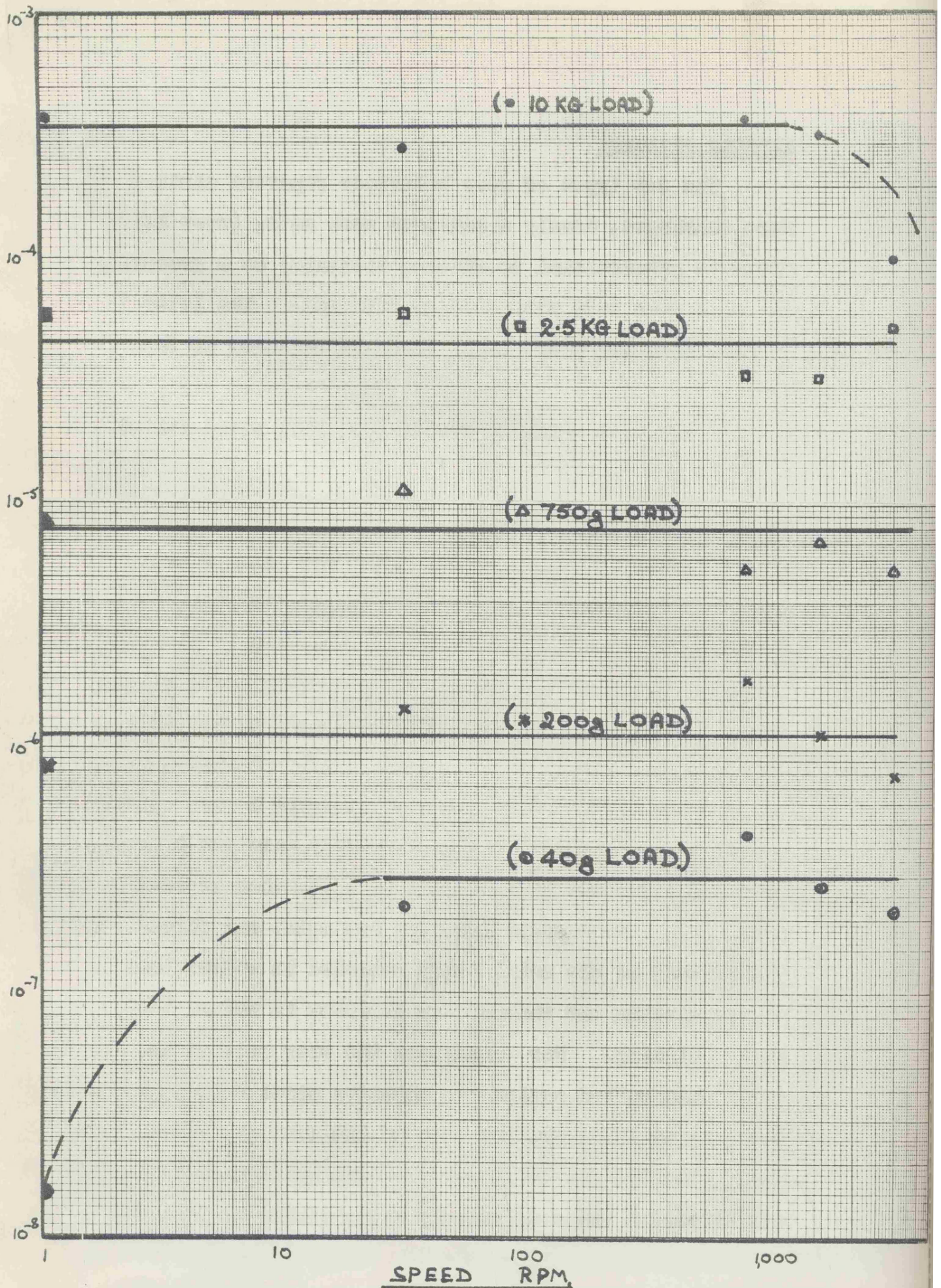


Fig. 4.12 Wear rate against speed for 20Cr steel rubbing against 60grit wheels under various loads.

Sliding distance.

The two types of wear behaviour reported earlier were confirmed, namely a constant wear rate, (wear being directly proportional to sliding distance) or a gradually changing wear rate with sliding distance. The latter type of behaviour was only observed at the extremes of the conditions studied or with abrasive pins; most tests carried out with abrasive wheels gave wear rates directly proportional to sliding distance.

4.5.3. Effects of Configuration.

A series of tests were carried out using a cross cylinders arrangement consisting of a $\frac{1}{4}$ " diameter carborundum pin and a 0.6% C steel (CNM) ring 1" diameter. The tests were carried out at 750rpm. using loads varying from 40g to 10Kg. The wear curves showed a gradual fall in wear rate with sliding distance, the equilibrium wear rates being difficult to assess. However a more sensible result was obtained if the initial wear rate was determined for each curve and then plotted as a function of load (fig 4.8). Wear rates for both the metal and abrasive are shown; that of the metal being recorded in weight loss in gms/cm sliding and that of the abrasive in volume loss cm^3/cm sliding. For comparison the wear rate of the same steel when rubbed against an abrasive wheel BA60 - L5 - VFBLU rotating at 1,500 rpm. is shown on the same diagram. The wear rates for the steel are the same using either configuration and are directly proportional to load.

It is of interest to note that the wear rates of the abrasive pins follow the same pattern as those of the steel. The grinding ratio (ratio of metal removed to abrasive removed) ranges from 3.3:1 with a load of 40g up to 1.7:1 with a load of 5Kg. Hahn (1965) has reported similar values with controlled force grinding when conditions were particularly unfavourable. The high values of grinding ratio are probably accounted for by the unusual test conditions, the same area of the abrasive pin being continually in contact with the work.

4.5.4 Effects of Material.

All the materials used were steels; the hardness range covered was relatively small ($198-356 \text{ Kg/mm}^2$). It was not intended at this stage to make a detailed study of the effects of hardness variations on wear rates.

Each of the materials tested gave a similar pattern of wear behaviour, a typical set of results being shown in figure 4.10. The effects of hardness are not completely consistent but in the range of hardnesses covered the harder materials tend to have the lower wear rates.

4.5.5 Discussion.

Over a wide range of speeds and loads wear rates were independent of speed and directly proportional to load. The results therefore give the type of wear behaviour which is predicted by the wear equation 3.30. To carry out precise predictions the value of the K factor must be known. A value for K was obtained from the results for the ferritic

stainless steel; a theoretical wear curve was produced using the formula,

$$\text{Wear rate} = \frac{K \cdot W \cdot \rho}{2 \cdot P_m \cdot 10^5} \text{ gms/cm sliding.} \quad (4.1)$$

where,

K	=	assumed to be unity.
W	=	normal load in gms.
ρ	=	density of steel 7.9 gms/cm ³
P_m	=	flow pressure Kg/mm ² (198VPM.)

and is shown on figure 4.9. The calculated wear curve assumed $K = 1$ but to reconcile the theoretical and practical curves a value of K in the region of 0.1 to 0.05 is required. The desired value of K could be obtained by altering the numerical values of the parameters from which it is made up (equation 3.31). For example, a value of 0.1 could be assumed for $\cot \theta$ or the values of α and β could be less than unity. Although a value of $\cot \theta = 0.1$ is typical of surface grinding, values of $\cot \theta = 0.25$ were typical of abrasive wear test using a 60 grit wheel. In this instance, it would appear that the value of $K = 0.1$ depends not only on the width depth ratio of the scratches formed but also on the proportion of the scratch volume removed or the proportion of active grits.

Although a linear wear rate was not obtained in the abrasive pin experiments and some abrasive wheel experiments, if the initial wear rates were determined these compared favourably with the linear rates observed

with abrasive wheels. This suggests that the abrasive cuts at the start but conditions are such that the cutting action falls off and a clogged glazed surface results. This surface is similar to that formed on superfinishing abrasives, where conditions are similar to those in the abrasive pin experiments in that the same portion of the abrasive is continuously in contact with the work.

4.5.6 Conclusions.

(1) Two types of wear curve were observed (i) wear increases in a linear manner with sliding distance and (ii) wear rate gradually falls with increasing sliding distance.

(2) For the ferritic stainless steel in particular and to a lesser extent with the other steels, wear was almost independent of speed over a wide range and increased in approximately direct proportion to load.

(3) Over a wide range of speeds and loads metal was removed as metallic particles c.f. severe wear.

(4) At very light loads a mild wear condition was observed characterised by the production of dust or oxide rather than metallic particles c.f. mild wear. The surface of the wheel gradually became glazed.

(5) A mild wear condition was also observed at very high speeds and again the abrasive wheel took on a glazed appearance.

(6) When rates of material removal reported elsewhere in the literature for grinding conditions are re-interpreted as a rate of abrasive wear they agree closely with the wear rates reported here.

(7) Linear wear rates correspond to the grinding process working satisfactorily; the gradual deterioration of the grinding wheel due to glazing is represented by a wear curve. The latter condition is representative of superfinishing.

(8) The wear results obtained using the pin and ring machine show that it is not only possible to simulate the grinding process but to a lesser extent such specialised processes as superfinishing. This implies that the same basic mechanism applies to each process and that each can be interpreted in abrasive wear terms.

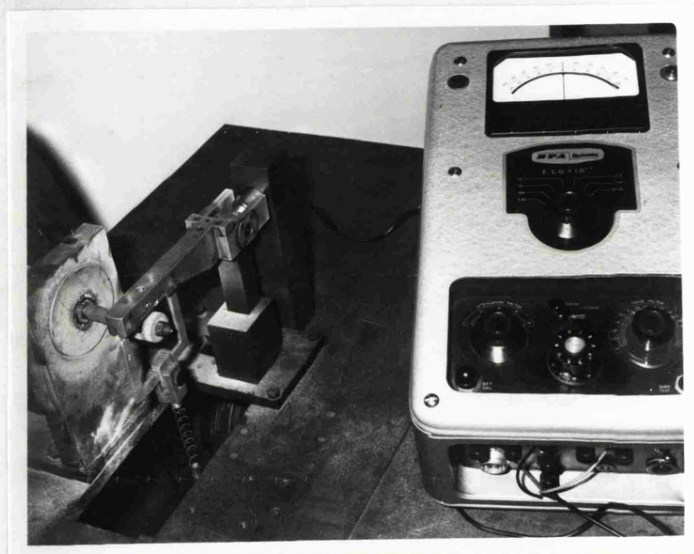


Fig. 5.1 Pin and ring wear machine fitted with a transducer to measure tangential force.

5. Grinding Dynamometer and Associated Tests.

5.1 Introduction.

Both wear tests and a study of the literature have shown that the grinding process could be usefully examined in abrasive wear terms.

Unfortunately there are no recorded experiments involving both grinding and abrasion in which all the parameters for a complete analysis have been measured. It was therefore decided to perform such a series of tests. The measurement of grinding forces involved the construction of a simple grinding dynamometer described later.

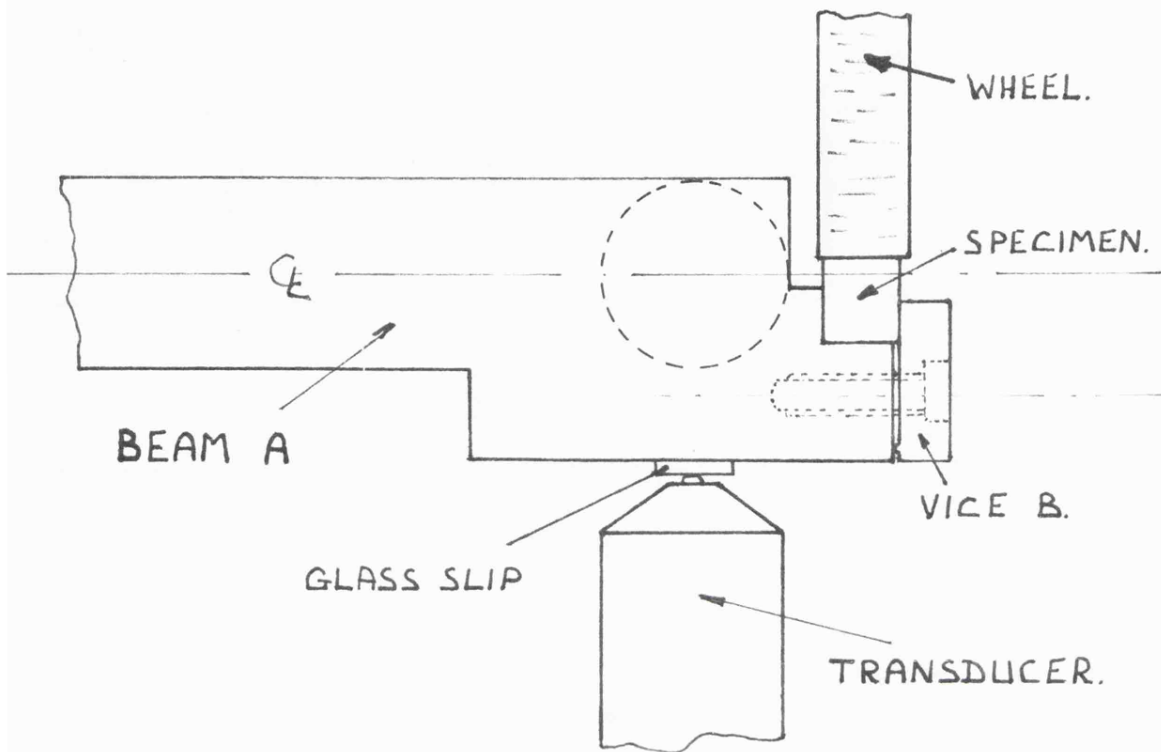
One of the more significant facts revealed by a study of the literature was the anomalous behaviour of hardened steel when abraded and ground. (Abrasive wear tests had shown that hardened steels wear more readily than would be expected whilst grinding experiments indicated similar cutting forces for hard and soft steels.) The present series of experiments were therefore designed to make a particular study of the grinding and abrasion of heat-treated steels of various hardnesses. The effects of grit size on both processes was also included in the programme.

5.2 Apparatus.

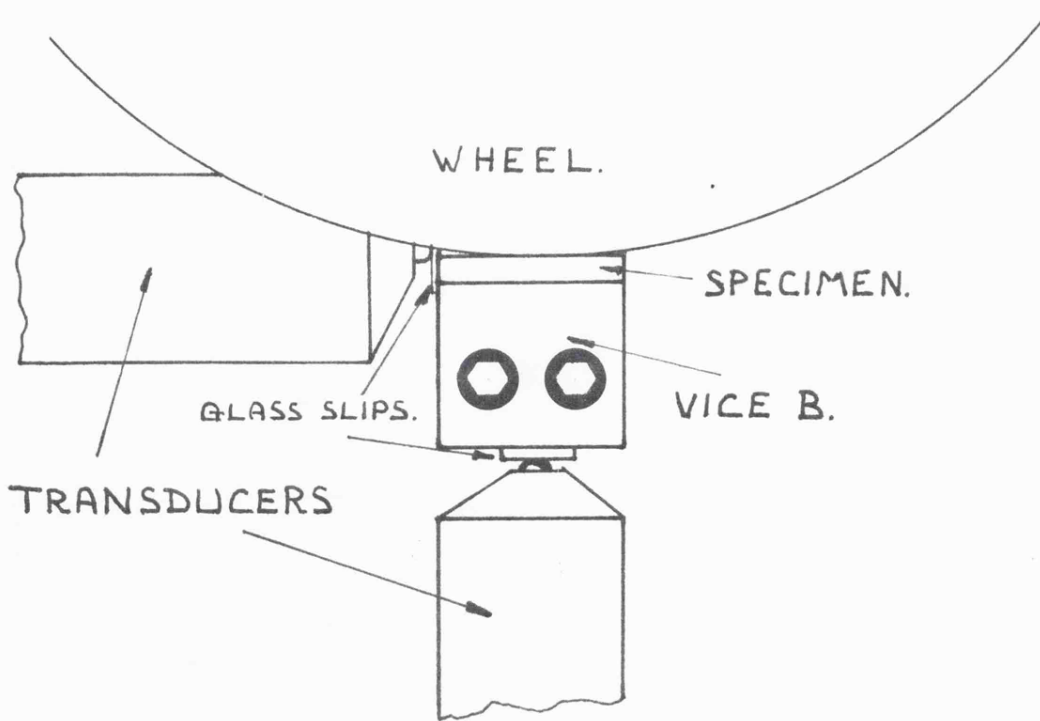
Wear Tests.

Tests using steel pins and abrasive wheels were carried out on the pin and ring machine described earlier. The steel pins were preformed and used in the vertical position (fig 4.1a). The wear of the pin was measured by loss in weight.

DYNAMOMETER.



(a)



(b)

FIGURE 5.2.

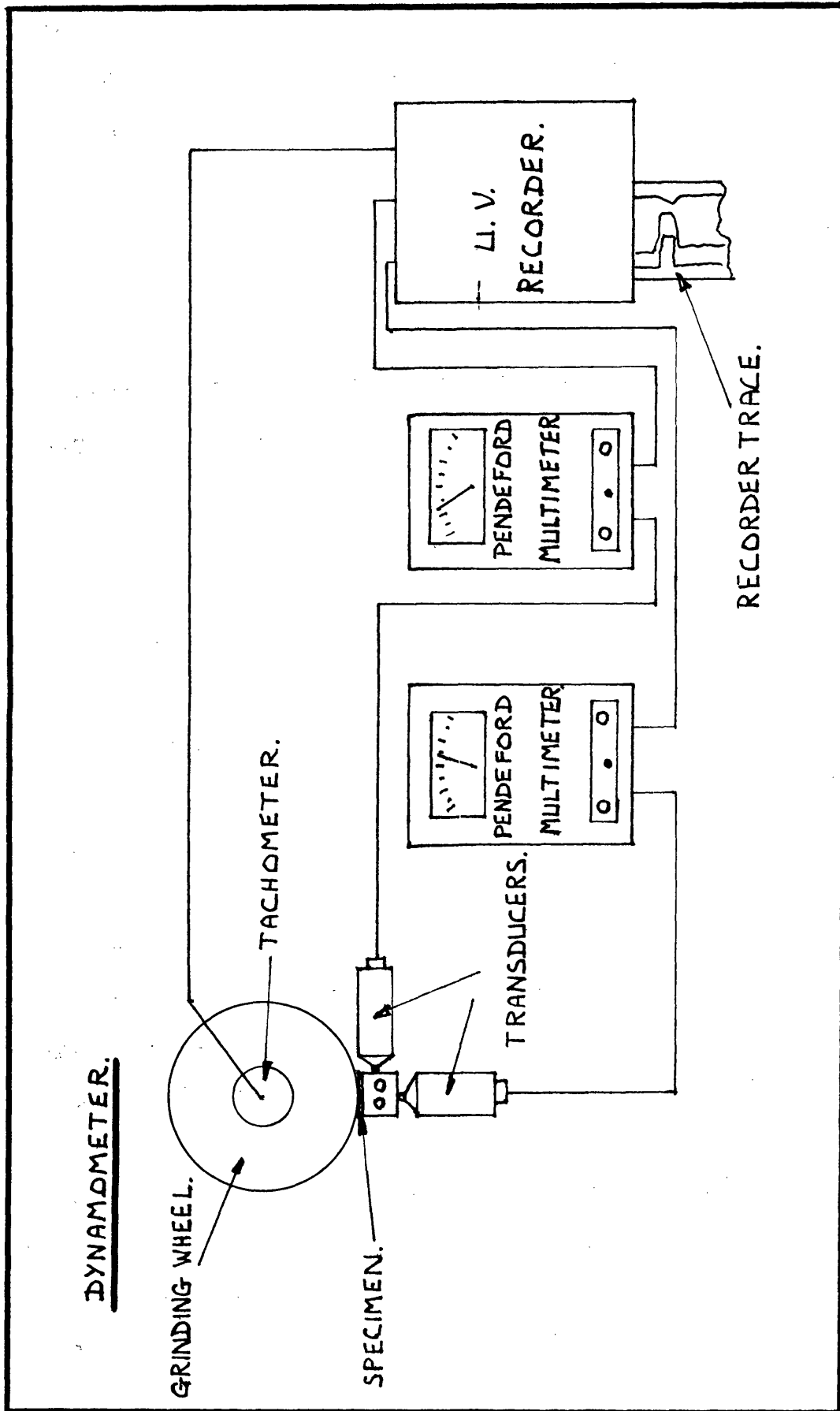


FIGURE 5.3 DYNAMOMETER MEASURING CIRCUIT.

Tangential force was measured during these experiments by observing the deflection of the loading arm by means of a transducer (fig 5.1), the system being calibrated against dead loads.

Grinding Experiments.

Surface Grinder.

All the grinding experiments were carried out on a Jones and Shipman 540 Surface Grinder. The only modification to the machine was to fit a tachometer to the grinding wheel shaft to monitor wheel speed. The output from the tachometer was displayed on a Honeywell U.V. Recorder.

Grinding Dynamometer.

General layouts of both the dynamometer and measuring circuits are shown in figures 5.2 and 5.3.

The dynamometer consists of a simple cantilever A with an integral vice B which holds the specimen. When the specimen is in place the surface to be ground is at the neutral axis of the cantilever; this arrangement was adopted to reduce twisting of the beam. The vertical and horizontal displacements of the beam under load were observed by two transducers C and D positioned at right angles to one another and locating against two glass flats. The transducers were connected to two Pendeford Multimeters whose outputs were in turn fed into a Honeywell U.V. Recorder. (fig 5.4). The dynamometer was calibrated against dead loads when in position on the surface grinder (fig 5.5). Interference between the horizontal and vertical force measurements was negligible. Calibration was checked at the beginning and end of each series of experiments.



Fig. 5.4 Photograph showing the dynamometer complete with measuring equipment, consisting of two Pendeford multimeters and a U.V. recorder.

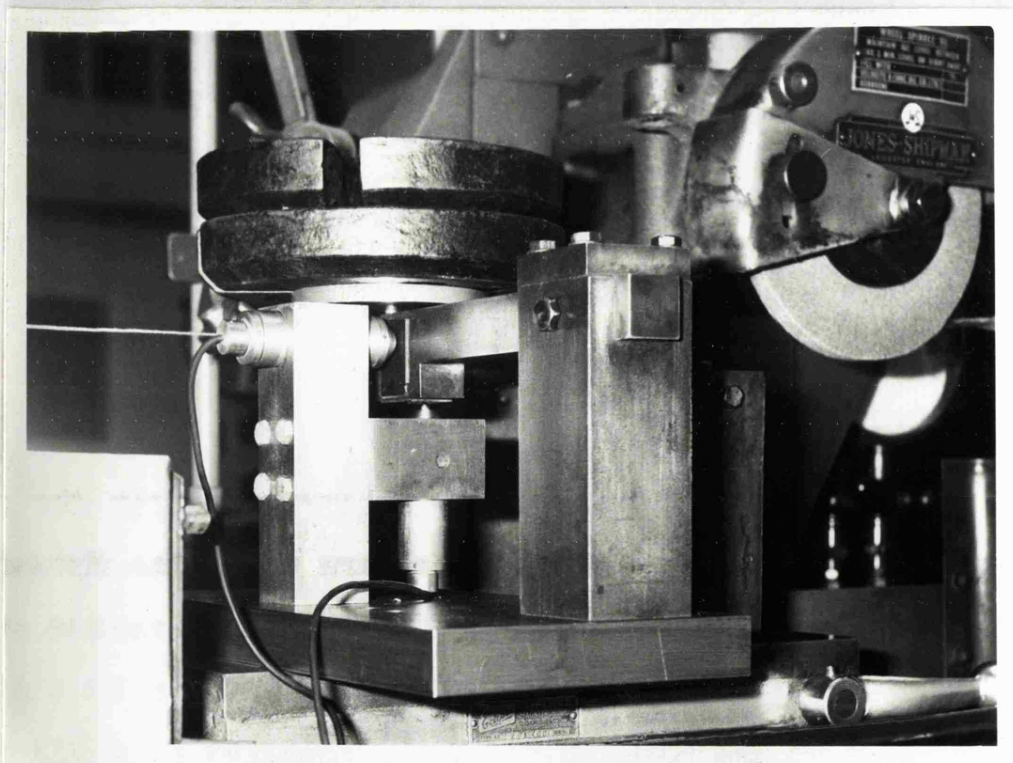


Fig. 5.5 Calibration of dynamometer in position on the surface grinding machine.

Table speed was obtained by measuring the time taken to make a cut from the U.V. Recorder trace and since specimens of known length were used the average table speed could be calculated.

5.3 Materials.

The grinding wheels used are listed in 4.3; the one inch diameter wheels for the pin and ring machine and the seven inch diameter for the surface grinder.

The specimens for surface grinding were 0.375" square by one inch long; preformed pins were used for the abrasive wear tests. The same range of materials was used to manufacture both types of specimen.

Steels.

DAK5 0.985%C. Hardened and Tempered to the following hardnesses.

890 V.P.N.	710 V.P.N.	573 V.P.N.
445 V.P.N.	314 V.P.N.	257 V.P.N.
Bright Drawn Mild Steel	184 V.P.N.	
Annealed Mild Steel.	112 V.P.N.	
Stellite 100.	823 V.P.N.	

5.4 Experimental Procedure.

5.4.1 Grinding Dynamometer.

A period of half an hour was allowed for both the grinding machine and measuring equipment to warm up. The dynamometer was calibrated at the start and finish of each series of tests. Wet grinding conditions were used for all the tests and the transducers on the dynamometer were protected from the coolant (Soluble oil, mixed 1 : 40 with water). The grinding wheels

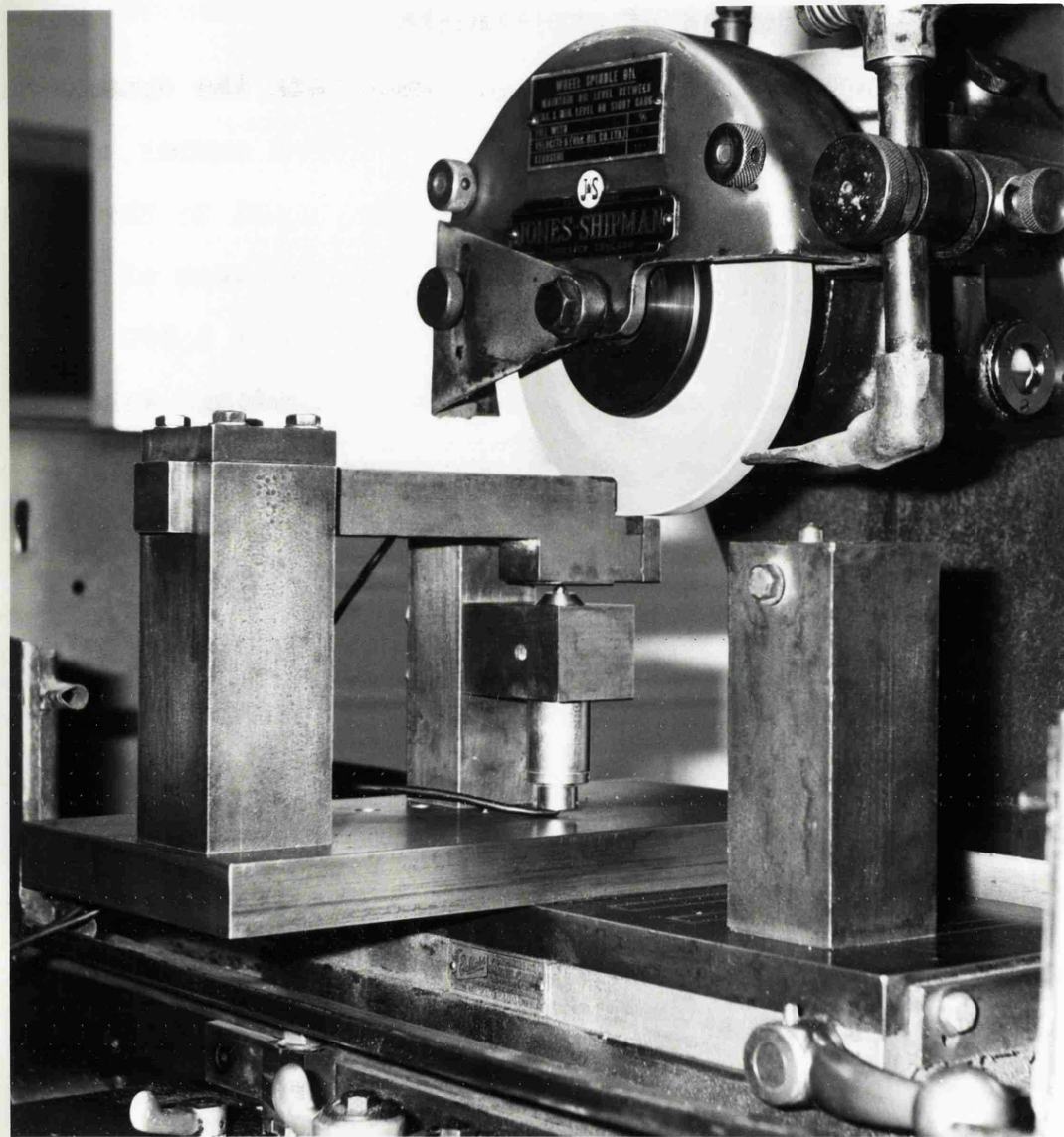


Fig. 5.6 Photograph of dynamometer passing under the grinding wheel as a cut is being made.

were diamond dressed; a standard procedure was adopted to ensure consistent results. As a further check hardened DAK 5 specimens ($p_m = 890\text{Kg/mm}^2$) were used as a control, force measurements being made with this material at the beginning and end of each series of experiments.

When a cut was put on the specimen both the dynamometer and the grinding machine deflected so that a number of cuts had to be taken before the down feed was equal to the material being removed. For the conditions used for most of the experiments (0.0003" depth of cut, wheel speed 2,800 rpm. and a table speed of $\sim 50'$ /min.) steady force readings were obtained after 40 passes. Force measurements were therefore taken after forty successive traverses; both the up and down cut forces were measured, a record being taken using the U.V. Recorder. The dynamometer is shown in action in fig.5.6; and a typical recorder trace in figure 5.7. A Talysurf trace was taken from each of the ground specimens using a X500 horizontal magnification and an appropriate vertical magnification; the width/depth ratio of a typical scratch was then determined by sampling the results.

Another specimen of the same material which had just been ground was then fitted into the dynamometer; this specimen had a micropolished surface. The grinding wheel was clamped to prevent rotation and then brought into contact with the specimen, the wheel was lowered until the dynamometer indicated the same normal load as recorded in the grinding test. The table was moved past the wheel by hand, force measurements being taken with the U.V.Recorder. Talysurf traces were taken

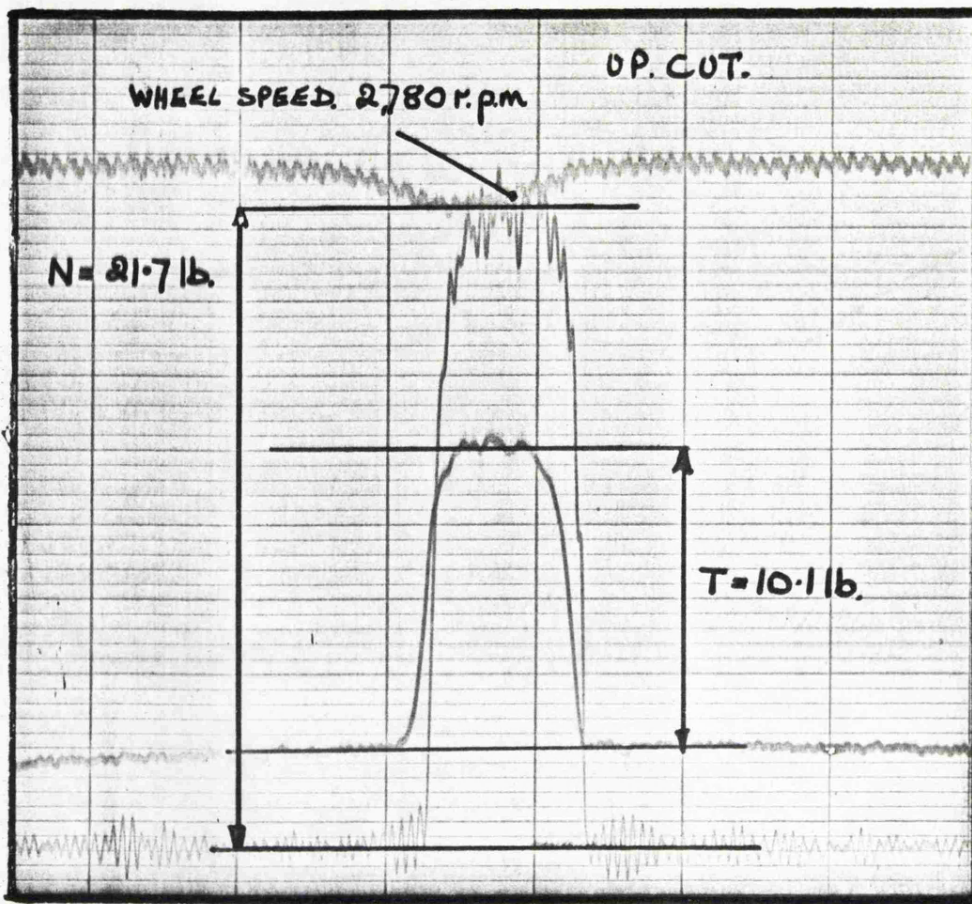


Fig. 5.7 Typical U.V. recorder trace, material hardened 1% C steel, wheel depth of cut 0.0003", table speed 50ft/min.

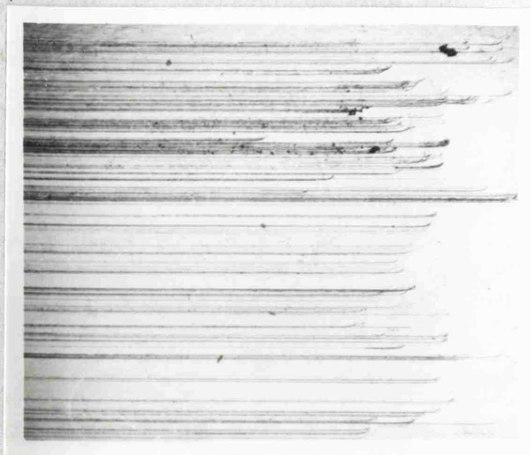


Fig. 5.8 Scratched 1% C steel specimen, X 18.

and the scratches examined microscopically. A typical scratched specimen is shown in figure 5.8.

5.4.2 Wear Tests.

The wear tests were carried out dry at a speed of 750rpm. the wear being measured after a run of one minute. Since the standard grinding conditions gave similar normal forces with all materials tests were carried out using an average normal force of 18 lb. A few tests involved a range of normal loads; these are described separately. Tangential forces were also measured in most of the experiments.

5.5 Results.

Grinding.

5.5.1 Effects of grit size and workpiece hardness.

The first series of experiments was arranged to study the effects of abrasive grit size and workpiece hardness on grinding forces and grinding coefficient.

Tests were carried out using three grit sizes (36, 60 and 100 grit) and workpiece hardnesses ranging from 250Kg/mm² to 890Kg/mm² (DAK 5 steel hardened and tempered). Grinding conditions were kept constant throughout the tests (0.0003" wheel depth of cut, 50 ft/min. table speed and a wheel speed of 2,800 rpm.).

The complete set of results for hardened and tempered DAK 5 is shown in figure 5.9; normal force, tangential force and grinding coefficient are plotted as a function of hardness. The results show that grinding forces are only slightly

NORMAL AND TANGENTIAL GRINDING FORCES FOR HARDENED AND TEMPERED DAKS STEEL.

CONDITIONS:

WHEEL DIAMETER 7 INCHES, WHEEL SPEED 2,800 R.P.M.
 DEPTH OF CUT 0.0003 INCHES, TABLE SPEED 50 FT/MIN.

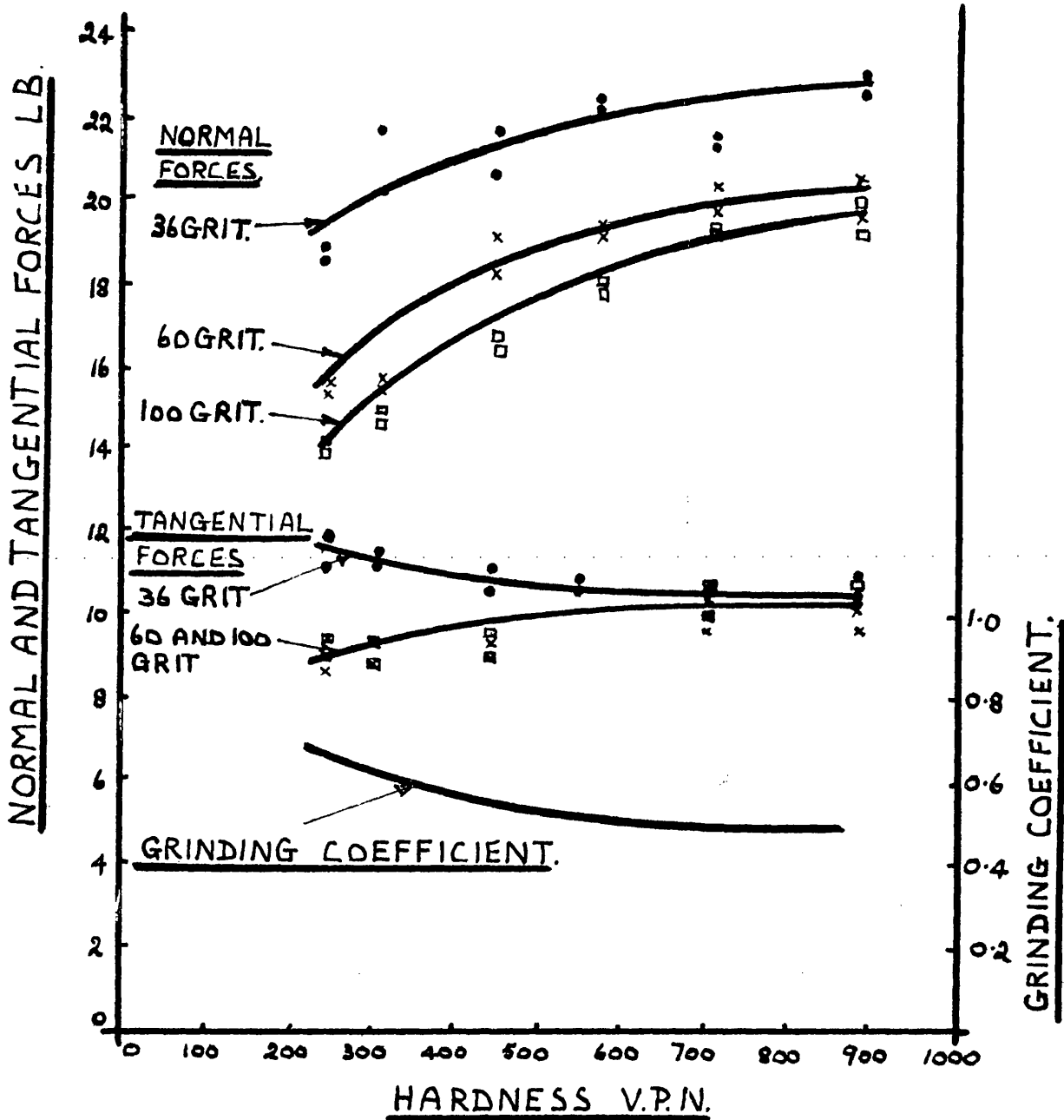


FIG. 5.9

dependent on hardness; reducing hardness by a factor of 3.5 reduces normal force by 15% with the 36 grit wheel, 20% with the 60 grit wheel and 30% with the 100 grit wheel. These reductions in normal force are partly associated with changes in grinding coefficient; reducing the hardness of the work-piece increases the grinding coefficient from ~ 0.5 to ~ 0.7 , higher values of grinding coefficient reduce both wheel and table speed with a corresponding drop in normal force.

Grit size can be seen to have some influence on normal force, the coarsest grit wheel giving the highest forces. These differences were found to be due mainly to variations in width/depth ratio for the three grinding wheels (determined from both the ground and scratched specimens as shown in table 5.1). Results from the two types of test show reasonable agreement and the mean width/depth ratio (although width/depth ratios are more difficult to determine from grinding than from scratching) can be seen to fall as grit size gets finer. This trend supports the experimental observations of normal grinding force (fig 5.9); theory predicts lower forces with smaller width/depth ratios. Width/depth ratio measurements also help to explain the particularly large drop in normal force observed with the 100 grit wheel when grinding soft steel (250Kg/mm^2). The hardened DAK5 specimen used as a control showed no change in the normal force with the 36 grit and 60 grit wheels. However, with the 100 grit wheel normal force obtained at the end of the test was 15% less than the original value. The width/depth ratio remained the same for all experiments with the 36 grit and 60 grit wheels but dropped by 12.5% with the

Table 5.1.

The relationship between the width/depth ratio obtained from ground specimens and scratched specimens for a number of abrasive wheels.

Wheel	Width/depth ratio		
	Grinding	Scratching	Average
36 grit	13.3 : 1	14.4 : 1	13.8 : 1
60 grit	13.7 : 1	12.8 : 1	13.3 : 1
100 grit	14.1 : 1	11.7 : 1	12.9 : 1

Table 5.2.

A comparison of observed and predicted normal forces for fully hardened and hardened and tempered DAK5 steel using a range of abrasives.

Wheel	Normal force lb.			
	Hardened specimen p_m = 890Kg/mm ²		Soft specimen p_m = 250Kg/mm ²	
	Observed	Predicted	Observed	Predicted
36 grit	22.2	22.3	19.0	4.98
60 grit	19.7	20.6	15.5	5.35
100 grit	20.1	20.8	14.1	4.83

100 grit wheel. One would therefore expect lower normal forces from the wheel having the smallest width/depth ratio.

5.5.2 Force predictions based on dynamometer tests.

The grinding conditions quoted in figure 5.9 are nominal and to calculate grinding forces the individual measurements appropriate to each experiment will be used.

Specimen calculations will be made for the grinding of fully hardened DAK5 ($p_m = 890\text{Kg/mm}^2$) with each grit size of wheel. In all calculations it is assumed that α and β are unity so that divergences between theoretical and experimental values should be capable of explanation by assuming other values of these parameters.

36 grit wheel.

Wheel diameter	6.581"	Width of specimen	0.375"
Normal force (average)	22.2 lb.	Wheel depth of cut	0.0003"
Wheel speed (average)	2,769 rpm.		
Table speed (average)	52.6 ft/min.		
Width/depth ratio	16.3 : 1 grinding	average	14.8 : 1
	13.4 : 1 scratching.		

Substituting in equation 3.41.

$$\begin{aligned}
 N &= \frac{10,830 \times 52.6 \times 0.0003 \times 0.375 \times 890}{6.851 \times 2,769 \times 1 \times 1 \times 0.135} \text{ lb.} \\
 &= \underline{22.3 \text{ lb.}}
 \end{aligned}$$

60 grit wheel.

Wheel diameter 6.765"	Width of specimen 0.375"
Average normal force 19.65 lb.	Wheel depth of cut 0.0003"
Wheel speed (average) 2,790 rpm.	
Table speed (average) 51.25 ft/min.	
Width/depth ration 14 : 1 grinding	
14 : 1 scratching	average 14 : 1

Substituting in equation 3.41

$$N = \frac{10,830 \times 51.25 \times 0.0003 \times 0.375 \times 890}{6.765 \times 2,790 \times 1 \times 1 \times 0.143} \quad 1b$$

$$= \underline{20.6 \text{ lb.}}$$

120 grit wheel.

Wheel diameter 6.843"	Width of specimen 0.375"
Normal force (average) 20.1 lb.	Wheel depth of cut 0.0003"
Wheel speed (average) 2,753 rpm.	
Table speed (average) 51.6 ft/min.	
Width/depth ratio 16 : 1 grinding	
12 : 1 scratching.	average 14 : 1

Substituting in equation 3.41

$$N = \frac{10,830 \times 51.6 \times 0.0003 \times 0.375 \times 890}{6.843 \times 2,753 \times 1 \times 1 \times 0.143} \quad 1b$$

$$= \underline{20.8 \text{ lb.}}$$

The same calculations were repeated for the completely softened DAK5 ($p_m = 250\text{Kg/mm}^2$) and these results are presented with those already shown in table 5.2.

GRAPH SHOWING THE VARIATION OF NORMAL GRINDING FORCE WITH TABLE SPEED FOR HARD AND SOFT STEEL (DAKS).

CONDITIONS:

WHEEL DIAMETER 7 INCHES.
WHEEL SPEED 2,800 R.P.M.
DEPTH OF CUT 0.0003 INCHES.

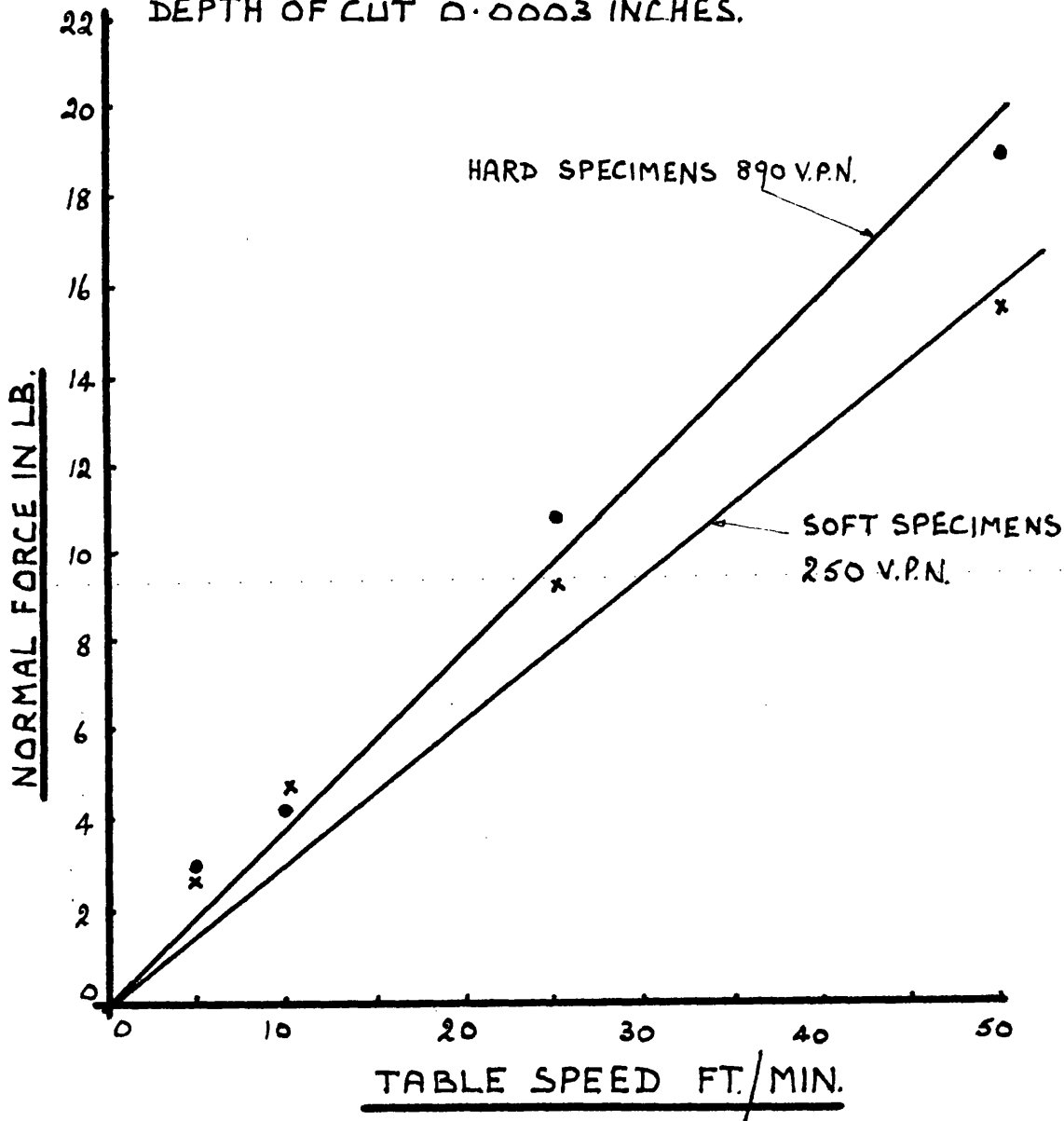


FIG. 5.10

The relationships between observed and predicted forces are very similar to those developed earlier when applying grinding theory to results available from the literature (namely predicted and observed forces are in good agreement for hard materials but with soft materials there is a marked divergence). As the hardness of the workpiece falls, the difference between observed and predicted force will increase. With completely soft DAK5 ($p_m = 250\text{Kg/mm}^2$) for example the predicted force is only $\sim 30\%$ of the observed force.

5.5.3 Grinding of Mild Steel and Stellite.

Specimens of mild steel in the bright drawn ($p_m = 184\text{Kg/mm}^2$) and annealed ($p_m = 112\text{Kg/mm}^2$) conditions were ground to study the effects of cold work on grinding force. Using the standard conditions (0.0003" depth of cut, 50ft/min table speed, 60 grit wheel and plunge grinding) both the bright drawn and annealed specimens gave similar normal forces; ~ 18 lb. These results are similar to those observed by Kruschov and Babichev (1960) who when abrading a range of materials on abrasive papers found that cold work did not increase wear resistance.

Experiments were carried out on Stellite as this is a material which is intrinsically hard ($p_m = 823\text{Kg/mm}^2$) unlike a steel which requires heat-treatment. The normal grinding force was particularly high ~ 90 lb when using the standard conditions. Grinding coefficient on the other hand was low, typically 0.19. It was noted that the grinding wheel exhibited slight glazing. The high forces were partly

WEIGHT LOSS OF A RANGE OF MATERIALS WHEN
RUBBED AGAINST ABRASIVE WHEELS (DIAMETER 1")
FOR ONE MINUTE AT 750 R.P.M. UNDER A LOAD
OF 18 L.B.

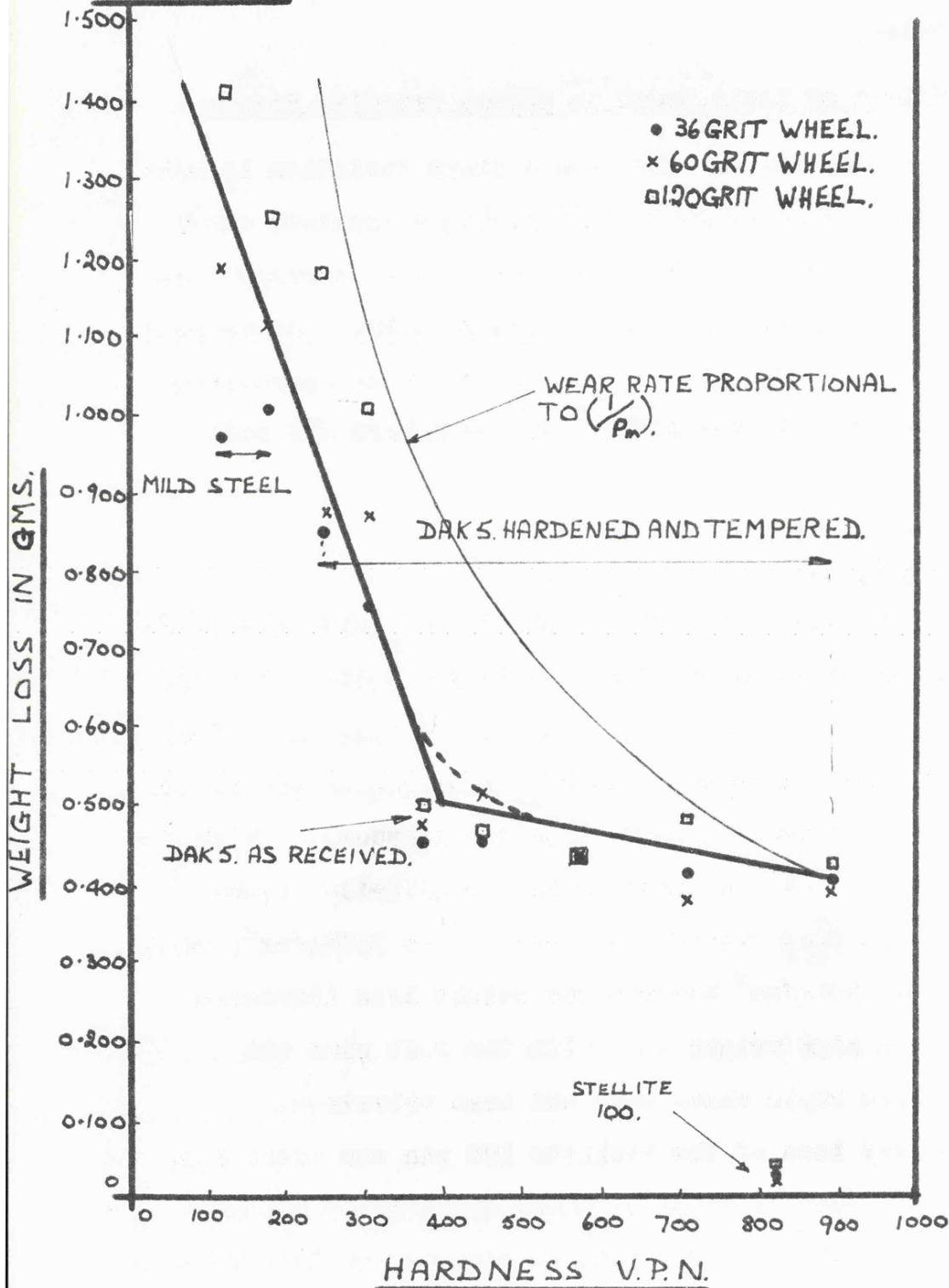


FIG 5.11.

accounted for by the high value of the width/depth ratio 35 : 1. Normal force predictions were 42 lb, only about 50% of the observed value.

5.5.4 Effects of Table Speed on Normal Grinding Force.

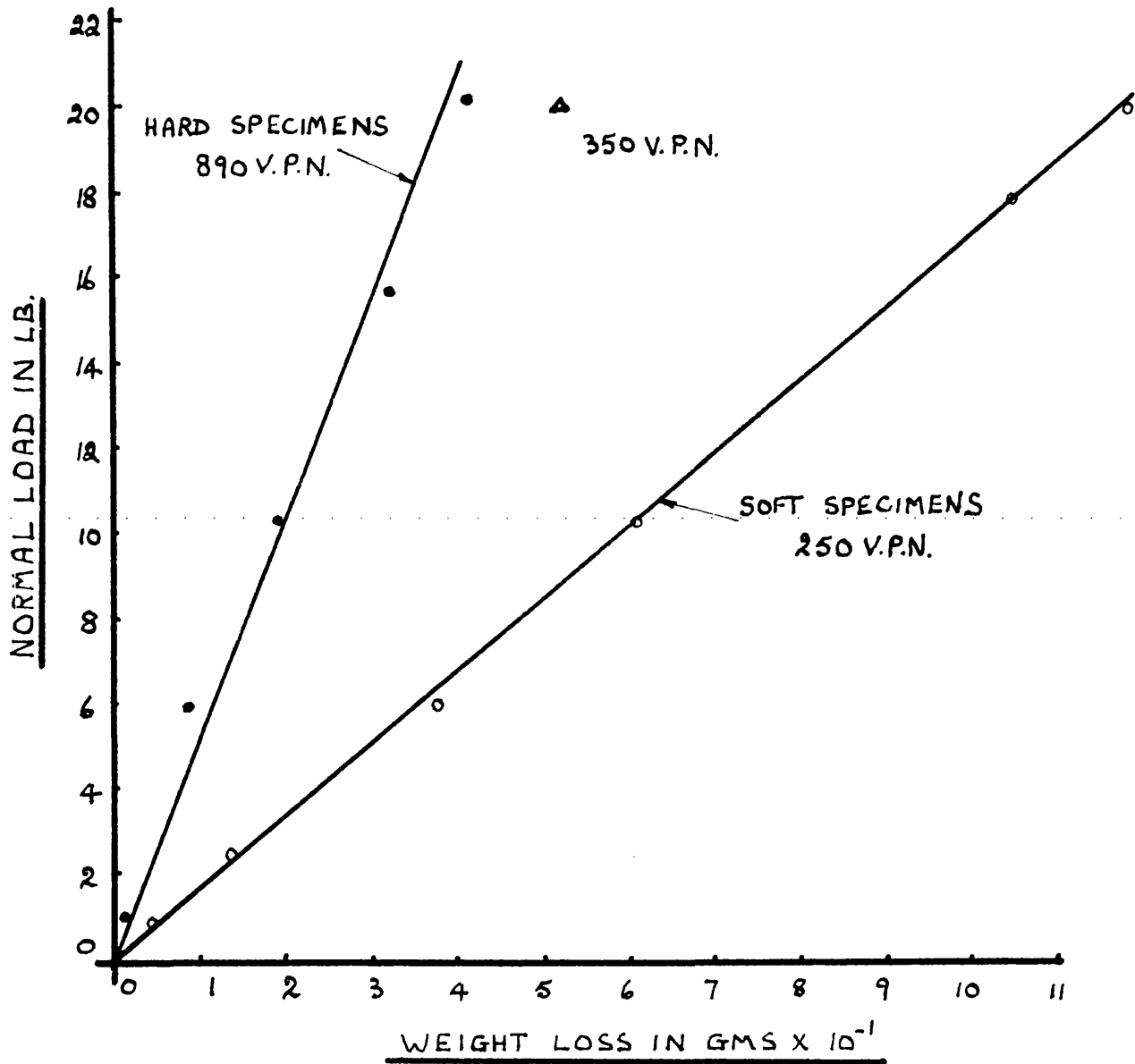
The simplest way of achieving a large variation in metal removal rate on a grinding machine having a constant wheel speed is to vary table speed. The results of varying table speed on normal force are shown in figure 5.10. As would be expected from wear theory normal force shows an approximately linear variation with table speed for both hard and soft materials.

5.5.5 Wear Tests.

Wear test results for the range of materials used in the dynamometer experiments are shown in figure 5.11. All the tests were carried out using a speed of 750 rpm., a load of 18 lb and one inch diameter wheels. The results are plotted as weight loss in grams against specimen hardness. With the DAK5 pins the weight loss only increases slightly as the hardness of the pins falls from 890Kg/mm² to 350Kg/mm²; below a hardness of 350Kg/mm² however the weight loss increases rapidly. The high weight loss with the soft pins was associated with rapid wheel wear and some vibration.

The weight loss of the Stellite 100 pin was small compared to that of the steel specimens. This observation is consistent with the large normal grinding force recorded by this material when compared with steel.

WEIGHT LOSS OF HARD AND SOFT DAK 5 PINS
RUBBING AGAINST A 60 GRIT WHEEL: WHEEL
SPEED 750 R.P.M., WHEEL DIAMETER 1", DURATION
OF RUN 1 MINUTE.



Δ 350 V.P.N. RESULT SHOWN FOR COMPARISON THIS BEING THE LOWEST HARDNESS BEFORE THE WHEEL STARTS TO BREAK UP AND VIBRATION BEGINS.

FIG. 5.12.

Table 5.3

A comparison of the grinding and friction coefficients with materials of different hardnesses and with a range of abrasives.

Material and hardness	Grinding and Friction Coefficients			
	36 grit wheel	60 grit wheel	*100-120 grit wheel	
	Grinding Friction	Grinding Friction	Grinding Friction	Grinding Friction
DAK5 hardened and tempered.				
890 VFN.	0.48	0.51	0.43	0.54
710 "	0.49	0.56	0.42	0.54
573 "	0.48	0.55	0.48	0.56
445 "	0.51	0.49	0.52	0.58
314 "	0.54	0.65	0.80	0.98
250 "	0.56	0.88	0.88	0.93
EDMS, 184 VFN	0.68	0.97	0.93	0.93
Annealed mild steel 112 VFN.		0.93	0.93	0.93
Stellite 100		-	0.36	-
823 VFN.		-	0.19	0.34

* Grinding coefficient 100 grit wheel, friction coefficient 120 grit wheel.

The weight losses of both cold worked and annealed mild steel were similar; again there was rapid wheel wear and some evidence of vibration.

To simulate the effects of changing table speed in surface grinding tests were carried out using progressively smaller normal loads; the results of these tests are shown in figure 5.12. With both the hard and soft materials weight loss falls in a linear manner with reduction in normal force. However the results show certain discrepancies with materials having a hardness below 300VFN. (see fig 5.11) probably due to rapid wheel wear and vibration. Discrepancies in this area occur in other tests and are discussed later.

5.5.6 Friction measurements.

The coefficient of grinding and the coefficient of friction were measured in the majority of experiments; the values for a wide range of hardnesses and different abrasive grit sizes are shown in table 5.3. The main feature of the results is that both grinding coefficient measured in the dynamometer tests and coefficient of friction measured in the wear tests increase steadily as hardness falls, the coefficient of friction showing the greater increase. With the exception of the softest materials, when the coefficient of friction was higher, both coefficients had similar values in comparative tests.

5.6 Discussion.

The dynamometer performed satisfactorily and the results produced were in good agreement with those of other workers reported earlier (Chapter 2). When grinding theory was applied to the present results good agreement was obtained with hard materials but soft materials showed considerable error. These inconsistencies are the same as those observed when the theory was applied to results available from the literature (Chapter 3).

Both wear and grinding theories are critically dependent on the value of the width/depth ratio of the scratches formed on the abraded surface. When obtaining the value of this ratio from, for example, a Talysurf trace the finer the scratches taken into account inevitably the smaller the value obtained for the width/depth ratio. Since in the present experiments the value of the width/depth ratio for both ground and scratched specimens are substantially the same the validity of the technique is not in doubt.

It was particularly reassuring to see the pattern of behaviour observed with the dynamometer repeated in the wear tests. For example, Stellite 100 was difficult to grind giving large normal forces and a low grinding coefficient. The corresponding wear tests showed that the material was wear resistant and had a low coefficient of friction. The anomalous behaviour of the softest materials is thought to be due to the rapid wheel wear and vibration which was observed with these materials. Vibration itself tends to increase

wear and the rapid breakdown of the wheel probably produces particularly sharp grits again increasing wear rate.

It is of interest to note that the wear rates in the tests with hardened steel ($6.7 \times 10^{-5} \text{ gm/cm sliding}$) were similar to that in the grinding experiments using the standard conditions ($5.76 \times 10^{-5} \text{ gm/cm sliding}$).

5.7 Conclusion.

(1) The grinding dynamometer worked satisfactorily and gave results similar to those of other workers.

(2) The method of determining width/depth ratio in the grinding experiments agrees with the results deduced from scratch tests.

(3) Grinding force predictions are accurate with hard materials but with soft materials the calculated forces assuming α and β are unity are as low as 25 to 30% of the observed values.

(4) Materials which are difficult to grind show good abrasion resistance and vice versa.

(5) Within the limited range of experiments carried out, grinding force and wear rate are unaffected by cold work.

(6) Friction measurements show the same behaviour pattern in both wear and grinding; grinding and friction coefficients are greater with soft than with hard materials.

6. Scratch tests with Rockwell and Vickers Indentors.

6.1. Introduction.

The fact that abrasive wear theory depends critically on the relationship between the abrasive grits and the scratches which they produce has stimulated a number of practical investigations of the mechanism of scratching using idealised cutting tools. Earlier, when discussing this work (2.4) it was pointed out that the majority of investigators used soft materials ($p_m = 10\text{Kg/mm}^2$ to $p_m = 200\text{Kg/mm}^2$) and tools with 90° face angles; such a tool gives a width/depth ratio of 2:1 when cutting at zero rake angle. These conditions are quite different from those occurring in grinding; a process usually applied to hard materials the width/depth ratio of a typical grinding scratch being 20:1. So that even ignoring the effects of speed, the conditions in grinding are very different from those used in the scratch tests reported in the literature.

The most critical feature of scratch tests, which a study of the literature leaves unresolved, is the possibility of metal removal by a cutter having a negative rake angle. Earlier theories of abrasive wear assume that the normal load is carried on the frontal facets of the grits and that such grits remove material; obviously if negative rake grits do not remove material then the basis of such theories of abrasive wear will be in question. On the other hand the work of Mulhearn and Samuels (1962) and Sedriks and Mulhearn (1963 and 1964) implies that grits with rake angles lower than

a critical value, close to zero, displace but do not remove material; material removal is then almost entirely due to grits with positive rake angles.

In the experiments reported below the scratching of materials having a wide range of hardness ($p_{1a} = 20\text{Kg/mm}^2$ to 890Kg/mm^2) was studied. In these tests the Vickers Diamond indenter and the Rockwell cone were used. Although these tools were used because of their ready availability they also have the merit that their width/depth ratios are similar to those of grinding scratches.

6.2 Apparatus and Materials.

A few exploratory experiments were carried out using the Vickers Projection Microscope Micro-hardness tester, the indenter being tracked across a micropolished specimen by means of the micrometer screws fitted to the microscope stage. In order to eliminate manual tracking of the indenter and to allow tangential force to be measured if required the majority of experiments were performed on a sliding friction machine (described elsewhere Archard 1956) with a mechanically driven stage; speed 4cms per minute.

The specimens were 1" X 0.375" square, the surface to be scratched being prepared to a micro-polished finish.

Materials.

0.9% C Steel (DAK5) Hardened and tempered to the following :-
 890VFN.
 710VFN.
 598VFN.
 441VFN.
 315VFN.
 263VFN.

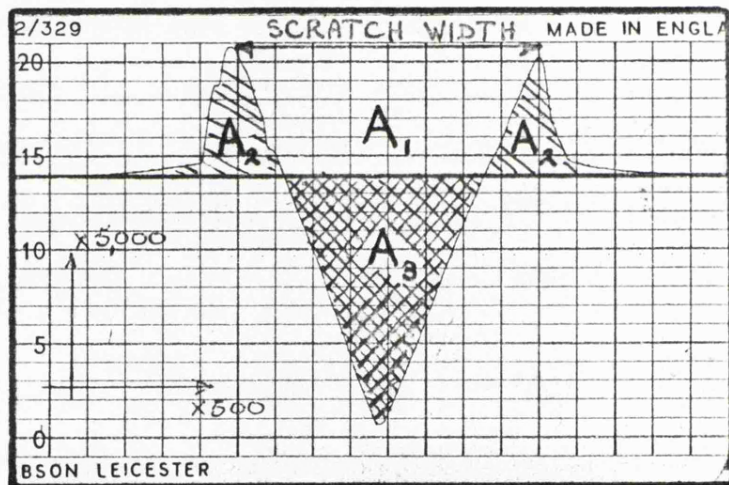


Fig. 6.1 A typical scratch showing pile-up, material Stellite 100, Vickers indenter edge-first orientation, load 2Kg.

<u>0.2% C Steel (BDMS)</u>	223VFN.
as above annealed	120VFN.
<u>Copper</u> (Bright Drawn)	102VFN.
(Annealed)	50VFN.
<u>Aluminium</u> (Bright Drawn)	40VFN.
(Annealed)	20VFN.
<u>Stellite 100.</u>	823VFN

6.3 Experimental Procedure.

A series of single scratches was formed on each specimen using both the Rockwell and Vickers, the latter being tracked using both the facet forward and the edge forward configurations. The scratches were then examined optically and a number of Talysurf traces were taken across each scratch using a X100 and X500 magnifications and the appropriate vertical magnifications. The Talysurf trace was used to measure the scratch width, including pile-up, as indicated in figure 5.1, and the amount of metal removed.

A study of the literature suggests that there exists some confusion about methods of characterising the geometry of the scratch. This is best understood by reference to a typical scratch, shown in figure 6.1, upon a surface which was originally optically smooth. Consider a scratch of unit length having the cross section shown. The volume of material displaced is equal to the area A_3 but, of this material, a volume equal to the area A_2 is retained upon the surface as piled-up material. Thus the volume of material removed (wear) is equal to $(A_3 - A_2)$. On the other hand, as already

RECIPROCAL OF THE SCRATCH WIDTH SQUARED
 $(\frac{1}{2a})^2$ AGAINST HARDNESS FOR A RANGE OF
MATERIALS.

CONDITIONS: ROCKWELL CONE,
 2 KG. LOAD.

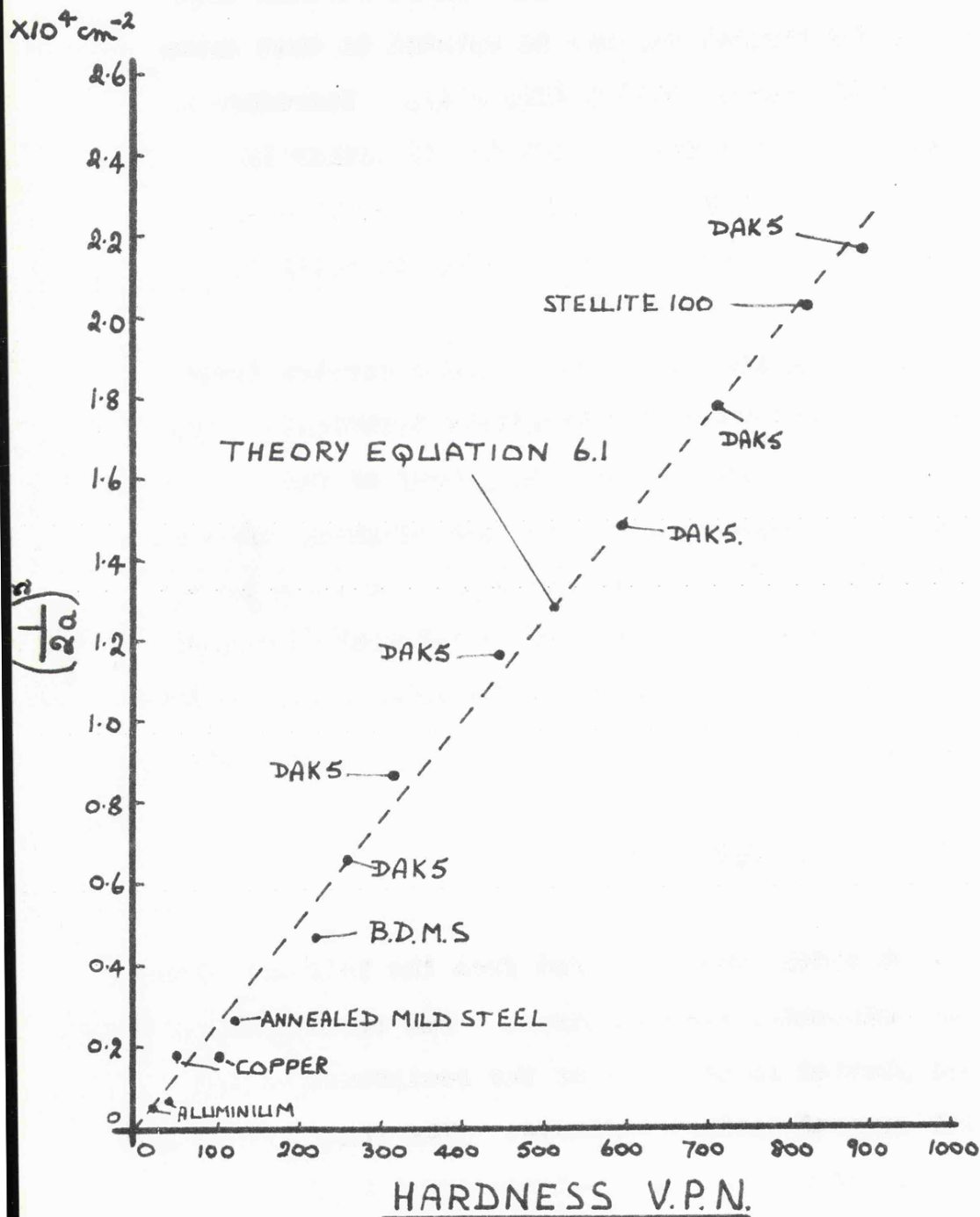


FIG. 6.2.

discussed, abrasive wear theory is concerned with the load supported upon the frontal regions of the indenter. To simplify the subsequent discussion it will be assumed that the pile-up in the frontal regions is related to that shown at the sides of the final scratch (fig 6.1). Therefore in terms of wear theory (Chapter 3), and in particular in connection with the factor β , one is concerned with the total scratch volume; this, in our example, is equal to $(A_3 + A_1)$.

In assessing the results of the present scratch tests the results were analysed by the following technique. The three volumes were obtained by cutting a copy of the Talysurf record into appropriate areas and weighing these on a chemical balance. The results are expressed below as the material removed either as a fraction of material displaced $\mathcal{G} = (A_3 - A_2)/A_3$, or as a fraction of the total groove volume $\beta = (A_3 - A_2)/(A_3 + A_1)$.

6.4 Results of Single Scratches.

Rockwell.

The scratch widths were measured from the Talysurf traces taken at X500 horizontal magnification. The results are shown in figure 6.2 plotted in the form of the reciprocal of the scratch width squared against hardness. The figure shows that the experimental results are in good agreement with theoretical values of the scratch width based upon the assumption that the load is supported only on the frontal half

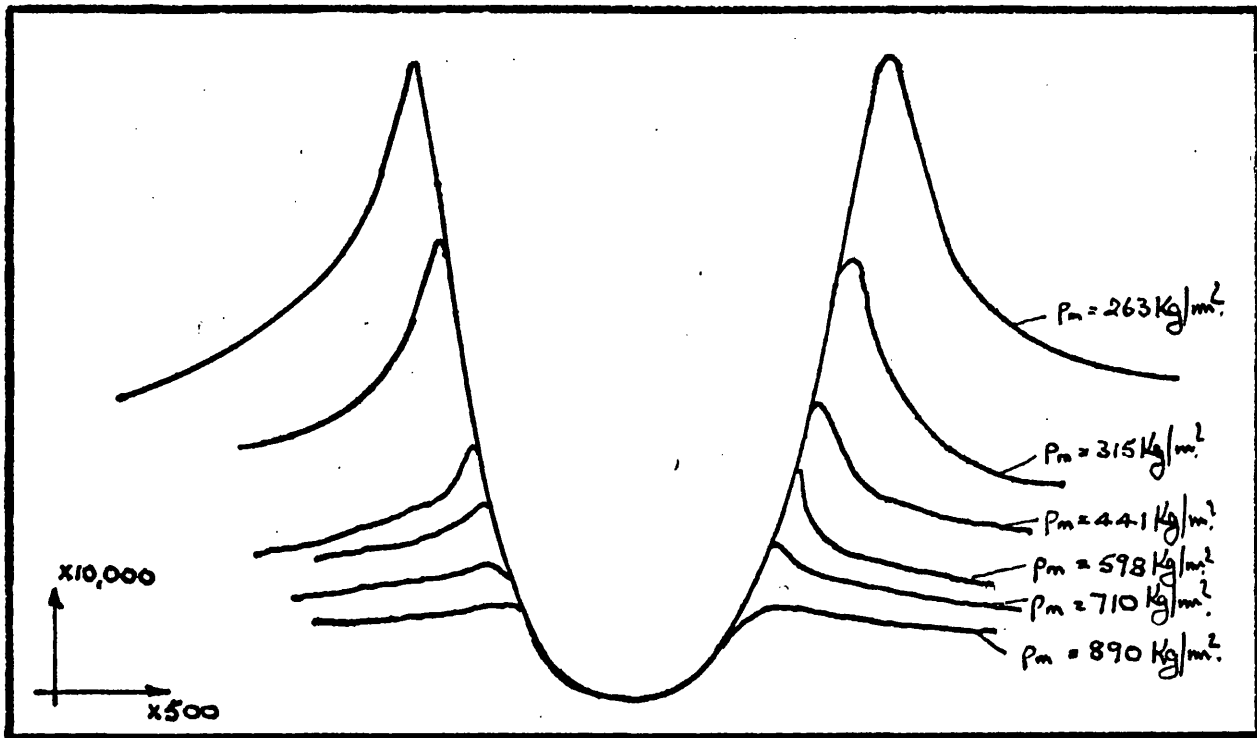


Fig. 6.3a Composite picture of a series of Rockwell scratches in hardened and tempered 1% C steel, load 2Kg.

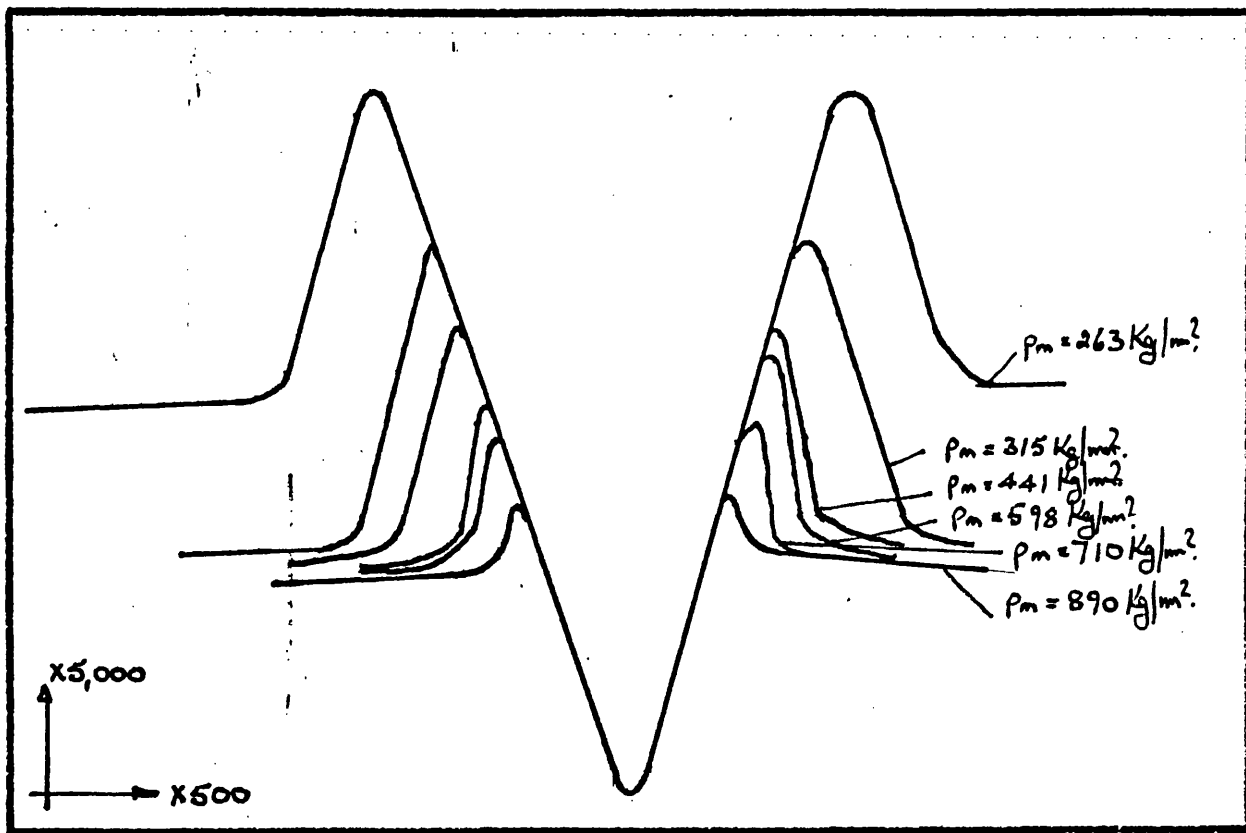


Fig. 6.3b Composite picture of a series of Vickers facet scratches in hardened and tempered 1% C steel, load 2Kg.

of the indenter and if a value of 0.5 is used for the constant of proportionality in the wear equation 3.30.

This assumption yields the result,

$$2a = 2 \sqrt{\frac{W}{2 \cdot p_m \cdot 10^2}} \text{ cm.} \quad (6.1)$$

where,

a = half the scratch width in cms.

W = normal load in Kg.

p_m = flow pressure Kg/mm^2 .

A particularly interesting feature of most of the scratches was the piled-up edges (fig 6.1), a phenomenon which has been noted by a number of other workers. An advantage of taking a Talysurf trace of each scratch was that this enabled a quantitative assessment to be made, of the effects of pile-up on metal removal. The results, which are shown in Table 6.1 are expressed in the form of per cent metal removed as a proportion of either metal displaced or total groove volume.

The effects of pile-up on scratch geometry are shown quite clearly in figure 6.3a in which all the traces for the hardened and tempered 1% C steel specimens have been assembled. These observations taken in conjunction with results shown in Table 6.1 indicate that pile-up at the edge of a scratch considerably affects the proportion of the groove volume removed. It can be seen that the softer the material the greater the degree of pile-up and as a consequence the smaller the proportion of the groove volume removed. With fully

Table 6.1

Material	Hardness VPH.	% metal removed of metal displaced	% metal removed of total groove volume.
0.9%C Steel (DAK5)	890	74	57
	710	61	39
	598	44	23
	441	33	15
	315	30	13
0.2%C Steel (Bright drawn) (annealed)	263	27	12
	223	40	14
Copper (Bright drawn) (annealed)	120	13	4
	102	1	$\frac{1}{4}$
Aluminium (Bright drawn) (annealed)	50	20	9
	40	too small to measure	too small to measure
Stellite 100.	823	69	52

hardened steel ($p_m = 890\text{Kg/mm}^2$) 57% of the total groove volume was removed but with the same material tempered to $p_m = 263\text{Kg/mm}^2$ this proportion had fallen to 12%. The behaviour of the softer materials (mild steel, copper and aluminium) although less consistent, provides further support for the assumption that the scratching process is more efficient with hard materials. Tests were also carried out with Stellite 100, a material which is intrinsically hard but having a metallurgical structure different from that of hardened steels; again a high proportion of the groove volume was removed and this suggests that these observations upon the effects of hardness have a wider, more general, significance.

Vickers Indentor.

The Vickers Diamond Indentor has a number of advantages over the Rockwell Cone; both facet and edgewise scratches can be made and the scratch geometry is constant. However, the Rockwell cone can produce only one type of scratch and, because the tip of the cone is radiused, the scratch geometry alters with depth of penetration.

Scratching with the Vickers indenor in the facet-first orientation gave similar results to those obtained with the Rockwell cone. A graph of the reciprocal of the scratch width squared against hardness is shown in figure 6.4 together with a theoretical line calculated from the equation (6.1) since, once again, it is assumed that the load is supported only on the frontal half of the indenor and due to pile-up at the front of the indenor the value of the constant of proportionality in the wear equation is again 0.5.

RECIPROCAL OF THE SCRATCH WIDTH SQUARED $(\frac{1}{2a})^2$
AGAINST HARDNESS FOR A RANGE OF MATERIALS.

CONDITIONS: VICKERS FACET.
2KG LOAD.

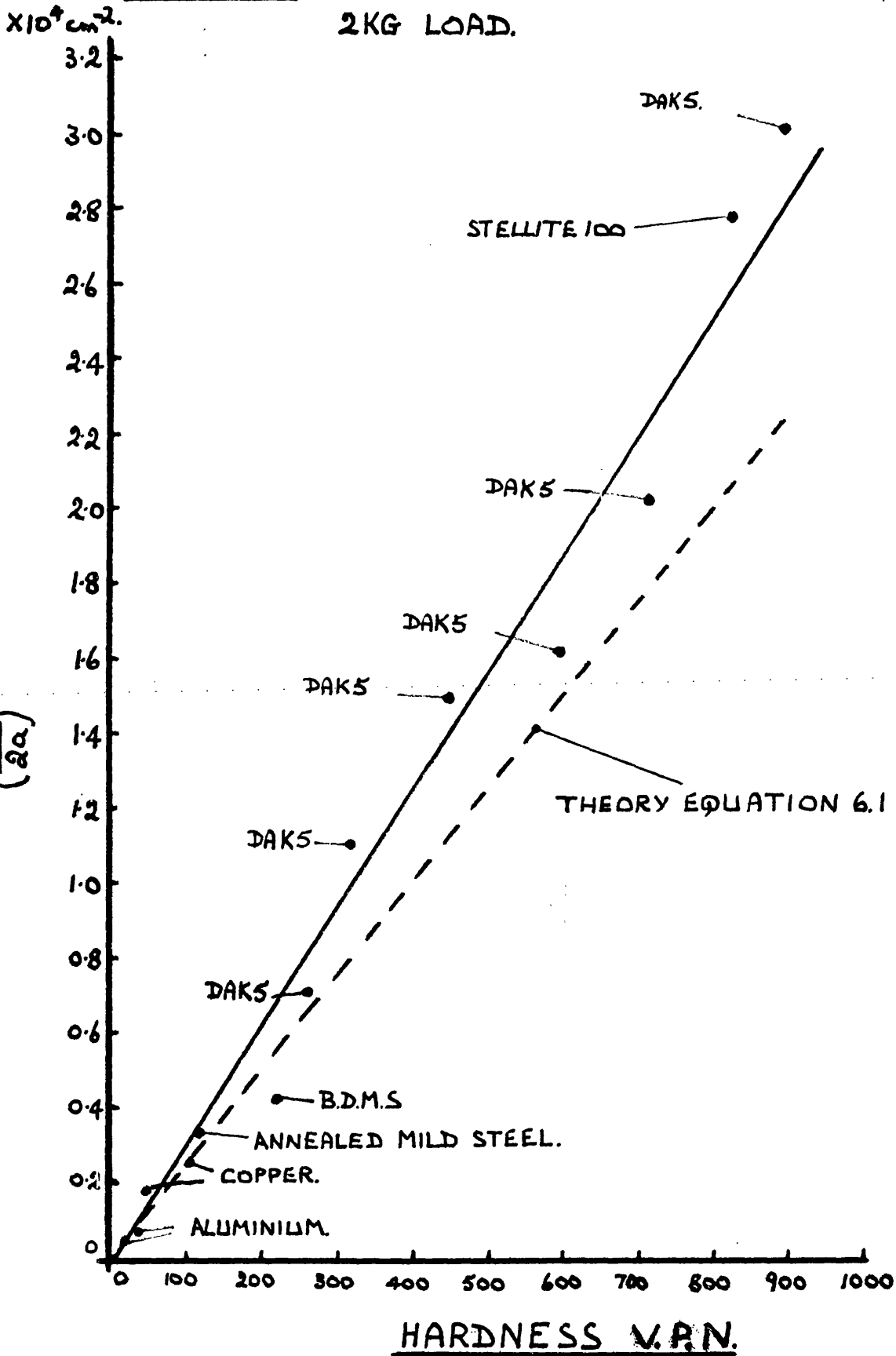


FIG. 6.4.

RECIPROCAL OF THE SCRATCH WIDTH SQUARED $(\frac{1}{2a})^2$
AGAINST HARDNESS FOR A RANGE OF MATERIALS.

CONDITIONS: VICKERS EDGE.
 2 KG. LOAD.

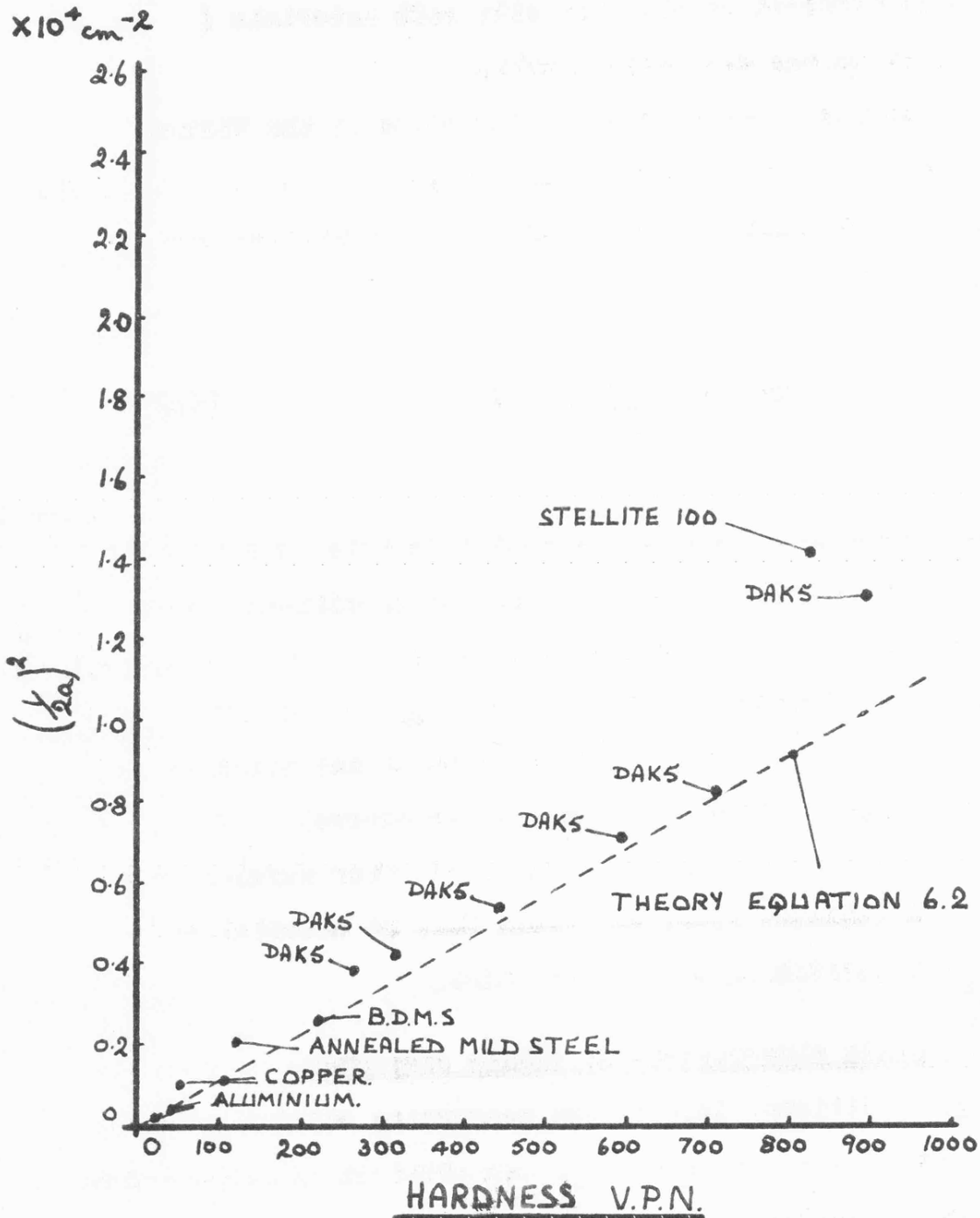


FIG. 6.5.

The theoretical scratch widths are slightly greater than those observed experimentally. Cutting efficiency was again found to be greater with hard materials ($\sim 50\%$ of total groove volume with hardened steel) than with soft materials ($\sim 10\%$ of total groove volume with mild steel).

The results obtained when scratching with the Vickers Indenter in the edge-first orientation are presented in fig.6.5. They are in good agreement with the theoretical line obtained from the expression,

$$2a = 2 \sqrt{\frac{W}{P_m 10^2}} \text{ cm.} \quad (6.2)$$

with the exception of the two hardest materials, Stellite 100 and the fully hardened steel. It may be significant that these were the only materials from which a measurable quantity of material was removed ($\sim 10\%$ of total groove volume). With the softer materials (below $600\text{Kg}/\text{mm}^2$) metal was piled-up at the edge of the scratches but nothing was removed. This observation is in agreement with those of other workers (e.g. Kruschov and Babichev 1960) who found that no material was removed when scratching with a cube edge.

6.5 Microscopic observations of single scratches.

Useful additional information concerning scratch geometry and the mechanism of metal removal was obtained by microscopic examination. Although the complete range of specimens was



Fig. 6.6 Vickers indenter facet-first orientation, material B.D.M.S., load 500g, magnification X 440.



Fig. 6.7 Vickers indenter facet-edge orientation, material hardened 1% C steel, load 500g, magnification X 1045.

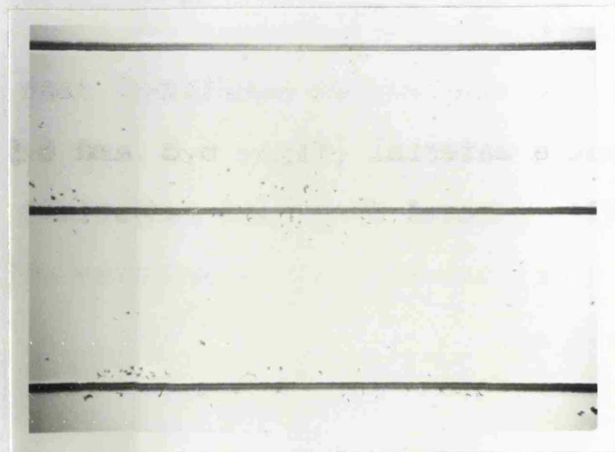


Fig 6.8 Vickers indenter facet-first orientation, material hardened 1% C steel, load 500g, magnification X 20.

studied the scratches on hardened steel and bright drawn mild steel were found to be representative and will be quoted as illustration. The scratches formed by the Vickers indenter were of particular interest since they can be made with either the facet-first or the edge-first orientation.

Most of the Talysurf traces had shown pile-up at the edge of the scratches an effect which could also be observed optically using a high resolution light-profile technique on the Vickers projection microscope. Stroud and Wilman (1962) used this method to study scratch geometry, and the proportion of the scratch removed. However, in the author's opinion the Talysurf method is more convenient and gives more reliable results.

The front end of the scratches is important when considering theoretical predictions; frontal pile-up was observed when scratching in the facet-first orientation (fig 6.6) but was absent when scratching in the edge-first orientation (fig 6.7). The extent of the pile-up at the front of the scratch formed by the facet face was equal to the depth of the scratch; this observation is in complete agreement with Sedriks and Mulhearn (1963).

Microscopic examination confirmed that facet-first scratches remove material (figs. 6.8 and 6.9) and that material is more readily removed from hard materials. There was no evidence of metal removal with scratches made with the edge-first orientation.

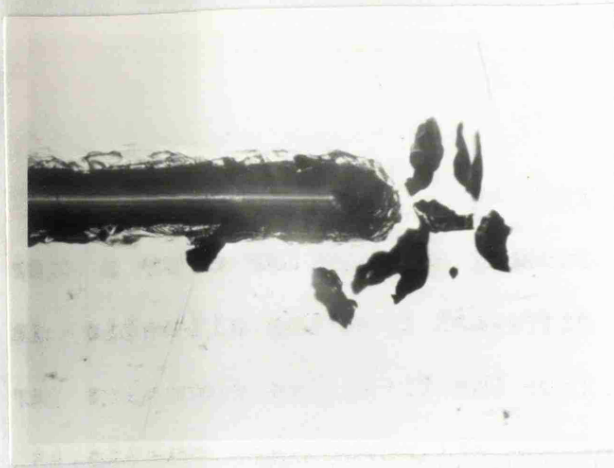


Fig. 6.9 Vickers indenter facet-first orientation, material B.M.N.S., load 500g, magnification X 110.

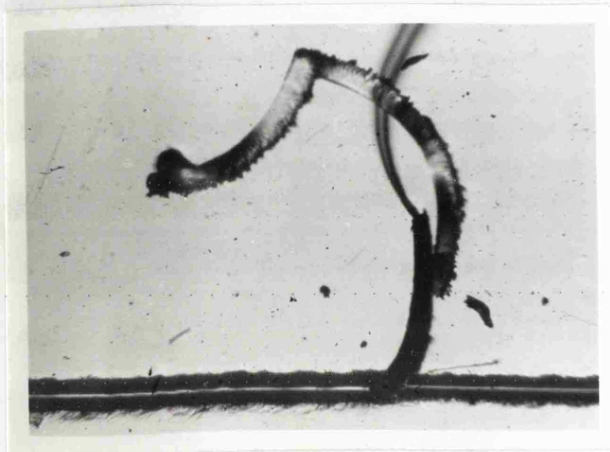


Fig. 6.10 Repeated track Vickers indenter facet-first orientation, material hardened 1% C steel, load 500g, magnification X110.



Fig. 6.11 Repeated track Vickers indenter facet-first orientation, material B.D.M.S., load 500g, magnification X 440.

6.6 Repeated scratches.

Obviously tracking an indenter over a micropolished surface is very different from the situation in normal abrasion where after the first few abrasive particles have scratched the surface all subsequent particles encounter material which has been abraded. Kruschov and Babichev (1960) for example, suggest as an explanation of their observation that the wear rate of metals is unaffected by cold work, that the maximum work hardened condition is achieved during abrasion. To get closer to practical conditions the effects of repeated tracking in the same groove were therefore studied.

Experiments were carried out with the Vickers Diamond Indenter using a 500g load; most of the tests involved hardened steel ($p_m = 890\text{Kg/mm}^2$). To carry out the experiments successfully the apparatus had to be carefully aligned; this being particularly critical with facet-first scratches.

When the Vickers indenter was tracked in the facet-first orientation in the same groove it readily cut a chip with hardened steel (fig 6.10) but with a softer material such as mild steel ($p_m = 223\text{Kg/mm}^2$) chips could only be formed with difficulty (fig 6.11). These observations confirm that scratching with a facet face, even one having a negative rake angle, will remove material.

Repeated scratching of hardened steel using the Vickers indenter in the edge-first orientation produced the most startling results. The original scratch had a relatively smooth piled-up edge (fig 6.12) but there was no evidence of

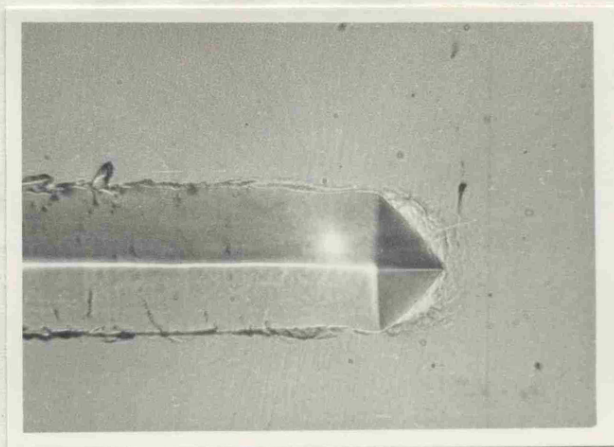


Fig. 6.12 Vickers indenter facet-edge orientation, material hardened 1% C steel, load 500g, magnification X 440.

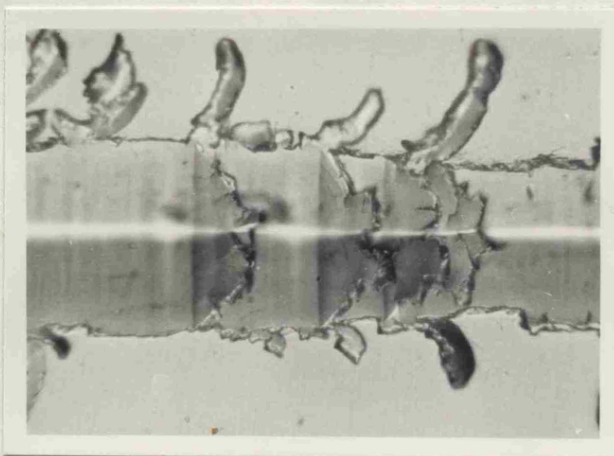


Fig 6.13 Repeated tracks using Vickers indenter facet-edge orientation, material hardened 1% C steel, load 500g, magnification X440.



Fig. 6.14 Repeated tracks Vickers indenter facet-edge orientation, material hardened 1% C steel, load 500g, magnification X 440.



Fig. 6.15 End of repeated tracks Vickers indenter facet-edge orientation, material hardened 1% C steel, load 500g, magnification X 1045.

TABLE 6.2.

Coefficients of friction during scratching under a load
of 2Kg, speed 4cm/min.

Material	Hardness V.P.N.	Coefficients of friction		
		Rockwell Indentor	Vickers Indentor edge-first	Vickers Indentor facet-first
1%Steel (DAK5)	890	0.16	0.45	0.50
" "	710	0.10	0.55	0.60
" "	573	0.24	0.55	0.60
" "	449	0.16	0.50	0.40
" "	310	0.24	0.45	0.50
" "	263	0.32	0.50	0.60
B.D.M.S.	223	0.60	0.48	0.50
Annealed M.S.	120	0.60	0.40	0.60
Cu. Hard.	102	0.60	0.40	0.50
Cu. Soft.	50	0.60	0.40	0.55
Al. Hard.	40	0.60	0.50	0.60
Al. Soft.	20	0.60	0.44	0.56

any material having been removed. When a series of traverses (six in all) were made in the same groove two effects were observed;

(i) a chip started to form in front of the indenter, several of which are shown in fig 6.13, and

(ii) chips started to appear due to breakaway of the piled-up edge at the side of the groove (fig 6.14).

Careful study of the edges of the groove showed that chips formed by the second mechanism were probably produced by a shearing action (fig 6.15). Thus edge-first scratches produce chips when scratching is repeated; however the process still appears to be less efficient than facet-first scratching.

6.7 Coefficients of friction.

In a number of runs on the friction machine the coefficient of friction was measured during scratching. Table 6.2 shows the values of the coefficient of friction obtained in this way.

These coefficients show no very marked trends although two tendencies may be noted. First, there is a trend towards lower values of friction with harder materials. Second, when using the Vickers indenter, the friction is generally somewhat higher in the facet-first orientation than in the edge-first orientation.

6.8. Theoretical analysis of scratch geometry.

For a scratch of given width the volume of material removed depends on two factors. The first of these is the width/depth ratio of the scratch which is already allowed for in the wear

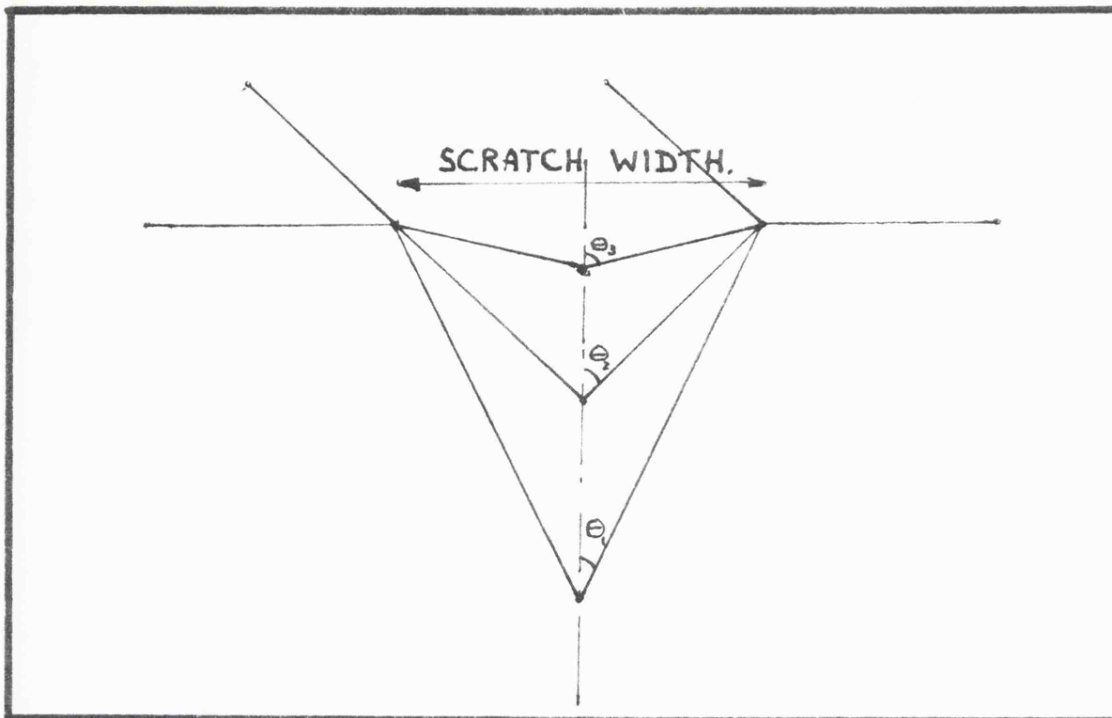


Fig 6.16a Showing the effect of θ on scratch volume.

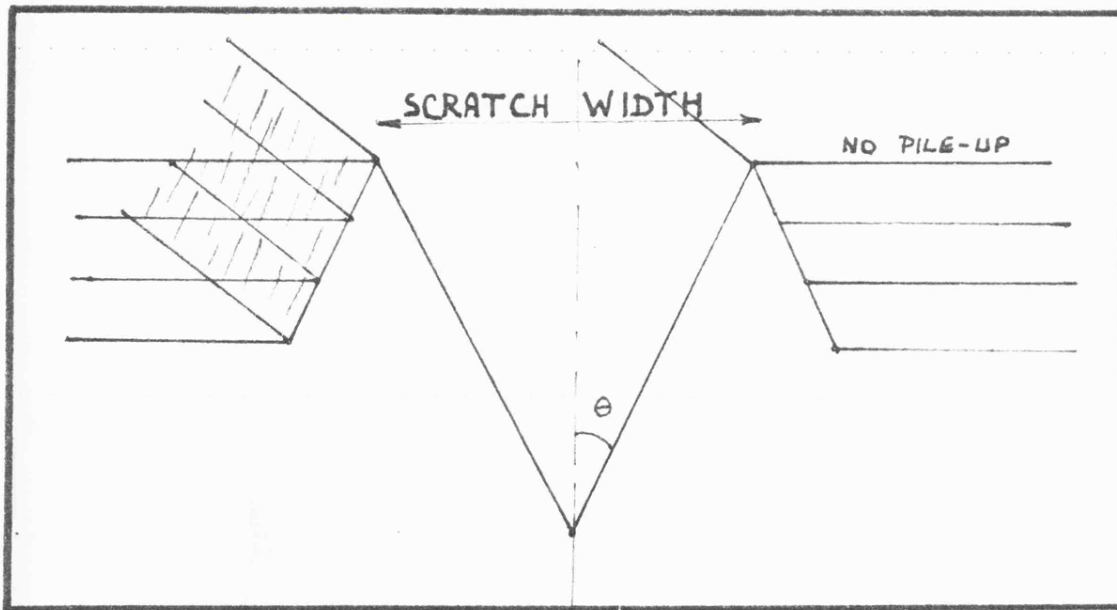


Fig 6.16b All the scratches have the same width and base angle but varying amounts of pile-up.

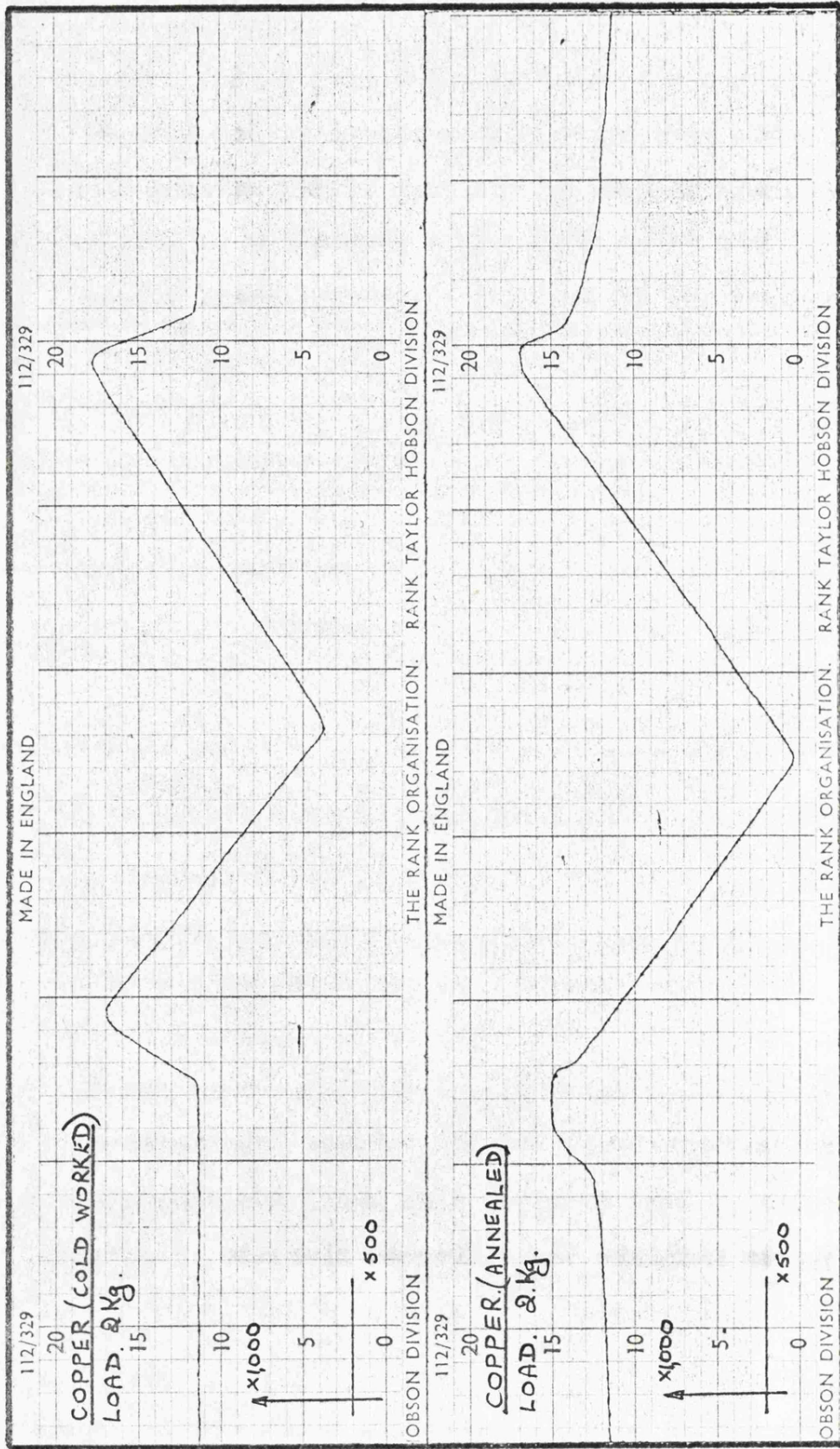


FIG. 6.17.

equation 3.30 being the value of $\cot \theta$ (fig 6.16a). However, the scratch tests have shown that a second factor must be considered, namely pile-up at the edge of the scratch (fig 6.16b). This means that only a proportion of the groove volume is removed and in the wear equation (equation 3.30) this is represented by the factor β .

A typical scratch with pile-up is shown in figure 6.1; the important parts of the scratch are the total groove volume ($A_1 + A_3$) the volume piled-up (A_2) and the volume displaced (A_3). The percentage of the total groove volume actually removed is given by the expression :-

$$\frac{A_3 - A_2}{A_1 + A_3} \times 100\% \quad (6.3)$$

Cutting efficiency is very sensitive to the amount of pile-up; and expressions for the volume of metal removed will be derived for the two types of pile-up which were observed in the experiments (6.17). Tabor (1951) has observed similar ridges at the sides of hardness indentations. In the theory which follows we shall consider the volumes associated with a regular scratch of unit length and we shall use the notation of figure 6.1 to indicate the different elements of material.

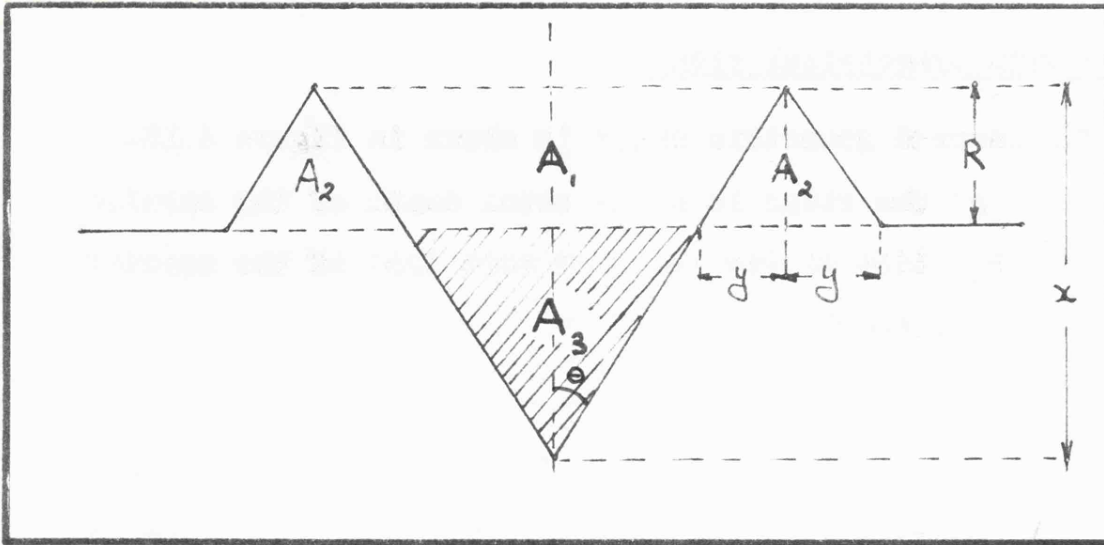


Fig. 6.18a Detail of scratch with symmetrical ridge.

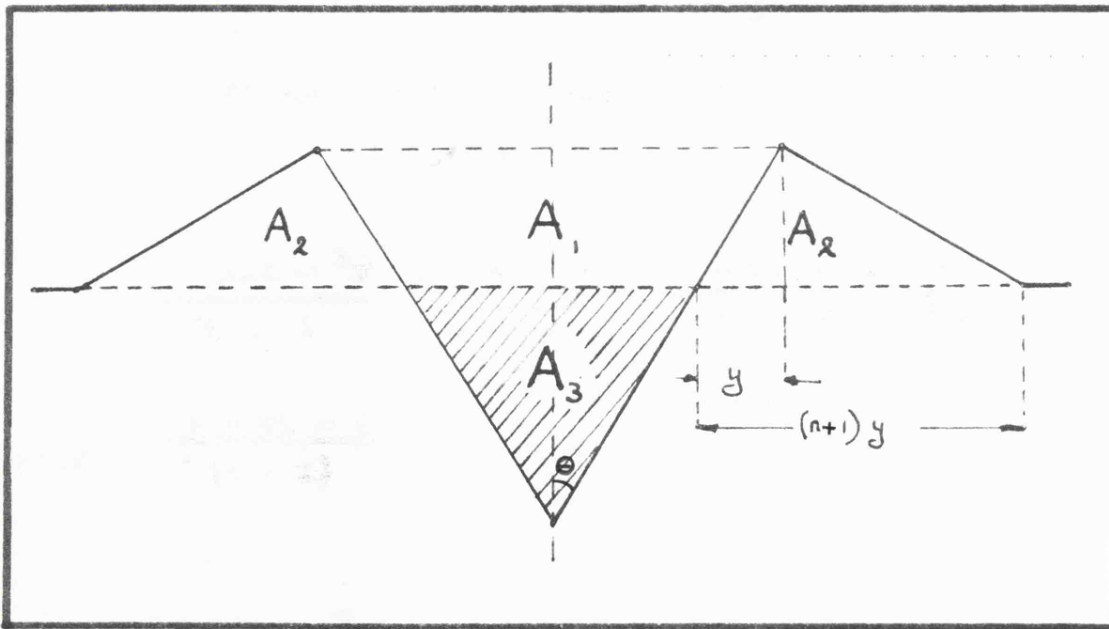


Fig. 6.18b Detail of scratch with asymmetrical ridge.

Groove with symmetrical ridge.

The assumed geometric shape is shown in figure 6.18a. The height of the ridge is R the total depth of the scratch is x and the width of the ridge on each side of the scratch is 2y where $y = R \tan \theta$

Then

$$\text{Volume of pile up} = A_2 = 2 R^2 \tan \theta \quad (6.4)$$

$$\text{Volume displaced} = A_3 = (x - R)^2 \tan \theta \quad (6.5)$$

$$\text{Total groove volume} = (A_1 + A_3) = x^2 \tan \theta \quad (6.6)$$

$$\text{Volume removed} = (A_3 - A_2) = (x^2 - 2xR - R^2) \tan \theta \quad (6.7)$$

We now denote the severity of pile-up by the factor r

where

$$r = \frac{R}{x} \quad (6.8)$$

It is now possible to express the volume removed by the two methods defined in section 6.3 above.

$$\begin{aligned} \beta_1 &= \frac{\text{Volume removed}}{\text{Volume displaced}} = \frac{A_3 - A_2}{A_3} = \frac{x^2 - 2xR - R^2}{(x - R)^2} \\ &= \frac{1 - 2r - r^2}{(1 - r)^2} \quad (6.9) \end{aligned}$$

and

$$\begin{aligned} \beta_2 &= \frac{\text{Volume removed}}{\text{Total groove volume}} = \frac{A_3 - A_2}{A_1 + A_3} = \frac{x^2 - 2xR - R^2}{x^2} \\ &= 1 - 2r - r^2 \quad (6.10) \end{aligned}$$

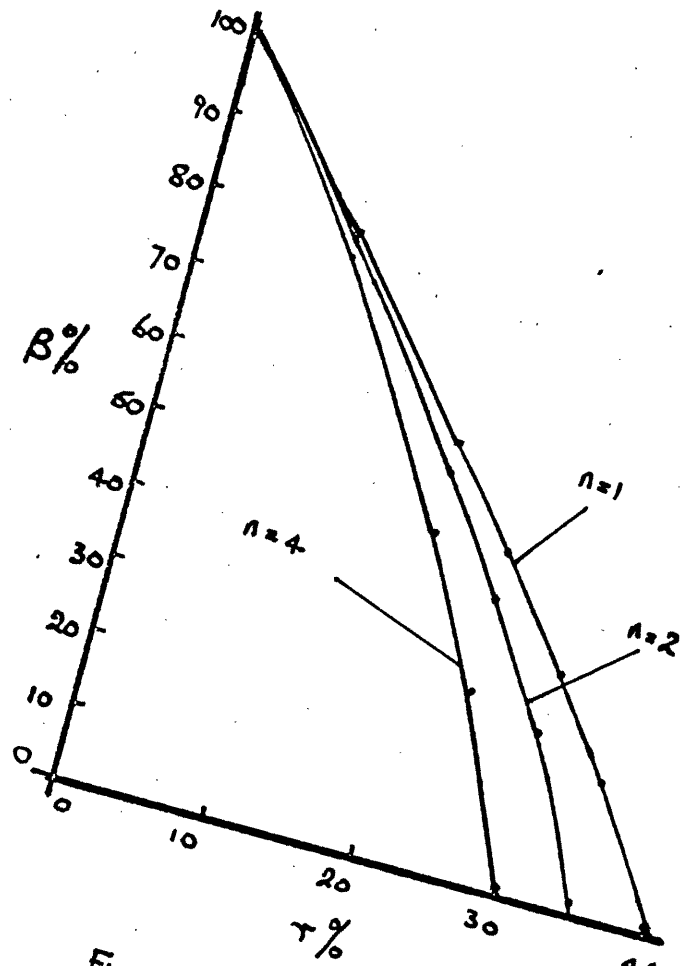


Fig. 6.19 (a)

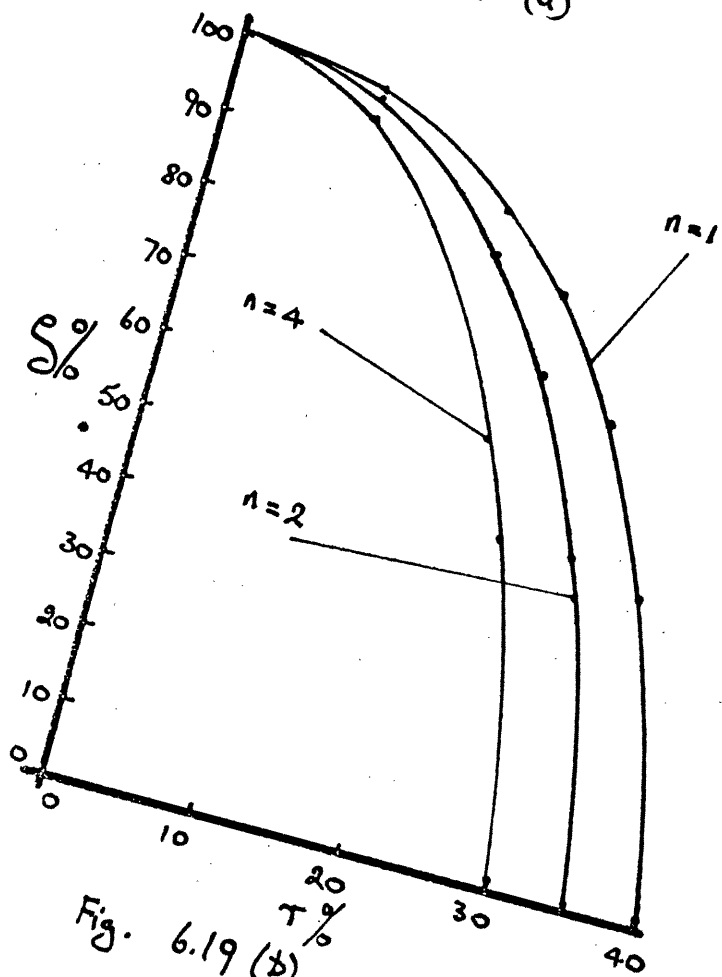


Fig. 6.19 (b)

Groove with an asymmetrical ridge.

For the more general case the width of the ridge on each side of the scratch is assumed to be $(n + 1) y$

Then, as before,

$$\text{Volume of pile-up} = A_2 = (n + 1)R^2 \tan \theta \quad (6.11)$$

$$\text{Volume displaced} = A_3 = (x - R)^2 \tan \theta \quad (6.12)$$

$$\text{Total groove volume} = (A_1 + A_3) = x^2 \tan \theta \quad (6.13)$$

$$\text{Volume removed} = (A_3 - A_2) = (x^2 - 2xR - nR^2) \tan \theta \quad (6.14)$$

As before, the volume removed may be expressed as

$$\mathcal{G}_n = \frac{\text{Volume removed}}{\text{Volume displaced}} = \frac{1 - 2r - nr^2}{(1 - r)^2} \quad (6.15)$$

$$\beta_n = \frac{\text{Volume removed}}{\text{Total groove volume}} = 1 - 2r - nr^2 \quad (6.16)$$

It will be observed that the groove with a symmetrical ridge is a special case of the general formulae with $n = 1$.

In figure 6.19a,b the ratios \mathcal{G} and β representing the volume removed are plotted against the ratio $r = (\text{ridge height})/(\text{total scratch depth})$ for different types of grooves. It will be observed that for a given ridge height, typically about 30 to 40% of the total scratch depth, the volume removed falls to zero.

In figure 6.20 is shown the interrelationship between the two methods of expressing the volume removed. Also plotted on this graph are the results obtained from Table 6.1

Fig. 6.20 Inter-relationship between methods of expressing the proportion of material removed.

- Rockwell indenter; 1% C steel (DAK5) Hardened and tempered.
- Rockwell indenter; other materials (Table 6.1).
- △ Vickers indenter, facet-forward orientation; 1% C steel.
- ▲ Vickers indenter, facet-forward orientation; other material

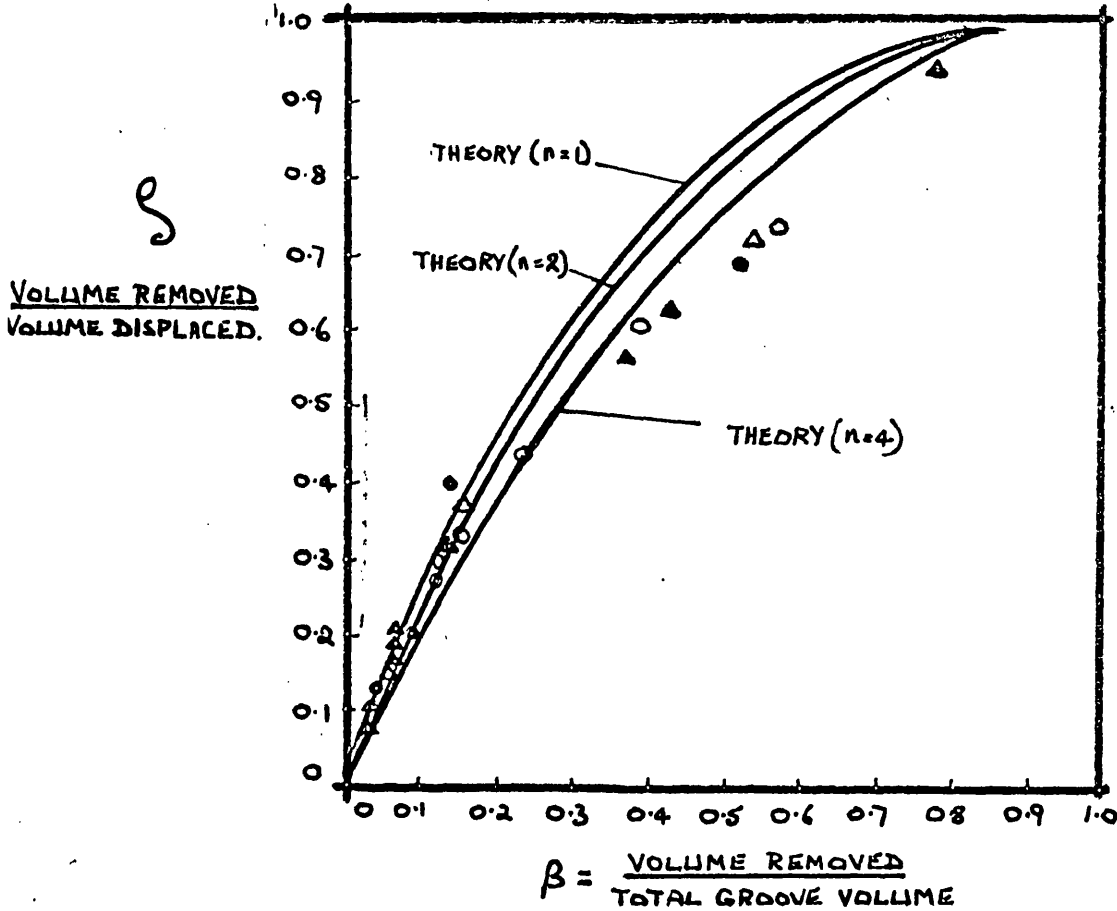
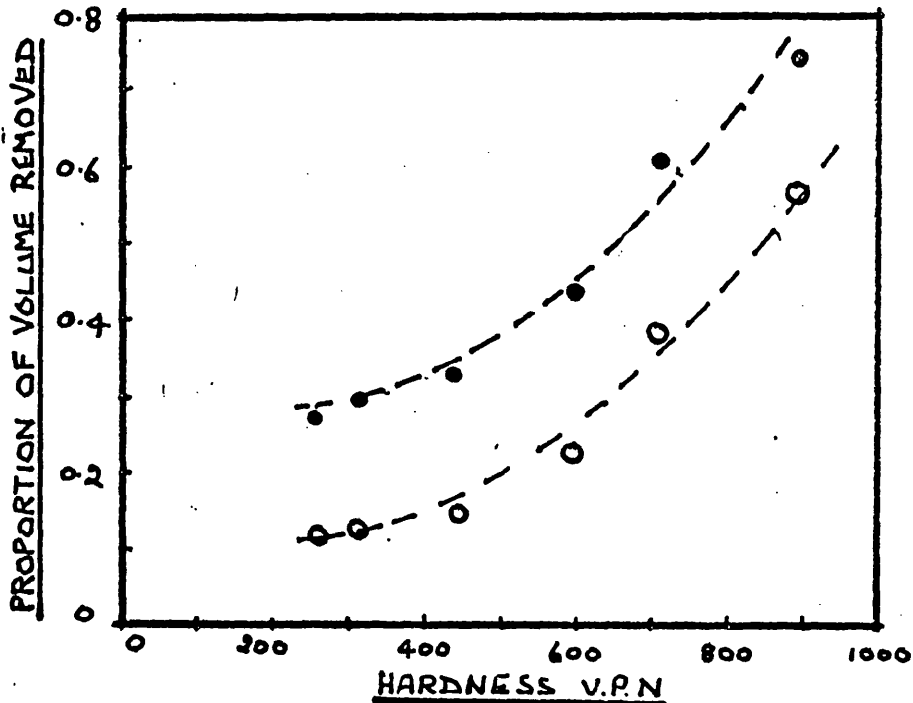


Fig. 6.21 Proportion of volume removed for scratch tests with Rockwell indenter on hardened and tempered 1% C steel.

- (Volume removed)/(Volume displaced)
- (Volume removed)/(Total groove volume)



(which refer to experiments with a Rockwell indenter) and similar results obtained with a Vickers indenter in the facet-first orientation. It will be observed that the experimental results are in reasonably good agreement with the theory. The experimental results plotted in figure 6.20 also seem to imply that with the harder materials, for which the proportion of material removed is larger, the pile-up tends to be more asymmetric (i.e. larger values of n in equations 6.15 and 6.16). There is an indication of this fact in the profiles of figure 6.3b.

Finally figure 6.21 shows the results of Table 6.1 for scratch tests in which hardened and tempered 1% C steel was used in conjunction with a Rockwell indenter. The proportion of the volume removed (expressed in the two alternative ways defined above) is plotted against the hardness. Results obtained with the same material using a Vickers indenter in the facet-first orientation show the same trend, with somewhat greater scatter, and the same conclusion applies to scratch tests with the other materials listed in Table 6.1. The general trend of the results is quite clear. As the hardness of the material is increased the efficiency of the scratching process becomes higher; a larger proportion of the material is removed and appears as worn debris.

6.9 Discussion.

The most important aspect of the work described in this Chapter is the discussion of the methods of characterising the geometry of the scratch. This is shown by the different

volumes of figure 6.1 and the analysis of the results in these terms given in section 6.8. Although the work of Kruschov and Babichev (1960) is of great importance in this field their results, upon closer examination, seem particularly confusing. Although they measured the width of their tracks with an optical microscope they claim that the track width corresponds to A_1 of figure 6.1. How this could be achieved in the presence of appreciable pile-up is difficult to understand.

In the present work the total width of the track, including the pile-up, has been taken as the parameter of greatest significance for abrasive wear theory. The comparison between theory and experiment shown in figures 6.2, 6.4 and 6.5 suggests that this assumption is fully justified. The agreement is very close indeed both for the Rockwell indenter and for the Vickers indenter in the edge-first orientation. For tests with the Vickers indenter in the facet-first orientation the agreement is a little less satisfactory but presumably this divergence is concerned with the assumed relationship between the pile-up at the front of the indenter and that observed at the sides of the scratch after the test. It may also be noted that the agreement between theory and experiment obtained in these tests is far more satisfactory than that obtained from an analysis of the results presented by Kruschov and Babichev.

The results of these scratch tests also have some significance for the theory of abrasive wear. The good agreement between theory and experiment suggest that, since

the wear equation (equation 3.30) is based upon the same assumptions, the value of 0.50 for the constant of proportionality in this equation is justified. However, because the total track width including pile-up is used, the inclusion of the factor β (representing the material removed as a proportion of the total track volume) is now an essential part of an acceptable wear equation.

The tests have shown that material can be removed by cutters having negative rake angles; but the ease with which material is removed depends on the way in which the cutter is presented (facet cuts more readily than edge), the number of times the material has been scratched and the material being scratched (hard materials show proportionally higher wear rates than soft materials). With repeated tracks in scratches with the edge-first orientation, the main mechanism of material removal appears to be shearing of the piled-up edge; the chips produced by this mechanism are relatively short compared with those produced by scratching in the facet-first orientation.

Finally, the fact that a higher proportion of the total groove volume is removed when scratching hard materials seems to be highly significant. It could go some way towards explaining the fact, noted by Kruschov and Babichev, that rates of abrasive wear fall less rapidly with increasing hardness than might be expected by simple theories. Secondly it could provide an explanation of the relative independence of grinding forces to changes in hardness of the workpiece. A more complete discussion of these questions will be given in Chapter 8.

6.10 Conclusions.

- (1) Material is removed by indentors having negative rake angles.
- (2) Theoretical and observed scratch widths were in good agreement provided allowance is made for pile-up.
- (3) Scratching in the facet-first orientation is a more efficient method of metal removal than scratching in the edge-first orientation.
- (4) Repeated tracks in the same groove, particularly with the Vickers indenter in the edge-first orientation, showed that breakaway of the piled-up edge is an important wear mechanism.
- (5) A higher proportion of the groove volume is removed with hard than with soft materials.
- (6) The proportion of the groove volume removed is related to the pile-up and the experimental results are in quite good agreement with simple theories which take this into account.
- (7) Scratching in the facet-first orientation tends to produce chips similar to those formed in single point cutting. Scratching in the edge-first orientation tends to produce relatively small chips which are cup shaped.
- (8) The use of a value of 0.5 for the constant of proportionality in the wear equation 3.30 is justified in the light of the results obtained by scratching.

7. Experiments with Abrasives.

7.1 Introduction.

Abrasive wear theory, and the experiments just reported for scratching with idealised indentors, make a number of assumptions about the nature of abrasive surfaces. These assumptions are a necessary simplification if calculations are to be made. Real abrasives with very sharp fracture facets may behave very differently to idealised cutters. To assess the extent to which the theoretical basis of wear theory is valid under practical conditions, a series of experiments was carried out using abrasives. These experiments were divided into two groups, (i) scratch tests using abrasives followed by an examination of the scratches formed by Talysurf and optical techniques (ii) an examination of abrasive surfaces using a wide variety of methods.

It was hoped that this series of experiments would provide further information about the mechanism of chip removal, scratch shape, the effects of material hardness on chip formation and the geometry and structure of abrasive surfaces.

7.2 Apparatus.

Scratch tests were carried out, as before, either on the Vickers Projection Microscope Micro-hardness Tester or on the Friction Machine.

The scratches produced were examined using optical and Talysurf techniques.

Abrasive surfaces were examined optically, by Talysurf and scanning electron microscope.

Where special techniques were used these are described at the appropriate stage.

7.3 Materials.

The bulk of the materials used in earlier experiments were studied but most of the results chosen for illustration involve either hardened or mild steel and BA60 - L5 - VFBLU abrasive wheels. Where results were obtained using other materials this is indicated in the text.

Except where indicated scratch tests were carried out on specimens having a micro-polished surface.

7.4. Preliminary Scratch tests with single abrasive grits.

A few preliminary tests were carried out on the Vickers Micro-hardness Tester using single grits projecting from an abrasive wheel. To obtain such grits the wheel was dressed in the usual way on the pin and ring machine; the wheel was then machined with the diamond so that a narrow band of abrasive about one grit wide was left projecting; a single grit could then be left proud of the surface by breaking away its neighbours.

Talysurf traces of the scratches formed by such grits showed that substantially the whole of the scratch volume was removed when abrading hard materials but with soft, the

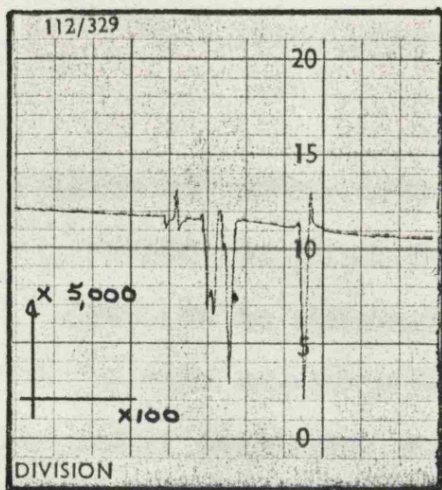


Fig. 7.1 Talysurf trace of scratch on hardened 1% C steel, load 500g, 36 grit wheel.

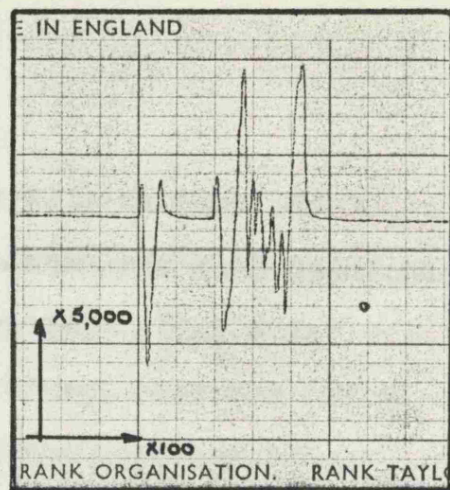


Fig. 7.2 Talysurf trace of scratch on B.D.M.S., load 500g, 36 grit wheel.

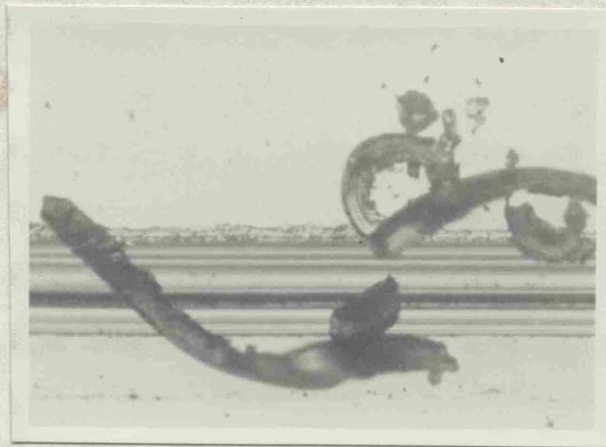


Fig. 7.3 Scratch on hardened 1% C steel, load 500g, 36 grit wheel, X 440.

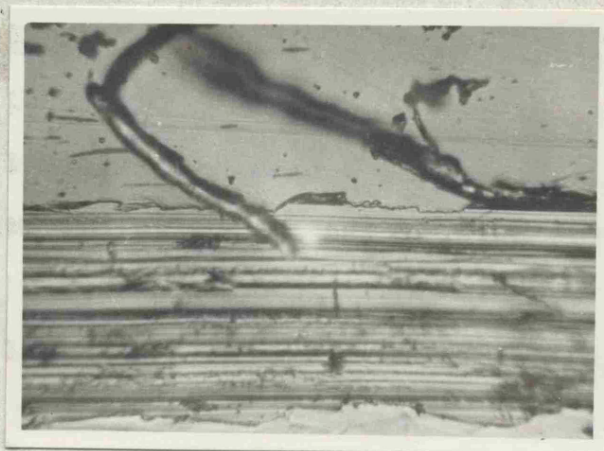


Fig. 7.4 Scratch on B.D.M.S., load 500g, 36 grit wheel, X 440.

materials, such as mild steel, the bulk of the material displaced from the scratch was piled-up at its edges (figs 7.1 & 7.2). The cutting performance of an abrasive grit is therefore sensitive to pile-up at the edge of the scratch in the same way as that of an idealised indenter.

Microscopic examination of the single grit scratches supported the Talysurf observations, chips being observed on the surface of the hardened steel specimen (fig 7.3) whilst the mild steel specimen had fewer chips and evidence of pile-up at the edges of the scratch (fig 7.4). It is of interest to note that some of the scratches on mild steel exhibited the mechanism of edge break-away observed earlier in repeated scratching with idealised indentors.

Both the Talysurf traces and optical examination showed that the use of the term a "single grit" is misleading; what had appeared to be a single grit often produced several quite separate scratches on the surface of the specimen showing that a single grit may have several cutting facets or edges.

7.5 Effects of material hardness on the cutting process.

Since the preliminary tests suggested that abrasive grits show the same behaviour pattern as idealised indentors, namely the bulk of the groove volume being removed with hard materials but reduced cutting efficiency with softer materials due to edge pile-up, it was decided to scratch test a range of specimens of differing hardness (DAK5

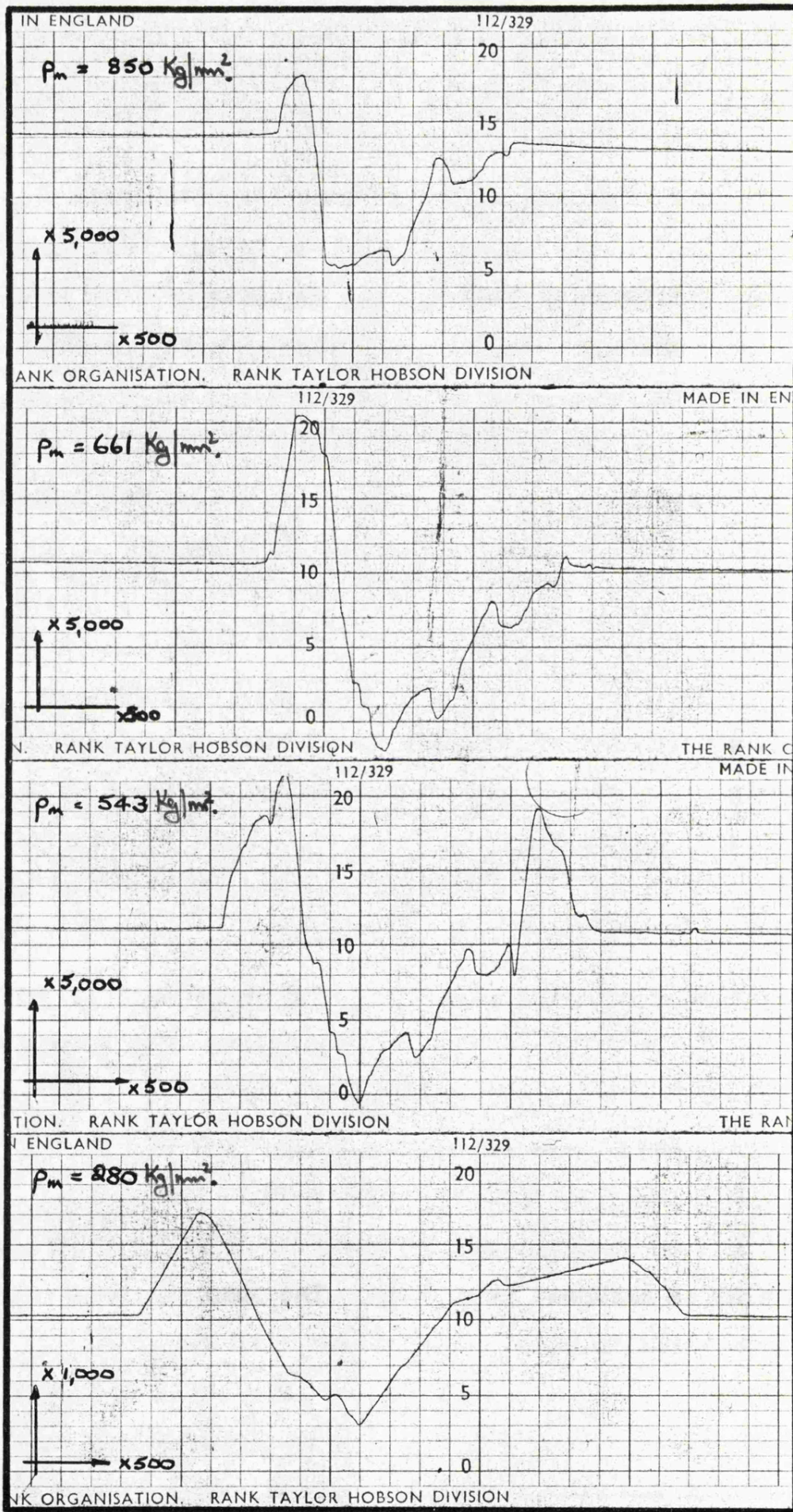


Fig. 7.5 Talysurf traces of a scratch, made with a single abrasive grain, on a specimen of steel heat-treated to give a hardness gradient, load 2Kg.

hardened and tempered) using the same abrasive grit. Unfortunately these experiments had to be abandoned as it was very difficult to preserve the abrasive grit in its original condition throughout the tests due to the ease with which fracture occurred. A different technique was therefore adopted; specimens were made from DAK5 and heat-treated in such a way that a hardness gradient was formed, the hard end being 890Kg/mm^2 falling to 300Kg/mm^2 at the soft end. The specimens were scratched on the friction machine using a load of 2Kg, and a single grit from a 36 grit wheel. Two types of test were performed; in one series scratching began at the soft end of the specimen, in the other at the hard end. When scratching began at the soft end of the specimen the grits fractured and friction measurements were erratic ($\sim 0.6-0.8$); when the test was begun at the hard end, the grit fractured when the soft end was approached. In both types of test the change in scratching mechanism occurred in the region of the specimen having a hardness of 300 to 400Kg/mm^2 , friction at the soft end being high (~ 0.6 to 0.8) falling to 0.4 to 0.5 at the hard end. Talysurf traces showed that as the grit scratched the specimen pile-up increased progressively with reduction in hardness (fig 7.5). The complete range of specimen hardness could not be covered as the high coefficients of friction associated with the soft end of each specimen and the tendency for the grits to dig in caused fracture in the regions having a hardness below about 400Kg/mm^2 .

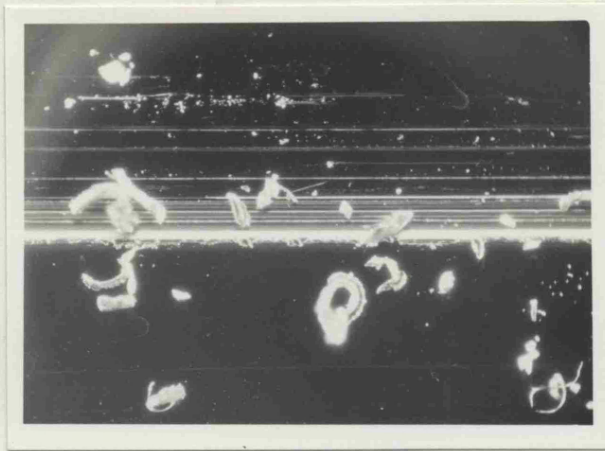


Fig. 7.6 Scratch at the hard end of the specimen, dark field illumination, X 100.

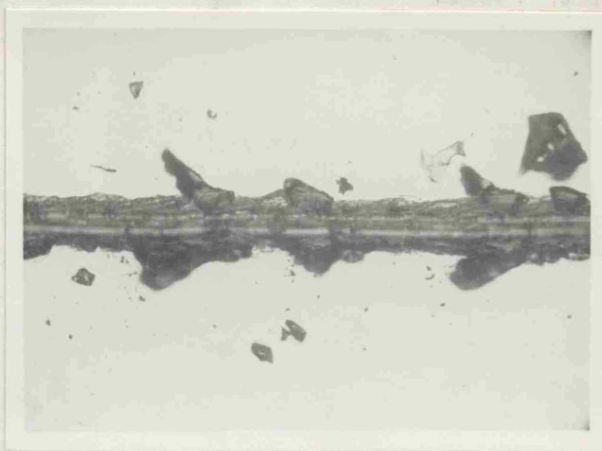


Fig. 7.7 Scratch at the soft end of the specimen, X 100.

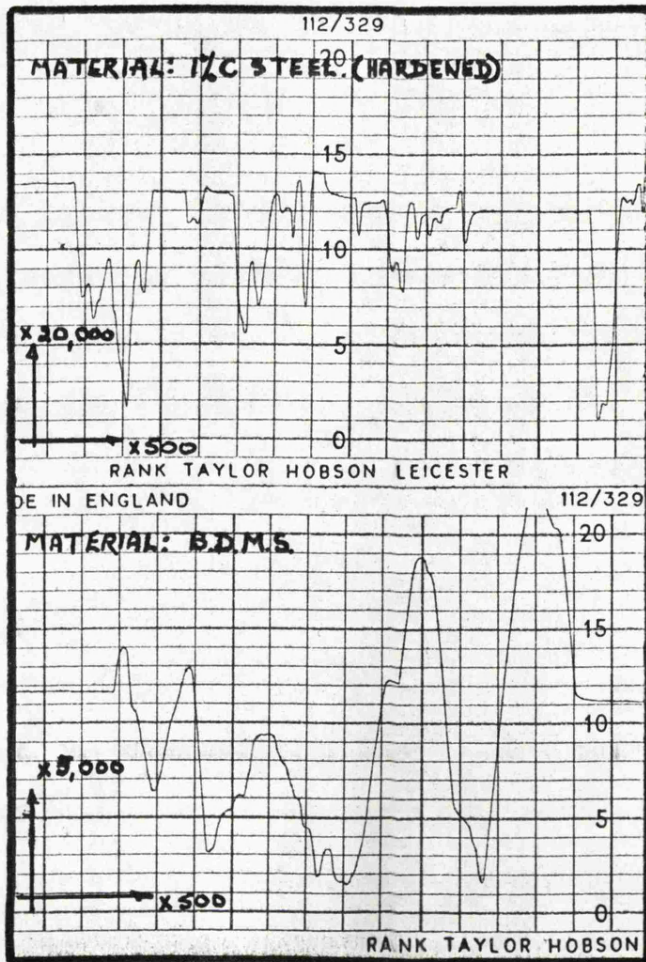


Fig. 7.8 Talysurf traces of scratches, made with a 100 grit grinding wheel during dynamometer tests, on hardened 1% C steel and B.D.M.S.

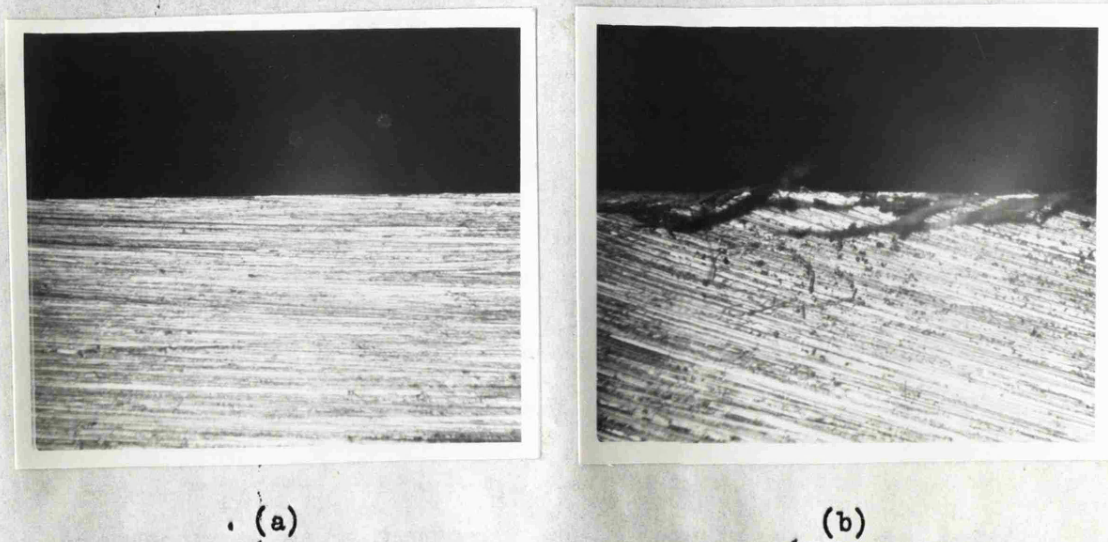


Fig. 7.9: Edges of ground specimens (a) hardened 1% C steel and (b) B.D.M.S., X 18.

Microscopic examination of typical scratches confirmed that chips were readily produced at the hard end of a specimen (fig 7.6) and that at the soft end grits fractured and there was considerable pile-up at the edge of the scratches (fig 7.7).

7.6 Scratch tests with grinding wheels.

In the dynamometer tests reported earlier (Chapter 6) scratch tests were made on a micropolished surface after each grinding run. The main purpose of these tests was to determine the width/depth ratio of the scratches formed and the coefficient of friction.

However it was noted that the behaviour pattern observed with both idealised indentors and single abrasive grits was repeated with grinding wheels. With hardened steels substantially the whole of the scratch volume was removed, but with softer materials ploughing occurred reducing scratching efficiency (fig 7.8).

The specimens used in the grinding experiments provided further evidence in support of the concept of ploughing with soft materials. After forty traverses using a depth of cut of 0.0003" the hardened steel retains a sharp edge but the soft specimen shows a rough edge (fig 7.9). It is suggested that the rough edge is formed by a ploughing mechanism, a small quantity of material being displaced over the side of the specimen with each traverse of the grinding wheel.

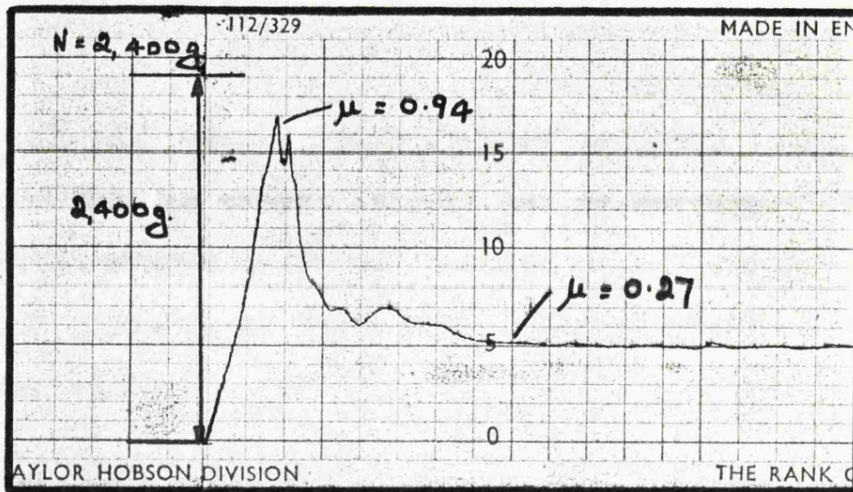


Fig. 7.10 Trace of tangential force in a single grit scratch test, normal force 2,400g, material 1% C steel hardened.

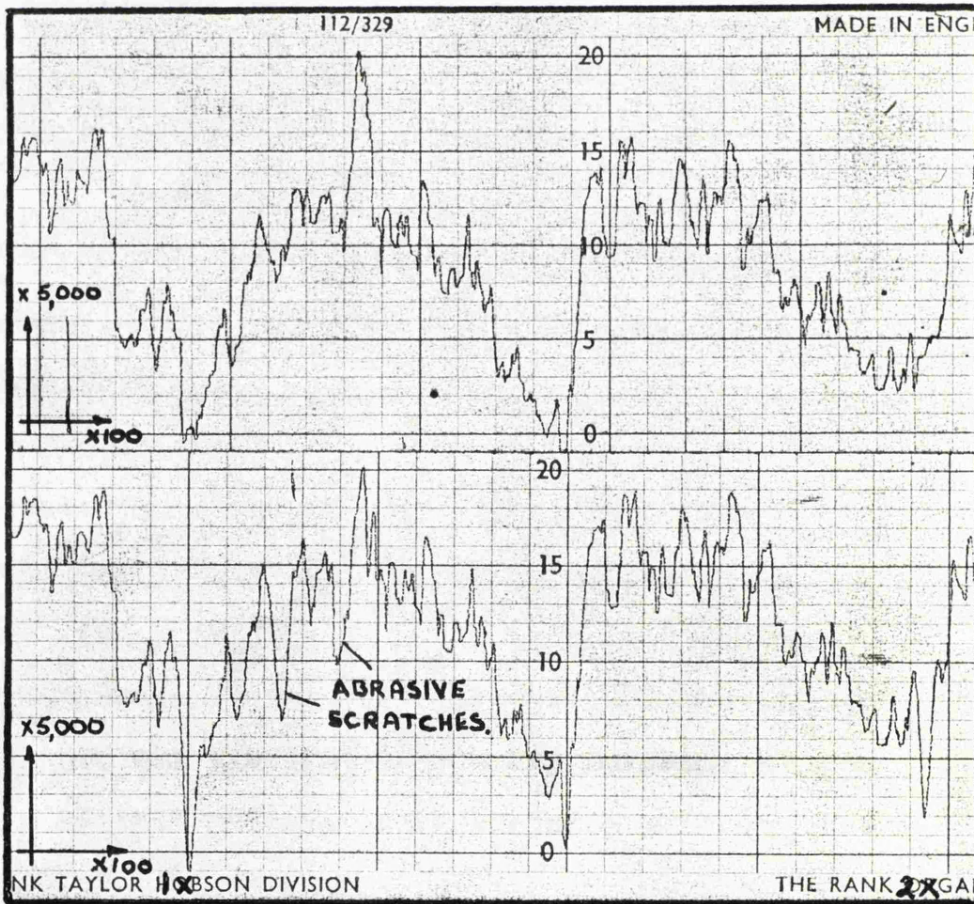


Fig. 7.11

Fig. 7.12

Talysurf traces of scratches on a ground surface, (fig 7.11) original surface, (fig. 7.12) the same surface scratched with Vickers indenter facet-first orientation (marked 1X and 2X) and with a 36 grit abrasive wheel as indicated, material hardened 1% C steel, load 500g.

7.7 Positive rake grits.

Most abrasive wear theories assume that the normal load is supported on the frontal facets of the abrasive grits and that it is these grits which remove material.

Positive rake grits do exist in abrasive surfaces and their role in the cutting process cannot be completely dismissed. Single grit scratch tests were therefore performed using positive rake grits isolated from a grinding wheel in the manner described earlier. (Examination of abrasives reported in Section 7.9 suggest that less than 10% of the grits had a positive rake angle).

The tests were carried out on the friction machine using a range of loads (400g to 2400g) and micropolished hardened steel ($p_m = 890\text{Kg/mm}^2$) specimens.

Two behaviour patterns were observed :- (1) under light loads the grits usually scratched the surface with a coefficient of friction of $\mu \approx 0.3$ (ii) with each grit there was a critical load at which it started to dig into the specimen, the coefficient of friction rapidly rose to a value of about $\mu = 1$, the grit fractured and the coefficient of friction fell to about $\mu = 0.3$ (fig 7.10). These observations can be explained if it is assumed that although the grit selected (at a comparatively low magnification) had a positive rake angle the cutting edge is slightly blunt so that at the tip the grit has a negative rake angle. At light loads the grit will present a negative rake angle to the specimen, the coefficient of friction being low; at

higher loads the grit penetrates further into the specimen and will have a positive rake angle and a high coefficient of friction. Due to the high value of μ the grit will fracture to give a new edge with a negative rake angle and the value of the coefficient of friction will return to 0.5.

7.8 Scratch tests on ground surfaces.

All the scratch tests reported so far have been carried out on micropolished surfaces; by adopting this technique the scratch geometry can be determined accurately but the conditions are unrepresentative of real abrasive processes where most of the grits encounter material which has already been abraded. A number of scratch tests were therefore carried out on surface ground specimens using both idealised cutters and single abrasive grits.

The method proposed for studying the removal of material was to take a Talysurf trace of the same area of the specimen before and after scratching and by comparing the two traces the scratch volume could be observed.

The technique consisted of fitting a small jig to the Talysurf table so that the specimen could be removed and then accurately replaced. Provided the Talysurf was operated very carefully the method worked successfully, repeated removal and replacement of the specimen giving identical traces.

The complete experimental procedure was accurately to locate the specimen on the Talysurf and take an initial



Fig. 7.13 Microsection of Aloxite pin, X 160.

trace, remove the specimen and scratch it with the idealised cutter or single abrasive grit, finally relocate the specimen on the Talysurf and take a second trace.

By superimposing the two traces the scratch was located and an estimate made of the material removed.

Typical results for fully hardened steel (DAK5) are shown in figures 7.11 and 7.12; with both the single abrasive grit and the Vickers facet effectively the whole of the scratch volume has been removed. Similar tests with softer materials showed that the cutting efficiency had been reduced by pile-up at the edges of the scratches, confirming previous observations with idealised cutters, single abrasive grits and grinding wheels when scratched on micropolished surfaces.

7.9 Examination of Abrasives.

Although a number of theories of abrasion have been developed assuming simple geometric models, remarkably little is known of the true nature of abrasive surfaces. The concluding phase of this chapter is concerned with methods of examining abrasive surfaces and in particular grinding wheels.

7.9.1 Micro-sections.

Mulhearn and Samuels (1962) developed a microscopic method of examining abrasive papers which in the present work was slightly modified before it was applied to solid abrasive pins. The surface of the pin was coated, by

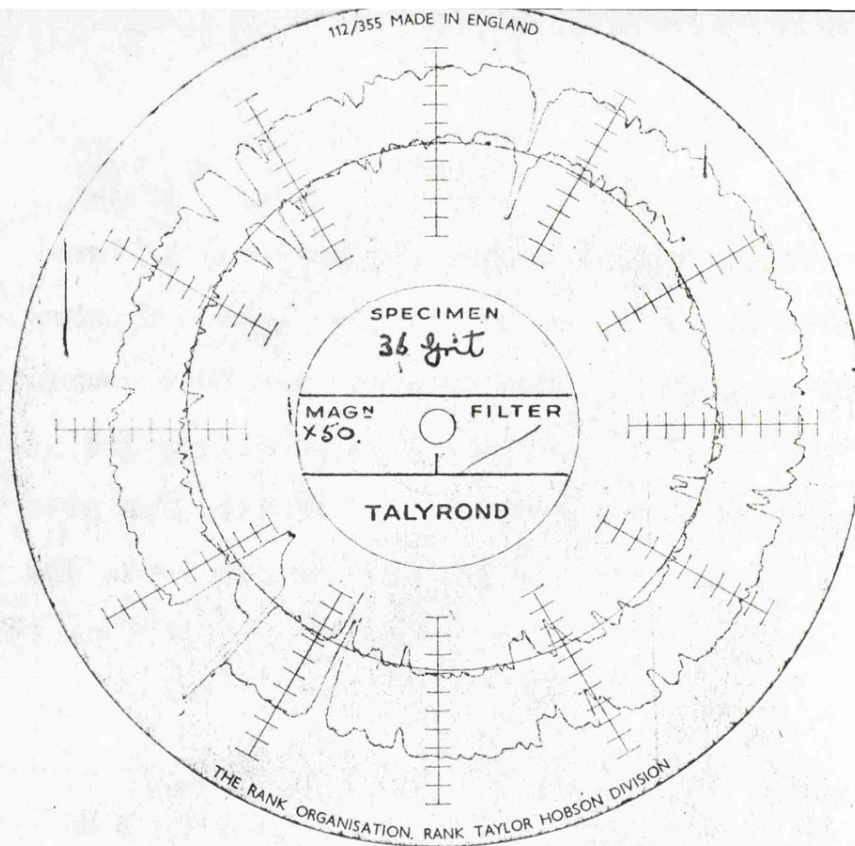


FIG. 7.14

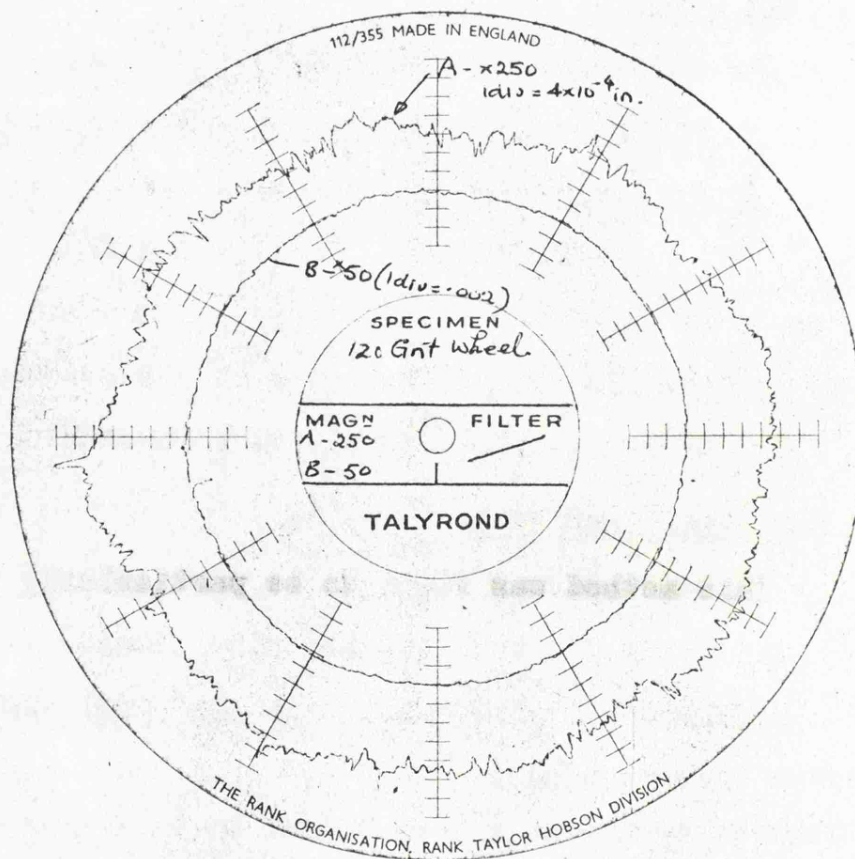


FIG 7.15

evaporation with a conducting material (silver); this was in turn coated by electroplating with a thicker protective layer of nickel. The specimen was then mounted in Diakon using a metallurgical mounting press and the press was maintained at the moulding temperature for several minutes to allow the mounting material to penetrate the pores of the abrasive. The specimens were then polished using diamond abrasives.

A typical section of an Aloxite pin is shown in figure 7.13; the structure of the abrasive and the attack angle of the grits can be seen. Unfortunately the technique is very time consuming, the specimen has to be destroyed and it is difficult to examine precise areas of the specimen.

7.9.2 Talyrond.

This instrument can examine round and cylindrical objects giving a very high vertical magnification. When applied to one inch diameter grinding wheels the traces were found to be reproducible (fig 7.14) and a fine grit wheel was shown to have more cutting edges than a coarse grit wheel (fig 7.15). The method gave little evidence of grit shape and no indication of positive rake cutting angles.

7.9.3 Optical Profile Methods.

This method was found to be particularly suited to the examination of the small abrasive wheels used in pin and ring experiments. The surface of the wheel was diamond dressed leaving a strip about one grit wide. A profile projection technique was then used to study the exposed



Fig. 7.16 Photograph of diamond dressed 60 grit wheel, X 7.



Fig. 7.17 Area 1 in fig. 7.16, X 125.



Fig. 7.18 Area 2 in fig. 7.16, X 125.



Fig. 7.19 Area 3 in fig. 7.16, X 125.

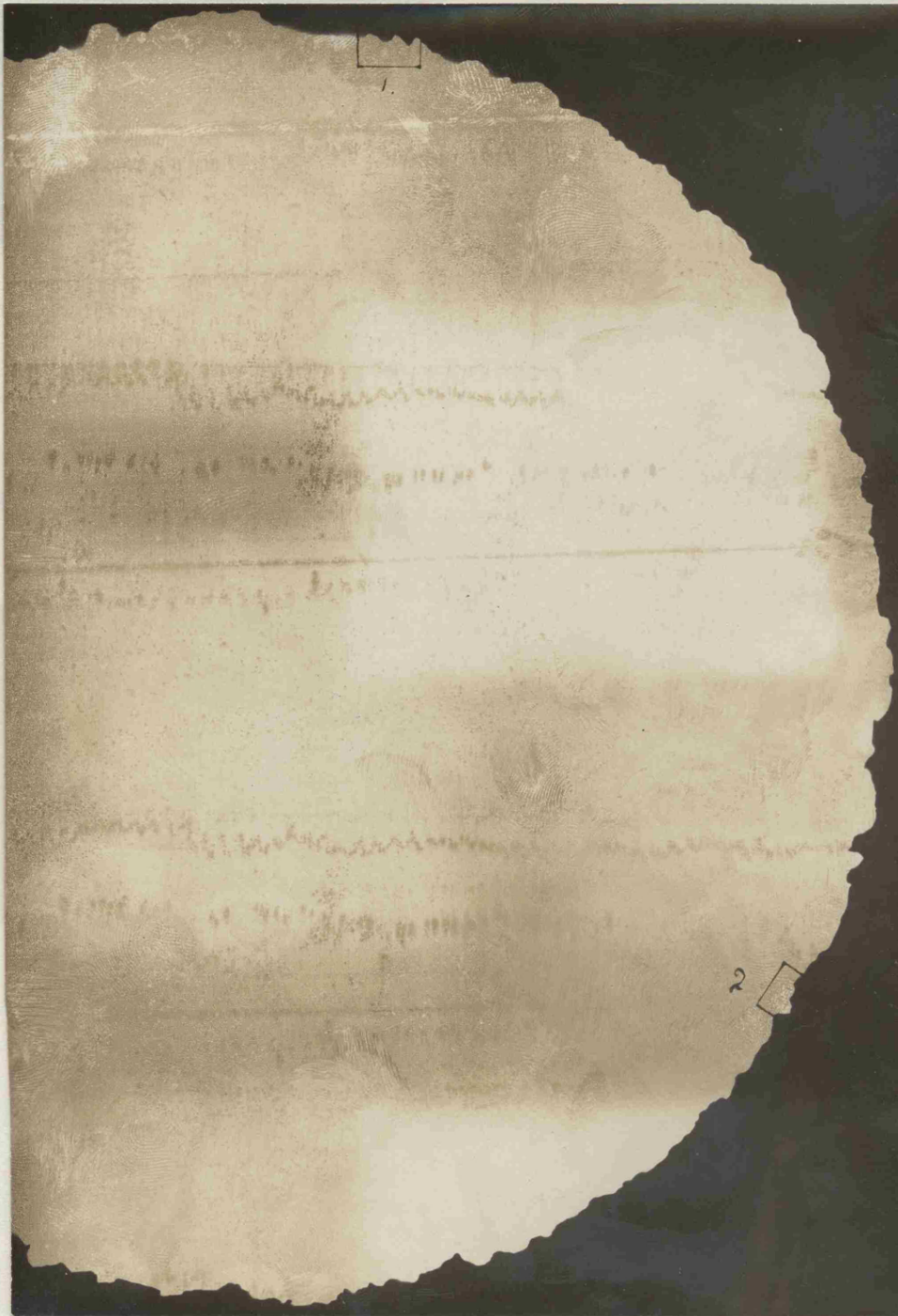


Fig. 7.20 Photogram of diamond dressed 36 grit wheel, X 7.

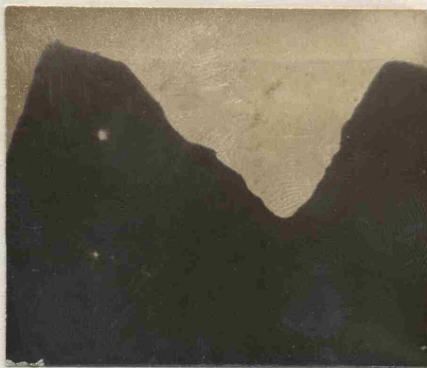


Fig. 7.21 Area 1 in fig. 7.20. X 125.



Fig. 7.22 Area 2 in fig. 7.20. X 125.



Fig. 7.23 Sharp grits in a diamond dressed 36 grit wheel, X 125.



Fig. 7.24 Glazed grits in a 36 grit wheel, X 125.

grains a permanent record being obtained by taking either a photogram or photograph.

An as dressed 60grit wheel is shown in figure 7.16 at a magnification of X7; the areas 1, 2 and 3 in figure 7.16 are shown enlarged to a magnification X125 in figures 7.17, 7.18 and 7.19. The very sharp facets of the abrasive can be readily seen and also the fact that there are very few positive rake grits. A similar set of results for a 36 grit wheel which is cutting satisfactorily are shown in figures 7.20, 7.21 and 7.22.

The method was also applied to wheels which had been used on the surface grinding machine. An as dressed 36grit wheel is shown in figure 7.23 and the grits are seen to be sharp, and in most cases have negative rake angles. The structure of a similar wheel which has been deliberately glazed is shown in figure 7.24 the flattened peaks of the abrasive grits being readily visible.

A severe limitation of optical methods is their poor depth of focus particularly at high magnifications. For example although the highly polished tip of a glazed grain can be studied optically at high magnifications no detail of the grit itself will be visible.

7.9.4 Scanning Electron Microscope.

The major advantages of this type of instrument are its great depth of focus, good relief contrast and high resolution, assets which are particularly useful when studying uneven surfaces such as abrasives. Another feature

FIG. 7.25. WEAR CURVE FOR 1% C STEEL (350 VPM) RUNNING AGAINST 60 GRIT WHEELS, SPEED 1,500 RPM, LOAD 1.25 KG

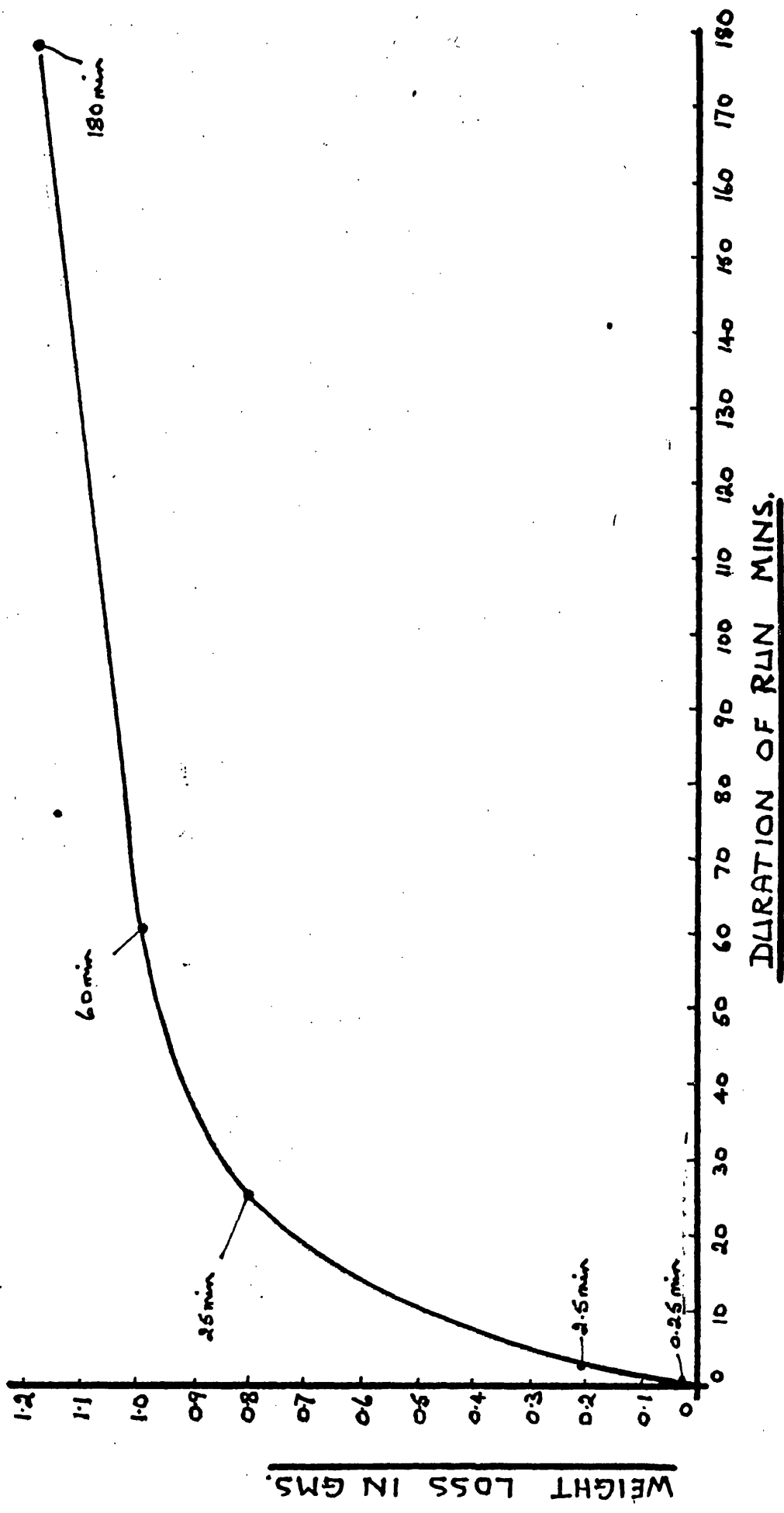


Table 7.1

Specimen No.	Figures No.	Condition.
1	7.26(a).	BA60 - L5 - VFBIJ wheel as received.
2	7.26(b), 7.27, } 7.30 }	BA60 - L5 - VFBIJ wheel diamond dressed.
		The remaining specimens had been run in wear tests, BA60 - L5 - VFBIJ wheels versus soft steel (DAK 5) speed 1,500rpm, load 1½Kg.
3	7.26(c), 7.29	Abrasive wheel running time 0.25 min.
4	7.26(d).	Abrasive wheel running time 2.5 min.
5	7.26(e).	Abrasive wheel running time 25 min.
6	7.26(f), 7.28, } 7.31, 7.32 }	Abrasive wheel running time 180 min.
7	7.34(a, c and e).	Steel pin running time 0.25 min.
8	7.34(b, d and f).	Steel pin running time 180 min.
9	7.33	Completely glazed abrasive pin included for comparison.



(a)



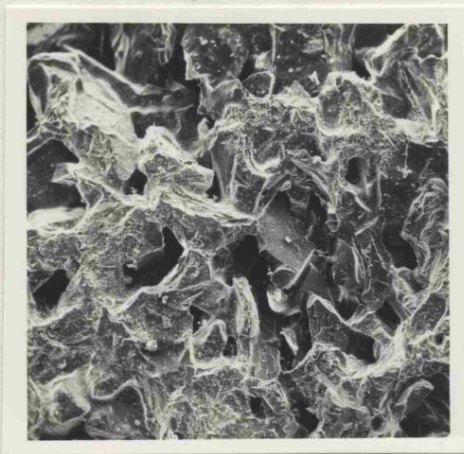
(b)



(c)



(d)

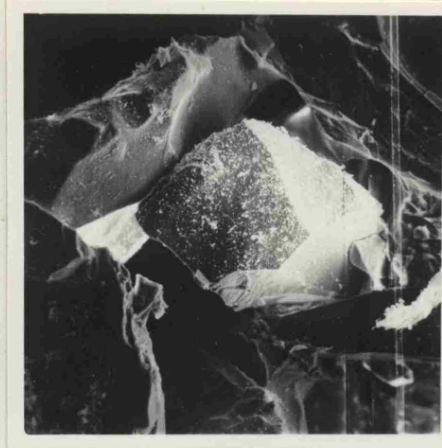
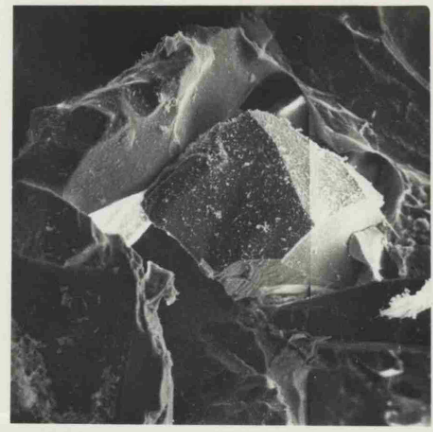


(e)

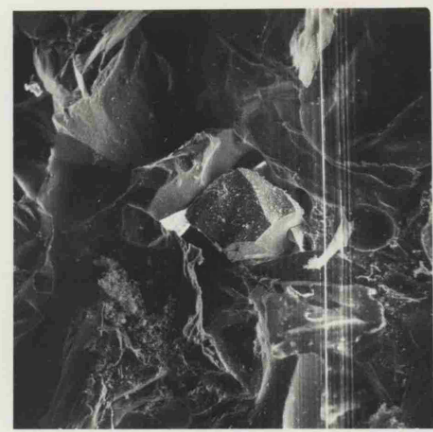


(f)

Fig. 7.26 60 grit wheels in various conditions (a) as received (b) diamond dressed (c) run 0.25min. (d) run 2.5 min. (e) run 25 min. (f) run 180min. Magnification X35 viewed vertically



(a)

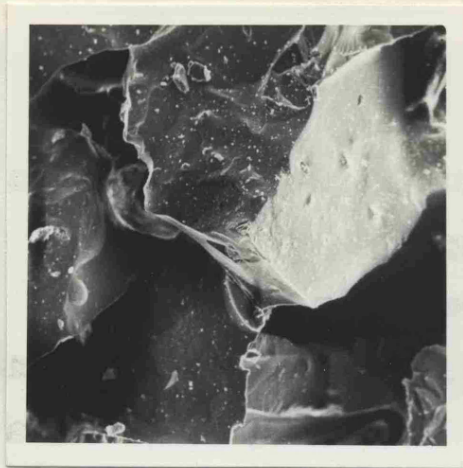


(b)

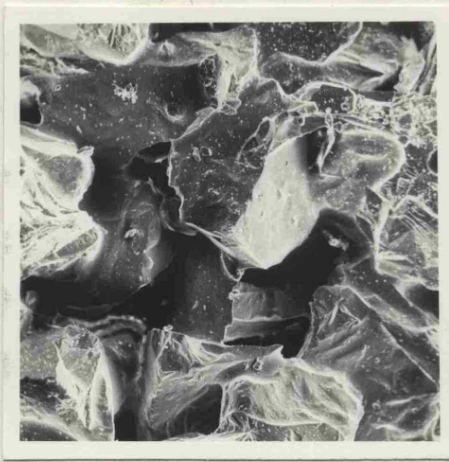


(c)

Fig. 7.28 Stereo-photographs of a 60 grit wheel which has run for 180 mins. (a) X 150 (b) X 75 (c) X 35. Viewed vertically.



(a)



(b)



(c)

Fig 7.27 Stereo-photographs of diamond dressed 60 grit wheel,
(a) X 125 (b) X 62 (c) X 35. Viewed vertically.

of the instrument is that it can produce stereoscopic photographs. However, during the present work only limited access to a scanning electron microscope was possible; therefore the results reported below should be regarded as an exploration of the utility of this technique.

Experiments were carried out to study abrasive wheels in various conditions ranging from as received to completely glazed. The wheels were prepared on the pin and ring machine (Chapter 4) the conditions being selected to give gradual glazing of the abrasive. A number of wheels were tested the experiments being stopped at progressively later stages in the glazing process. The wear curve for the experiments is shown in figure 7.25. A list of specimens is given in table 7.1.

Figure 7.26 shows the range of 60grit wheels viewed vertically. The as received specimen (7.26a) has a closely packed structure the abrasive grits presenting flat facets to the surface. Dressing (7.26b) gives a more open structure with a large number of very sharp cutting edges. Close examination of figures 7.26c to 7.26f reveals the progressive formation of flats on the tips of the cutting grits due to glazing. The differences between a freshly dressed wheel and one which has become glazed are shown in greater detail in stereoscopic photographs (figures 7.27 and 7.28).

The depth of focus given by the Scanning Electron Microscope is particularly advantageous when taking oblique photographs of a surface. An oblique stereo-photograph

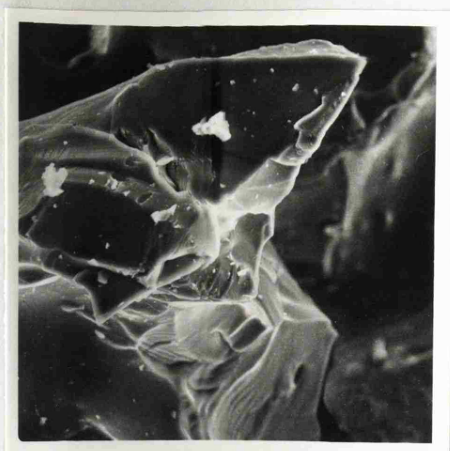
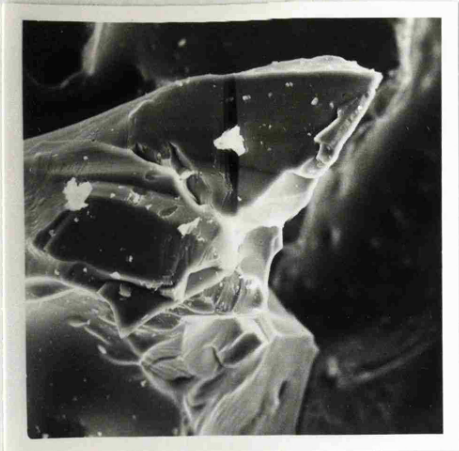


Fig. 7.29 Stereo- photograph of positive rake grit in a 60 grit wheel which has run for 0.25 min, viewed horizontally, X 320.



Fig. 7.30 Sharp grit viewed horizontally, X 550.



Fig. 7.33 Glazed abrasive pin viewed at 45° , X 70



Fig. 7.31 Glazed grit viewed horizontally, X 56.



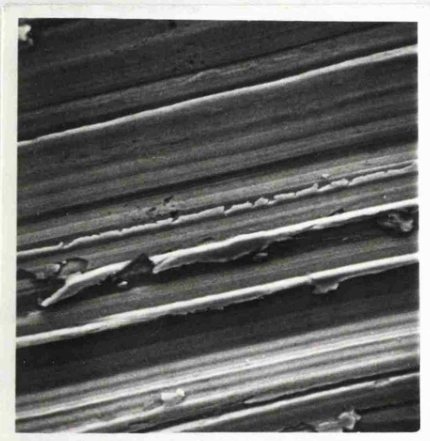
Fig. 7.32 As fig. 7.31. X 300.



(a) 0.25 min.



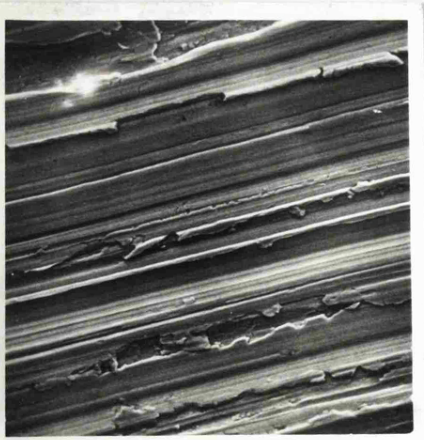
(b) 180 min.



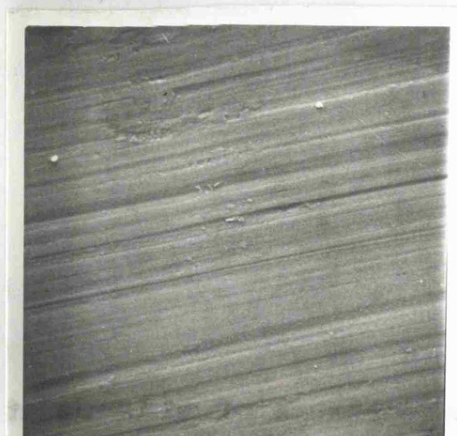
(c) 0.25 min.



(d) 180 min.



(e) 0.25 min.



(f) 180 min.

Fig. 7.34 Photographs of 1% (DAKS) pins which have run for 0.25 and 180 minutes. (a) and (b) X 1,500, (c) and (d) X 750, (e) and (f) X 375. Viewed at 17° to the horizontal.

of a grit with a positive rake angle is shown in figure 7.29 the cutting edges can be seen to be particularly sharp. The differences between the dressed and glazed wheels were found to be much more obvious when viewed at a shallow angle; figure 7.30 shows a sharp grit in the freshly dressed wheel figure 7.31 and 7.32 a glazed grain with a smooth top in the wheel which has run for 180 mins.

The wear scar on an aloscite pin is shown in fig (7.31) the abrasive is completely clogged with wear debris and has a very smooth surface. Similar effects were observed with abrasive wheels when glazing had been allowed to continue for very prolonged periods.

As the grinding wheel glazes the quality of the surface which it produces will also change, figure 7.32 shows the differences between the steel pin which has run for 0.25 mins. and the one which has run for 180 mins. The pin which ran for the shorter time has a rough surface and shows evidence of ploughing; the second pin has a very smooth surface which appears relatively undisturbed.

7.10 Discussion.

The scratch tests using abrasives were consistent with the earlier test involving idealised cutters the importance of pile-up at the edges of scratches in soft materials was again demonstrated. Although the tests used abrasive grits and in some cases ground specimens it must be remembered that the experiments are still not completely

representative of grinding as speeds were very low. Using coefficient of friction as guide to the cutting mechanism ($\mu = 2$ in single point cutting 0.5 in grinding) it was found that positive rake grits could only support a high coefficient of friction for a short time before fracturing to give a negative rake grit and a low coefficient of friction. This suggests that positive rake grits on grinding wheels play little part in the abrasion process and that the bulk of material is removed by grits with a negative rake angle.

Of the methods used to examine abrasives the optical profile and scanning electron microscope proved to be the most effective. The optical profile method did not involve sectioning the specimen so the specimen could be used again; this is particularly important with large grinding wheels. The specimens examined with the scanning electron microscope had to be broken up but, despite this, the results were very valuable. The differences between as received, dressed and glazed wheels were dramatically demonstrated. Examination of abraded steel pins also yielded interesting information concerning the effects of ploughing and metal removal rates.

7.11 Conclusions.

(1) Abrasive grits behave in a similar way to idealised cutters; the quantity of material actually removed from a specimen depends critically on pile-up at the edge of the scratches formed by the abrasive.

(2) Positive rake grits fracture very easily and are small in number; they probably account for the removal of only a small proportion of the abraded material.

(3) Dressing produces a grinding wheel with a large number of very sharp cutting edges.

(4) Glazing is the gradual blunting of the abrasive grits. The extreme situation observed in some abrasive pin experiments and some abrasive wear experiments when the abrasive becomes completely clogged with debris is more representative of super-finishing than grinding.

(5) When scratching a fully hardened steel ($p_m = 890\text{Kg/mm}^2$) almost the whole of the scratch volume is removed.

(6) There is need for further work on the relationship between the geometry of an abrasive grit and the scratch which it produces. The methods of examining abrasive wheels explored in this work could be further developed.

(7) When scratching hard materials a coefficient of friction of about 0.5 was observed.

8. General Conclusions.

This thesis has involved a broad investigation of a number of aspects of the allied subjects of grinding and abrasive wear. An attempt has been made to assess the extent to which similar considerations apply to the mechanisms which occur in both processes. The most obvious contrasts between the processes are the surface speeds involved, very high with grinding comparatively low in abrasive wear, and the materials to which each process is applied, usually hardened steels with grinding, fairly soft materials in abrasive wear studies. Previous theories of grinding have tacitly assumed that all the grits were cutting and that the process could be regarded as a form of micromilling. Abrasive wear predictions, on the other hand, have assumed that the normal force is supported on the frontal facets of the abrasive and that the contents of the scratches formed by abrasion are removed as wear. Theoretical studies of both processes have assumed that negative rake grits can remove material but experimental support, in the literature, for such an assumption is meagre.

Pin and ring wear tests were used to survey the broad range of behaviour primarily the rubbing of steels against grinding wheels. A wide range of loads and speeds were employed. With the exceptions discussed below throughout this range of conditions the wear was of a markedly abrasive type involving the removal of metallic

particles. To a reasonable first approximation the wear rate (worn volume per unit sliding distance) was found to increase proportionally with the load and was independent of the sliding speed.

Some anomalies in wear behaviour were noted. At extremes of load and speed effects were noted which could be attributed to thermal softening. However the most notable feature was a marked transition in wear behaviour from the production of metallic particles to the appearance of finely divided oxide debris. This caused glazing of the wheel and, after long periods of running, resulted in a clogging of the wheel. Thus although these mechanisms are, at first sight, similar to the severe and mild wear mechanism of adhesive wear, the detailed mechanisms involved in the transition are clearly different.

The development of a glazed wheel was therefore chosen as a suitable process to use for an exploratory investigation of the utility of the scanning electron microscope in the examination of abrasives. This work showed very clearly the potential value of the Stereoscan instrument in this field and further work is obviously desirable. In the present investigation the microscope showed very dramatically the development of flat worn surfaces upon the abrasive grits and, at a much later stage, the development of a flat surface when the abrasive becomes charged with oxide debris. These changes appear to be similar to those found in descriptions of the super

finishing process. It is not clear, at present what conditions are necessary to maintain an efficient abrasive mechanism which is required for grinding.

However, the major emphasis of this thesis has been to show that, in most important respects, abrasive wear and grinding must be regarded as similar mechanisms. But, as discussed earlier, there is a marked contrast in that grinding theory assumes that all grits remove material whereas most of the results obtained in abrasive wear lead to the conclusion that the process has an efficiency of about 10%, the most favoured assumption being that only 10% of the grits remove material. In this thesis some emphasis has been placed upon the study of heat treated steels since much of the anomalous behaviour is concerned with these materials. It has been shown, in many different types of test, that the efficiency of the abrasive process is closely linked with pile-up of the material. The percentage of material removed from an abraded track is directly related to this pile-up. With fully hardened steel the efficiency is high and it falls markedly with decreasing hardness. The major divergence between earlier results of abrasive wear and grinding tests therefore arises from the simple fact that most abrasive wear experiments have been concerned with soft materials and most grinding experiments with hardened steel.

This variation of efficiency with hardness could go some way to explain the major anomaly in the field of abrasive wear. This is the result of Kruschov and Babichev for heat treated steels. However other features, in particular excessive wear of the grinding wheel when grinding materials of low hardness, have been revealed in the course of the present work. Therefore we now examine the extent to which the present work presents a consistent and coherent picture. Consider first the consequences of an idealised model of the perfect abrasive in which all grits remove material and the efficiency of the abrasive process at each grit (represented by the factor β) is 100%. For this model in abrasive wear experiments the wear rate is inversely proportional to hardness and the coefficient of friction (which is dependent only upon the grit geometry) is independent of hardness. In grinding with a given depth of cut the normal and tangential forces would be directly proportional to hardness, the coefficient of grinding being independent of hardness.

These conclusions will, of course, be influenced by the variation of efficiency () with hardness. The model of the last paragraph is an adequate statement of the behaviour of our grinding wheels and fully hardened steel. However as the hardness falls the wear rate will increase less rapidly than expected (wear rate $\propto 1/p_m$) because of the fall in β . This is shown to be the case in figure 5.11.

In the grinding experiments, at a given wheel depth of cut, the expected decrease in normal force will be, to a large extent, offset by the change in β which means that the grit depth of cut will increase with decreasing hardness. An alternative statement of this same effect is to remark that as the hardness falls β falls and material, instead of being removed at the first cut, is involved in more than one cut.

The precise effect of the variation of β upon the normal forces cannot be specified on the basis of present knowledge. Consider a comparison of the grinding of hardened steel and soft steel with the same wheel depth of cut. For hardened steel, β approaches unity and each element of material removed is involved in only one individual abrasive process. Because, for soft steels β is lower, each element of material removed is involved in a number of individual abrasive processes before removal. This can come about either by an increase in the number of active grits or by an increase in the grit depth of cut or by both of these changes in unknown proportions. Likewise these factors could affect tangential forces. However, in broad terms, it is clear that the fall of efficiency (β) with decreasing hardness is capable of explaining both the relatively small effect of the hardness of heat treated steels upon the wear rate (in abrasive wear experiments) and upon the grinding forces (in grinding experiments).

At low values of hardness (less than about 300 VPN) another feature occurs which is a function of the characteristics of the grinding wheel. The scratch tests with grits (Chapter 7) show that with steels in this hardness range there was a rise in the coefficient of friction and an increased tendency for the grits to fracture. These features also occur in the wear and friction tests in sections 5.5.5 and 5.5.6 (fig 5.11 and Table 5.3). The rise in grinding coefficient with decreasing hardness is much less marked. However this might be expected if a decrease in hardness also produces an increase in the wear of the grinding wheel; this feature was noted in the wear tests. The effect of an increase in the wear of the grinding wheel would be to reduce the effective wheel depth of cut with a consequent reduction in forces. Once again this is an aspect worthy of further study.

The results for Stellite may also be briefly noted. It has been shown that the coefficient of friction in the wear tests and the grinding coefficients derived from the dynamometer tests are significantly lower than those obtained under otherwise similar conditions with steels. Broadly, these results are probably explained by glazing of the grits resulting in the marked increase in width/depth ratio which was observed. This aspect of the subject merits more detailed investigation and is an area where the techniques of examination of abrasives discussed in Chapter 7 could be

employed. Moreover, this is, perhaps, the only part of the experimental work reported in this thesis where the hardness of any constituent of the workpiece material (in this case the carbides which form part of the Stellite structure) approaches the hardness of the abrasive. If this were clearly established this factor could be an influence upon abrasion efficiency and the work of Richardson and co-workers (1967) would be relevant.

When the theories developed in this thesis are compared with conventional grinding theories two facts emerge. Firstly, both rely on the accurate determination of the value for the width/depth ratio of a typical grinding scratch. Secondly although the present theories have eliminated the controversial grit depth of cut this has been replaced by two other factors α and β (proportion of active grits and proportion of groove volume removed respectively). In the author's opinion the factor α could be abandoned as it is to a large extent taken into account in the β term, since if a grit is not removing material (active) it will pile-up a ridge. Such an inactive grit would be included in the mean value of β . As both theories are so critically dependent on the value of the width/depth ratio of a typical scratch and its geometrical relationship to the grit which produced it, it is this area which is considered to be the most important for further study.

BIBLIOGRAPHY.

- Alden, G.I. 1914. A.S.M.E. Vol. 36, p. 451.
- Archard J.F. 1958. Wear 2 (1) 21.
- Backer W.R. Shaw M.C. and Marshall E.R. 1952.
A.S.M.E. Vol. 74, p. 61.
- Bowden F.P. and Tabor D. 1950. The Friction and
Lubrication of Solids. Oxford, Clarendon Press.
- Farmer D.A., Brecker J.N. and Shaw M.C. 1968.
Paper No.8. Proc. Conf. Properties and Metrology
of Surfaces. Institution of Mechanical Engineers.
- Goddard J., Harker H.J. and Wilman H. 1959.
Nature, 184. p. 333.
- Goddard J. and Wilman H. 1962. Wear 5. p. 114.
- Grisbrook H. 1960 The Production Engineer Vol.39, No.5.
- Grisbrook H. 1962. Cutting points on the surface of a
grinding wheel and chips produced. Proc. 3rd
M.T.D.R. Conference, p.155.
- Hahn, R.S. 1955. A.S.M.E. Vol. 77, p. 1352.
- Hahn, R.S. 1956. A.S.M.E. Vol. 78, p. 807.
- Hahn, R.S. 1962. On the nature of the grinding process.
Proc. 3rd. M.T.D.R. Conference. p. 129.
- Hahn, R.S. 1964 J.Eng. for Industry. A.S.M.E.
Series B. 86, p. 287.
- Hahn, R.S. 1965. Some characteristics of controlled
force grinding. Proc. 6th. M.T.D.R.Conference p.597.

- Kragelskii, I.V. 1965. Friction and Wear (Translated from the Russian) London. Butterworths.
- K(h)ruschov, M.M. 1957. Paper 46. Proc. Conf. Lubrication and Wear. Institution of Mechanical Engineers, London.
- K(h)ruschov, M.M. and Babichev M.A. 1960. Research on the Wear of Metals. Moscow. N.E.L. Translation.
- Landberg, P. 1956. Experiments on Grinding. College International pour l'etude scientifique de techniques de production mecanique.
- Marshall E.R. and Shaw M.C. 1952. A.S.M.E. p. 51.
- Merchant M.E. 1945 J. Appl. Phys. 16. p. 267.
- Mulhearn T.O. and Samuels L.E. 1962. Wear 5. p. 478.
- Nathan G.K. and Jones, W.J.D. 1967. Paper No. 24. Fifth Lubrication and Wear Conference, Institution of Mechanical Engineers.
N.E.L. 1962. Leaflet No. 395.
- Opitz, H. Ernst, W., and Meyer, K.F. 1965. Grinding at high cutting speeds. Proc. 6th M.T.D.R. Conference p. 581.
- Rabinowicz, E. 1965. Friction and Wear of Solids. John Wiley & Sons, New York.
- Richardson, R.C.D. 1967-68. Proc. Inst. Mech. Engrs. Vol. 182, Pt. 3A, p. 410.
- Sedriks, A.J. and Mulhearn T.O. 1963. Wear 6, p. 457.
- Sedriks, A.J. and Mulhearn T.O. 1964. Wear 7, p. 451.
- Spurr R.T. and Newcomb T.P. 1957. Paper 28. Proc. Conf. Lubrication and Wear. Institution of Mechanical Engineers.

Stroud, M.F. and Wilman H. Brit. J. App. Phys. Vol. 13
p. 173.

Tabor D. 1951. The Hardness of Metals.
Oxford University Press. Oxford.

Tabor, D. 1954. Proc. Phys. Soc. (London) B. 67.
p. 249.

Welsh, N.C. 1965. Phil. Trans. Roy. Soc. (London) A.257
p. 31.

Wul'f, A.M., Shifrin A. Sh. and Shatsman, I.M. 1948.
Skorestnoe tochenie. (High-speed turning).
Moscow : Mashgiz.